2011

EFFECT OF AZITHROMYCIN ON MACROPHAGE PHENOTYPE DURING PULMONARY INFECTIONS AND CYSTIC FIBROSIS

Theodore James Cory
University of Kentucky, theodorecory@gmail.com

ABSTRACT OF DISSERTATION

Theodore James Cory

The Graduate School

University of Kentucky

2011

EFFECT OF AZITHROMYCIN ON MACROPHAGE PHENOTYPE DURING PULMONARY INFECTIONS AND CYSTIC FIBROSIS

ABSTRACT OF DISSERTATION

A dissertation submitted in partial fulfillment of the
Requirements for the degree of Doctor of Philosophy in the
College of Pharmacy at the University of Kentucky

By
Theodore James Cory

Lexington, Kentucky

Co-Directors: Dr. David Feola Professor of Pharmacy Practice and Science
and Dr. Patrick McNamara Professor of Pharmaceutical Sciences

Lexington, Kentucky

2011

ABSTRACT OF DISSERTATION

EFFECT OF AZITHROMYCIN ON MACROPHAGE PHENOTYPE DURING PULMONARY INFECTIONS AND CYSTIC FIBROSIS

Azithromycin improves clinical outcomes in patients with cystic fibrosis (CF), specifically in patients infected with Pseudomonas aeruginosa. Azithromycin shifts macrophage programming away from a pro-inflammatory classical (M1) phenotype, and towards an anti-inflammatory alternative (M2) phenotype; however, little is known about this mechanism, nor of its impact upon immune response to pulmonary infection. We set out to determine the mechanism by which azithromycin is able to alter macrophage phenotype, and assess the effect of azithromycin induced macrophage polarization on inflammation during pulmonary infections.

Utilizing macrophage cell culture, we found that azithromycin increased IKKβ, a signaling molecule in the NFκB pathway, which likely is altering macrophage programming. Using a Pseudomonas infection model in mice that lack physiologic alternative macrophage activation, we showed that azithromycin's ability to alter macrophage function and decrease lung damage was independent of interleukin control of macrophage programming. Azithromycin increased fibrotic protein production both in vivo and in vitro, but blunted immune-driven fibrotic damage. We extended our study to patients with CF, describing gene expression in macrophages isolated from sputum samples. We found markers consistent with a shift toward M2 polarization in these patients. These data suggest potential mechanisms by which azithromycin benefits patients with CF.

KEYWORDS: Azithromycin, Macrophage phenotype, Cystic fibrosis, *Pseudomonas Aeruginosa,* IKKβ

Theodore James Cory

August 2, 2011

EFFECT OF AZITHROMYCIN ON MACROPHAGE PHENOTYPE DURING PULMONARY INFECTIONS AND CYSTIC FIBROSIS

By

Theodore James Cory

Dr. David Feola
Co-Director of Dissertation

Dr. Patrick McNamara
Co-Director of Dissertation

August 2, 2011

RULES FOR THE
USE OF DISSERTATIONS

Unpublished dissertations submitted for the Doctor's degree and deposited in the University of Kentucky Library are as a rule open for inspection, but are to be used only with due regard to the rights of the authors. Bibliographical references may be noted, but quotations or summaries of parts may be published only with the permission of the author, and with the usual scholarly acknowledgements.

Extensive copying or publication of the dissertation in whole or in part also requires the consent of the Dean of the Graduate School of the University of Kentucky.

A library that borrows this dissertation for use by its patrons is expected to secure the signature of each user.

Name	Date

DISSERTATION

Theodore James Cory

The Graduate School

University of Kentucky

2011

EFFECT OF AZITHROMYCIN ON MACROPHAGE PHENOTYPE DURING PULMONARY INFECTIONS AND CYSTIC FIBROSIS

DISSERTATION

A dissertation submitted in partial fulfillment of the
Requirements for the degree of Doctor of Philosophy in the
College of Pharmacy at the University of Kentucky

By
Theodore James Cory

Lexington, Kentucky

Co-Directors: Dr. David Feola Professor of Pharmacy Practice and Science
and Dr. Patrick McNamara Professor of Pharmaceutical Sciences

Lexington, Kentucky

2011

To my wife Marie and my parents Jim and Laurie,
without whom I could not have achieved all that I have

The following dissertation, while an individual work, benefitted from the insights and directions of several people. First, my mentor Dr. David Feola. His patience, kindness, and support are just a few of the many qualities that I hope to be able to emulate in my own professional career. Second, Dr. Brian Murphy additionally greatly guided my scientific development, as well as provided a valuable sounding board through the difficulties I faced in graduate school. I additionally wish to thank the rest of my graduate committee and my outside examiner, respectively: Dr. Patrick McNamara, Dr. Val Adams, Dr. Don Cohen, and Dr. Melinda Wilson for their guidance and assistance.

Additionally, I received important assistance throughout my graduate work from many people, including Dr. Susan Birket, Dr. Jessica Breslow-Deckman, Ms. Cynthia Mattingly, and Ms. Kathleen Donoghue from the Feola and Murphy labs, as well as my former advisor at Drake University, Dr. Nita Pandit for her continued support. Dr. Heather Bush taught me how to utilize principal component analysis, and was incredibly patient with the innumerable questions that I had related to it. Ms. Catina Rossoll deserves special attention for being able to answer any question that I had for her, and making sure that I didn't miss any deadlines throughout my time in graduate school.

I additionally wish to thank my parents Jim and Laurie, as well as family friend Darlene Hazuka for their love and support, as well as hard work instilling in me a love of hard work and learning. Finally, I wish to thank my wife, Marie, for her love and support through my difficult time in graduate school. It would not be an understatement to say that I could not possibly have come as far as I have without the support of everyone I have mentioned, and countless others I have not.

TABLE OF CONTENTS

LIST OF TABLES

LIST OF FIGURES

Chapter 1: Introduction

A. Overview

Cystic Fibrosis (CF) is a genetic disorder characterized by a deficiency in the cystic fibrosis transmembrane regulator (CFTR) gene [11]. This deficiency results in impaired chloride transfer in epithelial cells. This impairment results in thickened secretions in the digestive and reproductive tracts, as well as in the lungs. While impairments in the digestive and reproductive tracts can commonly lead malnutrition and sterility, it is the pulmonary complications in patients that lead to long term complications and mortality, with the average life expectancy of patients with CF currently at 37 years [11]. Defects in the CFTR cause the lungs of these patients to be characterized by increased mucus formation, providing a breeding ground for a wide variety of bacteria to colonize, most notably the gram negative bacterium *Pseudomonas aeruginosa*. The progression of the disease is characterized by repeated acute bacterial flares, followed by a latent phase where the bacteria are held in check by the immune system. The inflammatory response in the lungs to these recurring infections contributes greatly to a decline in lung function in these patients over time [11].

During acute bacterial flares, the lungs of these patients are characterized by an influx of phagocytic and inflammatory cells, most notably neutrophils and macrophages [12]. These inflammatory cells produce a wide variety of pro-inflammatory cytokines in the lungs. Additionally, the production of molecules involved in the oxidative burst (e.g. nitric oxide) are up-regulated, resulting in destruction of bacteria [13]. Unfortunately, these oxidative molecules also cause considerable damage to the lungs of these patients. This inflammatory response is necessary, as without it bacteria would over-proliferate. If the response is overly zealous, however, a large amount of damage can occur in the lungs of these patients. This results in airway remodeling, scarring, and a decline in lung function over time in these patients. In the course of an individual infection of bacterial flare, macrophages initially play an important role in phagocytosis and inflammation; over time, however, they shift to an anti-inflammatory and pro-

fibrotic role. These cells play an important role in killing invading bacteria in the lungs, and are responsible for the initiation of the inflammatory response to a bacterial flare, [12]. These infections are treated with a wide variety of medications, including oral, IV, and inhaled antibiotics [14]. In an attempt to control the number of bacterial exacerbations, these patients also are commonly treated with anti-inflammatory medications, including traditional agents (e.g. corticosteroids and non-steroidal anti-inflammatory drugs). Ibuprofen has traditionally been shown in patients with CF to prevent decline in FEV1 % predicted, as well as improving survival. The medication is not routinely used in patients with CF, however, due to the side effect profile associated with the medication [15]. Additionally, azithromycin (AZM), an antibiotic that is utilized for its anti-inflammatory properties.

AZM is a macrolide antibiotic that is commonly used in this patient population. It has been shown in several clinical studies that chronic AZM therapy improves clinical parameters in patients with CF, including forced expiratory volume in one second (FEV1), incidence of acute bacterial flares, and patient quality of life [16-20]. Unfortunately, long term usage of AZM as an anti-inflammatory can contribute to increased bacterial resistance as well as to other forms of collateral damage resistance [17]. An increased understanding of how AZM alters immune responses and thereby improves clinical parameters in these patients may lead to potential new therapeutics that provide the beneficial effects of AZM without the need to for long-term antimicrobial use. Including much of the work in this dissertation, our group has shown that AZM alters the function and phenotype of macrophages in these patients, and hypothesize that this may be one of the methods by which patients benefit from taking the drug.

B. Cystic fibrosis

Cystic fibrosis is an autosomal recessive disorder that results in a non-functional CFTR channel. The CFTR is a chloride channel found in multiple organ systems, most notably the lung. The lung manifestations of CF are the most impactful to patients over the course of their lifetime, contributing the most

to morbidity and mortality. While literally hundreds of mutations in the CFTR have been observed, they can be grouped into 5 major groups. Class 1 mutations result in a shortened mRNA, and no CFTR protein production. Class 2 mutations result in misfolded mRNA, which is then degraded in the endoplasmic, resulting in no CFTR protein production. The ΔF508 mutation, which represents 70% of all mutations in patients with CF, is a class 2 mutation [11]. In class 3 mutations, an inactive CFTR is produced. Class 4 mutations result in a CFTR with decreased function. Finally, Class 5 mutations result in normal function, but decreased expression of the CFTR [11, 21]. Interestingly, while different classes of mutations can be correlated to disease severity for most organs affected with CF (e.g. the gut, pancreas, and reproductive tracts), with classes 4 and 5 mutations being associated with less serious disease, this correlation does not appear to exist in the lungs of patients with CF [22, 23].

In the lungs, a deficient CFTR leads to salt imbalances at the epithelial surfaces, which then results in thickened and dehydrated secretions [11]. Not only do these thickened secretions provide a breeding ground for a wide variety of pathogens, but this also alters immune cell function in the lungs, making it considerably more difficult for phagocytic cells to internalize and destroy bacteria [11]. Acute flares of CF also involve an extensive neutrophilic response. During an acute exacerbation of the disease, cytokines produced by macrophages, including IL8, IL1 and TNF-α result in the recruitment of neutrophils to the lung. Once they reach the lungs, they release elastases, and lyse, they release large amounts of DNA into the lung as well [24]. These secreted factors and released DNA provide the basis of the thickened secretions and impaired clearance of organisms that plague the lungs of patients with CF [11]. The prolonged inflammatory response that this causes also plays an important role in the decline of lung function in patients with CF. Disease progression is characterized by blockage of the small and medium bronchioles, although the alveoli are by and large spared [11]. Additionally, there is evidence that the CFTR plays an important role in the ability of phagocytic cells to acidify the phagosome. This results in macrophages and monocytes in CF patients being less able to destroy

bacteria that they have internalized [25]. This is likely an additional reason why patients with CF are unable to effectively clear the bacteriawith which they have been colonized.

Patients with CF are colonized with a wide variety of pathogens, and once colonized it is exceptionally difficult to clear these pathogens. The pattern of bacterial colonization in patients with CF has shifted over time. Traditionally, *P. aeruginosa,* methicillin-susceptible *Staphlococcus aureus*, and *Haemophilus influenzae* have been the primary pathogens that patients that CF are colonized with [26]. More recently, however, other bacteria are becoming increasingly common in patients with CF, most notably methicillin-resistant *Staphlococcus aureus*, although there has also been a great increase in patients colonized with *Stenotrophomonas maltophilia*, *Achromobacter xylosoxidans*, and various mycobacteria [11, 26].

By far, however, *P. aeruginosa* is the most significant pathogen in patients with CF [11]. The rate of colonization in patients with CF can exceed 70% in adults, and even in young children the rate of colonization can exceed 25% [27, 28]. This pathogen produces thick alginate biofilms that aid its ability to survive in this setting [29]. By hiding in biofilms, the bacteria is able to avoid phagocytosis by macrophages and neutrophils, as well as avoid antibiotics. Biofilms also may prevent complement from being able to bind to the organism's surface, preventing the bacteria from being targeted for destruction [30]. Indeed, conversion from a non-biofilm producing strain to a biofilm producing strain is considered one of the necessary steps for *P. aeruginosa* to permanently colonize the lungs of patients, as opposed to being present in the lungs intermittently [30]. *P. aeruginosa* additionally produces elastases and proteases that allow it to cleave host defense proteins, such as defensins, allowing it to remain in the lungs of these patients [13]. *P. aeruginosa* is able to respond quickly to changes in the host environment, allowing it to out-compete other bacteria [13]. The biofilms that are formed also impair the ability of these patients to breathe, and result in a decline in lung function for these patients over time. Evidence also

exists that *P. aeruginosa* is able to mutate more readily in patients with CF, allowing it to gain resistance to the antibiotics used to treat these patients [31].

Hartl et. al. have shown that the lungs of patients with CF colonized with *P. aeruginosa* showed increased concentrations of IL4 and IL13, and decreased concentrations of IFNγ, consistent with a shift towards a Th2 polarization in the lungs of these patients [32]. This difference was even more pronounced when they assessed mRNA expression via qRT-PCR [32]. They also found that patients colonized with *P. aeruginosa* displayed higher levels of the inflammatory cytokine interleukin (IL)6 in their bronchoalveolar lavage fluid. In their *P. aeruginosa* positive patients they additionally found a strong negative correlation between IL4 and IL13 concentrations and FEV1 % predicted [32]. This further suggests the negative repercussions associated with a shift to towards the Th2 phenotype in the lungs of these patients, and shows a method by which this shift occurs. Contrariwise, this may represent a reactionary response to a decline in lung function, with the increase in Th2 polarization being the response, rather than the cause of decreased lung function. This shift may be attempting to minimize further damage in the lungs of patients.

Patients with CF are treated with a wide variety of medications to manage their pulmonary symptoms. Nebulized tobramycin is approved for use in patients who have been colonized with *P. aeruginosa* [14]. Treatment with Dornase alfa, a recombinant DNase, is common as well to help degrade the thickened secretions that are common in patients with CF [14]. Patients receive a variety of other antibiotics to control bacterial infections, and to attempt to decrease the incidence of acute bacterial flares. Treatment with bronchodilators, as well as chest percussion is also commonly used and has been shown to improve lung function in these patients. It is also common for patients to receive dietary enzymes to aid in digestion, and to take proton pump inhibitors to deal with other symptoms associated with their disease [33]. While the wide variety of treatments used in these patients greatly improves life span and patient quality of

life, it makes clinical studies difficult due to confounding the data analysis in our studies and the studies of others.

C. Macrophage Polarization

Macrophages are important effector cells in the innate immune system [34]. Derived from circulating peripheral blood mononuclear cells (PBMCs), in their traditional roles, they reside in organs, and function both as a sentinel to invading bacteria, as well as one of the key phagocytic cells in the body. This response is characterized by phagocytosis of pathogens, and production of reactive oxygen species (ROS) [35]. Additionally, they secrete cytokines that recruit other inflammatory cells to the site of an acute infection, primarily neutrophils [36]. This robust inflammatory response, while necessary to destroy the invading pathogen, is not without cost. The production of pro-inflammatory cytokines, as well as ROS can lead to considerable tissue damage [37].

More recently, an additional phenotype for macrophage has been elucidated. Alternatively activated macrophages (M2), as opposed to the classically activated macrophages (M1) described above, play a very different role in host defense to infections. M2 macrophages are primarily involved in repairing the damage that is caused by a acute inflammatory injury. Their key effector molecules are arginase, as well as polyamines, which are the precursors to the extracellular (ECM) proteins fibronectin and collagen [38]. The production of these fibrotic molecules is a necessary part of the repair process. These molecules help damaged tissue regain integrity, and allow recovery from inflammatory damage. Overproduction, however, can lead to scarring, fibrosis, and organ damage. Indeed, in a variety of fibrotic lung diseases, it has been shown that the alternatively activated macrophage is the predominate phenotype in patients with these disorders [39]. Similar observations have been made for a number of autoimmune disorders as well, most notably multiple sclerosis and rheumatoid arthritis [38].

M1 and M2 macrophages are derived from inactive resident macrophages, as well as circulating monocytes. They are polarized to the classically or alternatively activated phenotype via signaling primarily from either Th-1 or Th-2 polarized T-cells, respectively [9, 35]. Cells are polarized to the classically activated phenotype via interferon-gamma (IFN-γ), in addition to signaling from the toll like receptors (TLRs) including TLR4 triggered by lipopolysaccharide (LPS). Macrophages can be polarized to the alternatively activated phenotype via signaling from both IL4 and IL13 [3]. The two prototypical effector proteins produced in the two phenotypes, iNOS and arginase 1, appear to be reciprocally regulated, sharing the common substrate L-arginine (Figure 1.1) [9, 10]. iNOS converts arginine to nitric oxide (NO) and citrulline. NO is a key component in the oxidative burst, leading to destruction of intracellular bacteria. It also, however, results in tissue damage, leading to inflammation at the site of infection. Conversely, with alternative macrophage polarization, the enzyme arginase is expressed and converts arginine to both urea and ornithine. Ornithine is then converted to polyamines, which can then be converted to precursors of matrix molecules including collagen. These proteins form the building blocks for tissue repair that is necessary to recover from an inflammatory response to bacteria, and if the damage is severe enough, results in irreversible fibrotic changes [40-42]. It is important to note that, unlike T cells, macrophage polarization occurs on a spectrum, and is not a terminal differentiation. A cell polarized to the classically activated phenotype can later be polarized to the alternatively activated phenotype, and vice versa [35].

The terminology used to describe macrophage polarization is a topic of ongoing discussion. It is generally accepted that the classically activated phenotype is relatively homogenous in its polarization and function. However, alternatively activated macrophages are considerably more variable in their description in terms of gene expression. An overview of the different phenotypes of macrophages can be seen in Table 1.1. Mantovani et. al. describe 3 different types of alternatively activated macrophages. M2a are polarized by IL4 and IL13. These cells display high expression of surface mannose receptor, and

express proteins including IL10, IL1ra, and the decoy IL1RII. They describe these macrophages as being heavily involved in type 2 inflammation, allergy, and the killing and encapsulation of parasites. They describe M2b macrophages as being activated by immune complexes and TLR or IL1R. M2b macrophages express high levels of CD86, IL10, TNF, IL1 and IL6. These macrophages are also known as type II macrophages, and are involved in immunoregulation and Th2 activation. Finally, they describe an M2c phenotype. These macrophages are activated by IL10, and express high levels of IL10, TGF-β, MR, and produce pro-fibrotic proteins involved in matrix deposition [3]. Others group one or more of these phenotypes together [1, 35]. In fact, rather than view macrophage polarization as a spectrum with M1 or M2 macrophages on either pole of the spectrum, some view there to be three primary poles of macrophage polarization, with classically activated macrophages, wound healing macrophages (essentially M2 macrophages), and regulatory macrophages representing the three poles, and various tissue macrophages that display markers of the three different phenotypes [35]. For the purposes of this dissertation, however, I will be treating macrophage polarization as a duality. I will be describing macrophages as either M1 or M2, although the M2 macrophages that I will be focusing on most closely resemble the M2a phenotype that Mantovani et. al. described. This does not, however, eliminate the possibility that AZM polarizes macrophages to a novel phenotype, as opposed to polarizing to the traditionally thought of alternatively activated phenotype. AZM may be polarizing macrophages to a novel phenotype that avoids both the inflammatory component of an M1 macrophage and the pro-fibrotic component of the M2 macrophage.

In the lung of the patient with CF during an acute bacterial infection, or during an acute flare of a chronic infection, both resident and infiltrating macrophages are quickly polarized by the cytokines in the lung milieu to the M1 phenotype. Additionally, M1 macrophages produce cytokines, including IL8, that result in a strong neutrophilic response [11, 43]. The strong M1 polarization in the lungs during an acute infection results in phagocytosis and destruction of bacteria in the lung. This results in the up-regulation of inflammatory markers, as

well as free radical levels in the lung [44]. There is also evidence that macrophages with deficient CFTR may indeed be playing a disproportionate role in this strong inflammatory shiftby producing higher amounts of proinflammatory cytokines including IL6 and TNFα as compared to macrophages with normal CFTR function [45].

T cells play an important role in the orchestration of the immune response. CD4+ T cells can be classified as having a T helper (Th) type 1, or a type 2 response. A Th1 response is characterized by production of the cytokine IFNγ, and leads to activation of macrophages to efficiently kill phagocytosed organisms, and a robust pro-inflammatory response [46]. A Th2 response, on the other hand, is primarily characterized by IL4 production, and leads to activation of humoral immunity. In addition, activation of the Th2 response leads to production of cytokines that polarize macrophages towards the alternatively activated phenotype in response to some pathogens [46]. In the lungs of patients with CF, the Th1 polarization is traditionally associated with improved outcomes. However, over time, a net shift to a Th2 polarization is observed in these patients. This shift is associated with a worsening in outcomes in patients with CF [47]. Indeed in other fibrotic lung diseases, most notably idiopathic pulmonary fibrosis, a vicious cycle persists in the lungs, wherein the Th2 polarization shifts macrophages to the alternatively activated phenotype, leading to increased production of collagen in the lungs of these patients, and a decline in lung function [48]. Others have shown that targeting IL4 and IL13-responsive cells (including macrophages and fibroblasts) in fibrotic lung disease in animals can lead to decreased fibrosis [49]. While similar findings have not yet been observed in patients with CF, it is reasonable to surmise that the damage caused during acute flares of CF results in an inordinately strong shift to the M2 phenotype, causing scarring and fibrosis in the lungs of these patients. While T cells coordinate the adaptive and chronic phases of host defense, macrophages also coordinate aspects of chronic inflammation in the lungs and in other tissues [50, 51]. Instead of the inflammatory response maturing into a more T cell-dominated process, in CF the response continues to be neutrophil-driven,

described by other investigators as more of a “sustained acute response” in contrast to a maturing, chronic inflammation [52]. While in normal circumstances this repair and remodeling is both necessary and beneficial in patients, in the face of the dysregulated inflammatory response in CF and the excessive damage that then results, it leads to pulmonary functional decline.

This exaggerated immune response, while necessary to respond to the acute infection, is not without costs. Considerable debris is accumulated in the lungs in the aftermath of an infection. This debris consists of portions of bacteria, as well as dead and dying epithelial cells and macrophages [53]. Alternatively activated macrophages are able to efficiently internalize and destroy this cellular debris [35]. They also produce profibrotic proteins, providing the necessary building materials for tissue repair to occur [54]. This repair commonly results in scarring and fibrosis of the lungs, especially when the initial immune response is robust [55]. Unfortunately, this scarring can lead to decreases in the parameters of lung function, including FEV1 % predicted [11]. This decline additionally increases the probability of a future acute bacterial flare, and the cycle of a damaging inflammatory response followed by tissue repair and remodeling is responsible for much of the mortality associated with CF [15]. The remodeling occurs primarily in the peribronchiolar regions of the lungs, with considerable bronchiectasis and scarring occurring in the lungs of these patients over time. Damage to the alveoli of the lungs is much less common, and also less severe in patients with CF, although it does occur in some patients, especially those with severe disease [56].

D. Azithromycin

AZM is a macrolide antibiotic that is commonly used for a variety of infections. It functions as a bacteriostatic agent and has clinically effective activity against both gram positive and negative organisms [57]. It binds to the 50s subunit of bacterial ribosomes and inhibits bacterial protein synthesis by blocking elongation of the peptide chain [58]. Interestingly, the drug is

extensively concentrated in immune cells:concentrations in alveolar macrophages have been reported to be 170 fold higher than in serum [58].

AZM is one of the drugs of choice for a wide variety of infections. The drug has been shown to be effective in a large percentage of community acquired pneumonia cases caused by the typical pathogens associated with this infection, including *Streptococcus pneumoniae*, and atypical organisms such as *Chlamydia pneumoniae*, *Legionella* sp., and *Mycoplasma pneumoniae*. [58]. Its spectrum of activity combined with the ease of administration results in it commonly being used for acute exacerbations of chronic bronchitis, otitis media infections, streptococcal pharyngitis, sinusitis, and both upper and lower respiratory tract infections [58].

Additionally, it has been shown that the macrolides exert anti-inflammatory effects independent of their effects on microorganisms [59]. Patients with advanced CF derive their benefits from the anti-inflammatory, rather than the anti-infective properties of the medication. Indeed, it appears to be a class effect of the macrolides, with clarithromycin displaying a less potent effect on inflammation, while roxithromycin (not approved for clinical use in the United States) is more potent [59]. Macrolides have also been shown to decrease inflammatory cytokine concentrations in the lungs, including IL6, IL8, and TNFα [37, 60]. It has been shown that while AZM does not destroy *P. aeruginosa*, it does exert indirect effects on the bacteria. AZM decreases transcription of the quorum sensing genes *lasR* and *rhlR*, resulting in a decrease in the production of bacterial virulence factors [61]. Importantly, it has been shown that treatment with macrolides decreases neutrophil influx in the lungs of patients with CF [62]. The importance of this effect, as well as the determination of a molecular mechanism by which this effect occurs is currently unknown.

Key to the development of this project, our lab has demonstrated that AZM is able to shift macrophage polarization away from the classically activated phenotype, and towards the alternatively activated phenotype, even in the presence of M1 stimulating cytokines [63]. We showed that macrophages

treated with AZM, bacterial LPS, and IFNγ increased expression of macrophage surface markers that was consistent with macrophages treated with IL4/IL13 and LPS. We also published that AZM treated macrophages exhibit increased arginase activity, as well as decreased expression of the iNOS protein. Finally, we showed that the pattern of cytokine expression in macrophages treated with AZM is less inflammatory, and more anti-inflammatory than macrophages that did not receive AZM [63].

AZM has been shown in a variety of studies to be beneficial for patients with CF. It has been shown to improve lung function, measured via the FEV1% predicted [16, 18]. Saimin et. al. have found this is a mild increase, on the order of 3-4% over the placebo group over the course of 3-6 months. Subjects with CF were randomized to receive either AZM or a placebo. Interestingly, this difference disappeared once the patients were taken off the medication [18]. This group went on to separately analyze data from both patients colonized with *P. aeruginosa*, as well as patients who have not been colonized with the organism. While differences in FEV1% predicted occur in both patients in both groups, the effect is much more pronounced in subjects who have been colonized with *P. aeruginosa* [17, 18]. Additionally, they found that CF patients treated with AZM are more likely to go longer without an acute lung exacerbation of their disease, a result that was consistent over 2 trials performed by this group [18, 19]. Additionally, AZM increases the time to a first exacerbation in both patients colonized with *P. aeruginosa*, as well as patients who have not been colonized with *P. aeruginosa* [17, 18].

Equi et. al. utilized a cross-over design with both AZM and a placebo, and found that the treatment group had a slight but significant increase in FEV1 % predicted on the order of 10% [16]. They also found that differences in FEV1% predicted declined when patients were taken off of the medication. Subjects who were receiving AZM were additionally less likely to be taking other oral antibiotics to control their symptoms, although they did not find significant differences in hospitalization rates between the two groups [16].

Finally, Wolter et. al., in addition to finding similar results as the other groups with regard to lung function, also found that AZM treated patients were significantly less likely to receive IV antibiotics. They also investigated C-reactive protein levels, a marker of systemic inflammation in the blood of these patients. They found that patients treated with AZM showed decreased C-reactive protein levels in their blood at the end of 3 months of treatment with AZM, as compared to patients that received a placebo. Finally they had patients complete quality of life questionnaires both before and after treatment. Patients reported less dyspnea and fatigue, as well as general improvements in their quality of life [20].

As one might expect, long term treatment with AZM is not without repercussions in these patients. In patients with CF treated with AZM, there were significant increases in the amount of bacteria resistant to macrolides in one of the trials outlined above [17]. Specifically, the rates of macrolide resistant *S. aureus* increased from 28% to 37% over 6 months, while the rates of macrolide resistant *H. influenzae* increased from 1% to 8% [17]. Additionally, the collateral damage inflicted by long-term AZM exposure to pathogen susceptibility to other antimicrobials is unknown.

In summary, the studies investigating AZM have shown that patients receiving the drug have slight but significant improvements in lung function, most notably measured by FEV 1% predicted. Additional improvements were observed for number and time to an acute exacerbation of the disease, and general patient quality of life. Because of these investigations, the Cystic Fibrosis Foundation currently recommends chronic AZM therapy for patients over the age of 6 years who are colonized with *P. aeruginosa*, as a method to improve lung function [14]. A recent meta-analysis reviewed 8 different studies assessing the effect of AZM in CF. Combining the data resulted in the drug inducing an overall increase in FEV1% predicted [64]. This improvement was again more pronounced in patients who were colonized with *P. aeruginosa* [64]. They also showed that these patients were less likely to experience an acute exacerbation of the disease, as well as a decrease in hospitalizations [64]. While it considers

the potential benefit to be great, the CF Foundation considers the strength of the data to only be fair. Thus it is currently classified as grade “B”, and not as a gold-standard therapy [14]. Improvements in the medications that patients with CF take has lead to great improvements in the length of time that patients with CF live, although the average age still is in the mid 30’s [11]. The consensus is that AZM contributes to this success.

Others have also investigated the positive effects of AZM in other pulmonary disorders. Notably, Beigelman et. al. showed that in an experimental asthma model that mice treated with AZM displayed decreased influx of macrophages and neutrophils, as well as a decrease in the influx of eosinophils [65]. AZM treated mice also displayed fewer inflammatory cells around the airways in their lungs [65]. Others have shown that AZM decreases acute exacerbations and hospitalization in patients with COPD [66]. These findings suggest a role for AZM in a wide variety of inflammatory and fibrotic lung diseases, and further the importance of discovering the mechanism by which AZM improves symptoms.

E. Cell signaling and macrophage phenotype

The NF-κB signaling pathway

The NF-κB signaling cascade is an important pathway that leads to the up-regulation of many pro-inflammatory genes, and is a major transcription factor that controls inflammation. A schematic of the NF-κB signaling pathway can be seen in figure 1.2. Activation begins with stimulation from an external signal. When macrophages are exposed to Gram-negative bacteria, including *P. aeruginosa*, it is signaling through TLR4, which responds to binding to bacterial LPS. The I kappa kinase (IKK) complex consists of three subunits, α,β, and γ. The complex is next phosphorylated via TLR4 bound My88. Upon phosphorylation of this complex, the complex phosphorylates IκB. In its unphosphorylated form, IκB is bound to the p50 and p65 subunits of NF-κB in the cytoplasm, and prevents these subunits from translocating to the nucleus. Upon

phosphorylation, however, IκB is targeted for ubiquitination and destruction. With the loss of its chaperone, NF-κB translocates to the nucleus, and upregulates the expression of a wide variety of pro-inflammatory cytokines and other cellular mediators [6-8]. The activation of the NF-κB cascade is one of the two steps necessary for macrophages to be polarized to the M1 phenotype.

The interferon-γ STAT1 cascade

M1 macrophages additionally require signaling from IFNγ which has been produced from Th1 polarized T cells (Figure 1.3). IFNγ binding signals through the STAT1 signaling cascade. Briefly, IFNγ binds to both the type 1 IFNγr, and the type 2 IFNγr. These receptors are pre-associated with either Janus associated Kinase (JAK) 1 or 2. Upon IFNγ binding, these receptors oligomerize. This allows JAK1 and JAK2 to phosphorylate both of the IFNγRs. Phosphorylation of the IFNγRs creates binding sites on the IFNγR for STAT1. Upon the binding of STAT1 to the cytoplasmic portion of the IFNγR, it is then phosphorylated by JAK2. P-STAT1 then dimerizes, and is able to translocate to the nucleus, and binds to IFNγ associated sequences. This induces the expression of proteins associated with inflammation and the M1 macrophage phenotype [4, 5].

Crosstalk between the two signaling cascades

For a macrophage to be polarized to the classically activated phenotype, signaling from both of these pathways is necessary [67]. Stimulating macrophages with either IFNγ or LPS is insufficient to achieve classical activation. Likewise, if we stimulate cells with AZM alone, or with both IFNγ and AZM, we are unable to shift the polarization of the macrophages to the M2 phenotype. Both cytokine signaling, as well as signaling from LPS are necessary to achieve macrophage polarization [10]. It is reasonable to believe that these cells are wired to require signaling from both of these pathways to polarize a macrophage to an M1 phenotype in order to ensure that a strong inflammatory and destructive cell type is not needlessly activated. However, there are

increasing indications that the two pathways directly interact with each other, rather than macrophage polarization being an additive effect of the pathways (Figure 1.4).

Fong et. al. described a series of experiments suggesting a more direct interaction between the two pathways. Utilizing Cre-recombinase technology, they created mice that were deficient in IKKβ in either their airway epithelial tissue, or in their myeloid cells (including macrophages). They then infected the mice intranasally with group B streptococcus. As they expected, mice with IKKβ selectively knocked out of their lung epithelial cells displayed a decrease in inflammation, and increased proliferation of group B strep. More interestingly, however, was the data from the mice deficient in IKKβ in their myeloid cells. These mice actually had fewer bacteria in their lungs, indicating that they responded well to clear the infection. They also displayed increased serum levels of pro-inflammatory cytokines, as well as decreased arginase 1 mRNA in their spleens. The cells also showed increased iNOS protein expression [68]. The authors suggested that IKKβ decreased M1 polarization. It is, however, reasonable to assume that M2 polarization would also be increased. They next found that IKKβ deficient cells displayed increased amounts of phosphorylated STAT1, suggesting that activated IKKβ was inhibiting the activation of the IFNγ signaling cascade, and that this was the mechanism by which they saw an increase in M1 macrophage polarization in the IKKβ KO cells [68]. They suggest that the crosstalk between the two pathways may exist as a mechanism by which the body can prevent an overly-zealous M1 response to an infection, and prevent any damage that may result from such a strong polarization.

IL4rα chain and M2 macrophage signaling

Inactive macrophages are polarized to an M2 phenotype via signaling from interleukins 4 and 13 (IL4, IL13) produced by Th2 cells, mast cells, and basophils [69-73]. What is interesting about alternative macrophage polarization, however, is that both IL4 and IL13 share a common receptor chain for their cell signaling (Figure 1.5). IL4 binds when the IL4rα chain and the common γc

receptor chain dimerize, forming the type I receptor. The binding of IL13, on the other hand, causes the IL4rα chain and the IL13rα chain to dimerize, forming the type II receptor. IL4 can, however, also bind to the type II receptor as well as the type I receptor [71]. Once either cytokine binds to either the type I or type II receptor, it recruits JAK 1 to the intracellular portion of the receptor, and induces phosphorylation. This allows STAT6 to bind to the receptor and be phosphorylated. Once phosphorylated, STAT6 dimerizes, translocates to the nucleus, and induces gene expression for genes that are upregulated in the M2 phenotype [71]. In our work, we will take advantage of the commonality among IL4 and IL13 receptors, and employ an IL4rαKO mouse strain that lacks the ability to respond to either cytokine. In using these animals, we will investigate the impact of an absence of the M2 subtype upon the immune response to *P. aeruginosa* infection.

F. Overview of the dissertation

With AZM, we have a commonly used medication in CF, with an unknown mechanism of action. While we have previously shown that AZM is able to polarize macrophages to an alternatively activated phenotype, the mechanism by which this occurs is currently unknown. It has been shown that one potential mechanism is via inhibition of NF-κB activation, although it is important to note that this inhibition is markedly less than by corticosteroids [74]. There is also evidence that there is cross-talk in the signaling pathways between the NF-κB signaling cascade and the IFNγ signaling cascade. Specifically, it appears that IKK-β, a molecule in the NF-κB cascade that inhibits activation of NF-κB, is also able to inhibit phosphorylation and activation of STAT1. STAT1 is activated by IFNγ, and once activated, it translocates to the nucleus and up-regulates the production of classically activated macrophage makers. We show below that one method by which AZM may polarize macrophages to the alternatively activated phenotype is via increasing activation of IKK-β, without a resulting increase in NFκB activation.

We also are interested in what the role of increased M2 activation in the lungs of patients with CF may mean in the long term for these patients. The three major studies assessing AZM in CF have been conducted over a short time period (3-12 months) [16, 18, 20]. The long term effects of the medication are unknown. On first consideration, changing the polarization of macrophages towards a pro-fibrotic phenotype is counterintuitive. Indeed, there is data suggesting that in other fibrotic lung diseases a Th2 polarization leads to alternatively activated macrophages, and results in increased scarring and fibrosis [55]. Another possibility, however, is that by altering macrophage polarization away from the M1 phenotype and towards the M2 phenotype, AZM is able to blunt an overly zealous inflammatory response. By doing so, there will be less damage to the lung parenchyma and peribronchiolar tissues, and a resultant decrease in scarring and fibrosis in the lungs of these patients. This possibility is also consistent with data showing that AZM treatment results in a decrease in acute exacerbations of CF, as well as a decline in the amount of courses of intravenous antibiotics that patients taking AZM experience [18, 20].

We hypothesize that AZM polarizes macrophages to an alternatively activated phenotype via IKKβ dependent mechanisms. We also hypothesize that by increasing M2 activation and decreasing M1 activation, AZM will improve the response of mice and humans to pulmonary infections and CF. This will be investigated through a variety of *in vitro, in vivo*, and human based studies.

In this dissertation, I will utilize a combination of cell culture, *in vivo* experiments with mice, and human clinical research to test the mechanism and importance of AZM dependent macrophage polarization in inflammatory lung diseases. I will describe how AZM polarized macrophages alter the production of fibrotic markers in a co-culture system of macrophages and fibroblasts. Alternatively activated macrophages produce the precursors to fibrotic proteins, and we hypothesized that macrophages polarized by AZM would increase the production of fibrotic proteins in the co-culture system [2]. At first thought, increasing the amount of a pro-fibrotic macrophage phenotype in a fibrotic lung

disease such as CF seems counterproductive. Indeed, if a Th2 polarization in the lungs is associated with a decline in outcomes in patients with CF, it would be reasonable to suggest that a shift to an M2 phenotype would be associated with a decline in outcomes in these patients [32]. A greater understanding of the effector functions of AZM polarized macrophages will allow us to understand whether the drug is polarizing macrophages to a novel phenotype, which may function in a manner different than a traditional alternatively activated macrophage.

Second, I will describe a potential mechanism by which AZM is able to alter the polarization of macrophages, towards an M2-like phenotype. The manner by which macrolide antibiotics are able to polarize to an alternatively activated-like phenotype is currently unknown. A greater understanding of this could provide future targets for medications that provide the immunomodulatory effects of macrolides, without the need to place patients on antibiotics chronically. I will additionally describe the role of M2 macrophages in the context of acute infections with PA, and whether AZM is able to polarize macrophages to the alternatively activated phenotype in a manner independent of IL4 and IL13 signaling, continuing the investigations into potential mechanisms by which AZM is able to alter macrophage polarization. We have access in our laboratory to a mouse strain that is deficient in the IL4rα chain. This receptor subchain is necessary for both IL4 and IL13 to properly signal [2]. Macrophages from mice deficient in the IL4rα chain display an impaired ability to be polarized to the alternatively activated phenotype. We have used these mice to first characterize the host response to *P. aeruginosa* infection with a lack of alternative macrophage activation by the cytokines. These results describe the importance of M2 macrophages in the response to intratracheal infection with *P. aeruginosa*. Then, by treating mice deficient in the IL4rα chain with AZM, as well as conducting *ex vivo* experiments on the cells collected from these mice, we were able to assess whether the ability of AZM to polarize macrophages is dependent on IL4 or IL13 signaling.

Finally, I will describe a pilot human study that was conducted in conjunction with our translational team of investigators. We collected sputum samples from patients with CF, isolated mRNA, and performed quantitative real-time PCR on a variety of M1 and M2 proteins, as well as inflammatory and fibrotic markers. We then correlated these gene markers to the clinical parameters of the patients. We additionally performed principal component analysis as a data reduction method to assess which gene markers are correlated with each other. By doing this, we were able to place our subjects into subgroups that are high or low in the various components, and assess whether these patient groupings corresponded with certain clinical features. This allowed us to determine if differences in gene expression were associated with clinical outcomes or disease severity in subjects with CF. We hypothesized that increased markers of M2 activation would be associated with AZM use and declines in lung function in these subjects. An increased understanding of macrophage associated gene expression in subjects with CF will lead to clinical validation of our molecular and animal data, to provide a basis for future research in therapeutic target discovery.

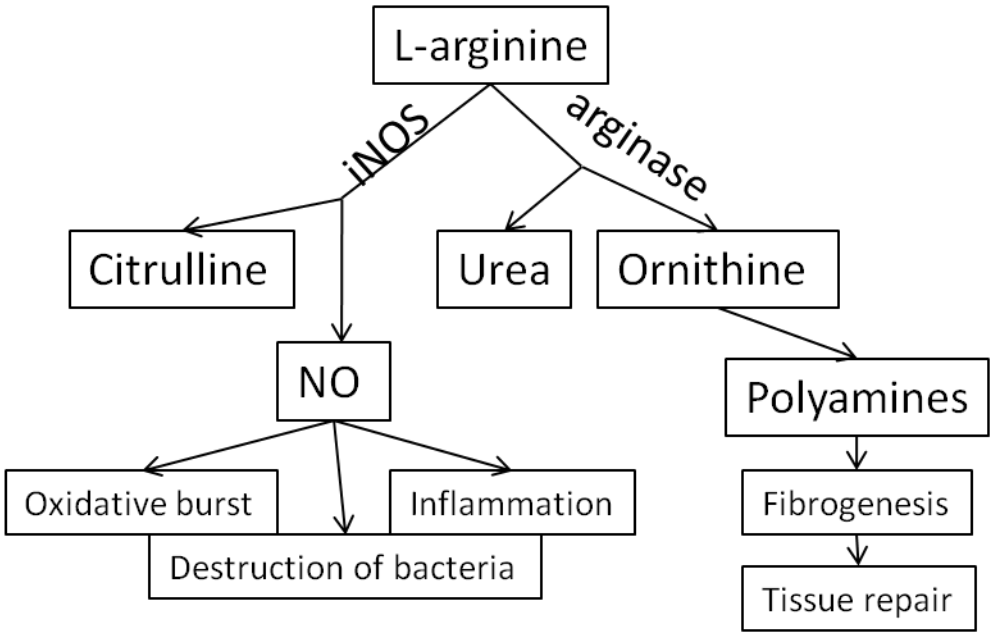

Figure 1.1. Overview of arginine metabolism with macrophage polarization. M1 macrophages upregulate iNOS, leading to the conversion of arginine to citrulline and nitric oxide. The produced nitric oxide is part of an oxidative burst in macrophages, leading to destruction of internalized bacteria and localized inflammation. M2 macrophages upregulate arginase. Arginase competes with iNOS for arginine, and catalyzes arginine to urea and ornithine. Ornithine is a necessary component of polyamines, which are then converted into fibrotic molecules including collagen. Collagen production and incorporation into the extracellular matrix is essential for tissue repair and fibrogenesis. Adapted from [9, 10].

Cell Type	Stimulus	Function	Surface Markers	Functional markers	Cytokines produced
M1 (Classically Activated Macrophage)	IFNγ, LPS	Phagocytosis, destruction of intracellular pathogens	TLR4 CD80 CCR7	iNOS ROS	IL-1 IL-6 IL-12 IL-23 TNFα
M2a (Alternatively Activated Macrophage)	IL4, IL13	Tissue repair, encapsulation of parasites	MR CD23	Arginase I Polyamines IL1ra	IL-10
M2b (Type II Macrophage)	Immune Complexes, TLR signaling	Th2 activation, Immuno-regulation	Scavenger Receptor (SR) 1, SR2 CD86		IL-10 IL-1 IL-6 TNFα
M2c (Deactivated Macrophage)	IL-10	Matrix deposition, Tissue remodeling	MR CD14	Polyamines	IL-10 TGFβ

Table 1.1. Function and markers of different macrophage phenotypes. Listed are the macrophage phenotype, the stimulation necessary to polarize an inactive macrophage to that phenotype, the function of the cell, surface markers, functional markers, and the cytokines produced (adapted from [1-3]).

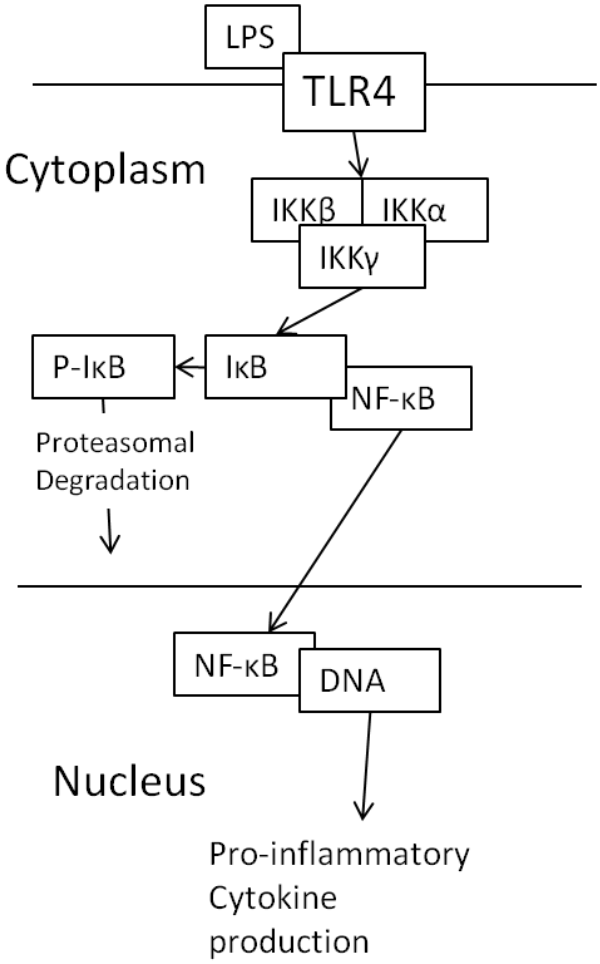

Figure 1.2. Activation of the NF-κB signaling cascade. LPS binds to TLR4, eventually leading to activation of the IKK complex. Upon activation of the IKK complex, it phosphorylates IκB, leading to the destruction of IκB. IκB had been bound to NF-κB, preventing it from translocating to the nucleus of the cell. When NFκB translocates to the nucleus, it binds to DNA leading to the transcription of genes associated with inflammation. Adapted from [6-8]

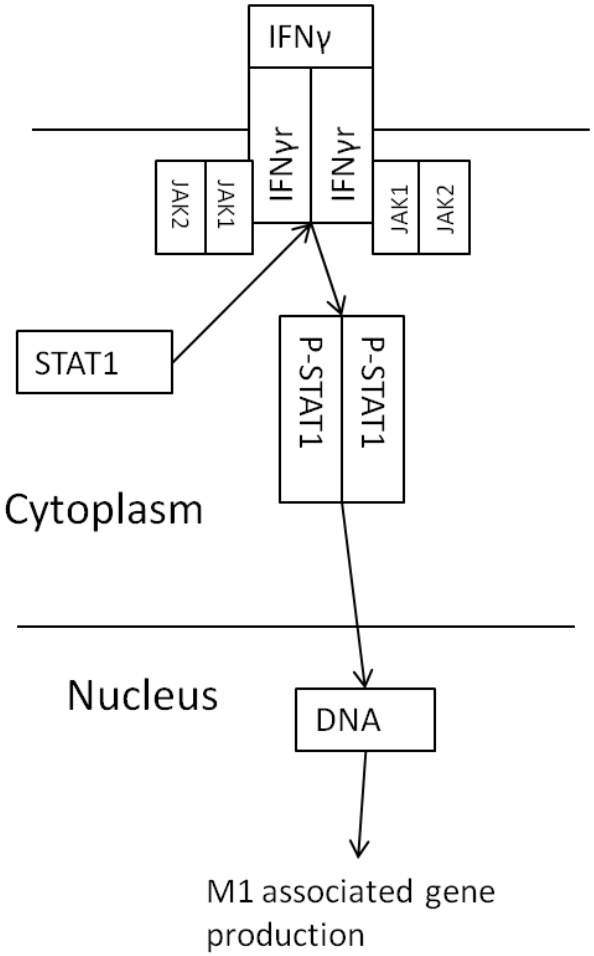

Figure 1.3. Activation of the IFNγ-STAT1 cascade. IFNγ binds to the IFNγr, leading to the recruitment of JAK1 and JAK2 to the receptor. The binding of these two molecules allows STAT1 to bind to the receptor and become phosphorylated. P-STAT1 dimerizes and translocates to the nucleus, leading to the transcription of genes associated with M1 macrophage polarization. Adapted from [4, 5].

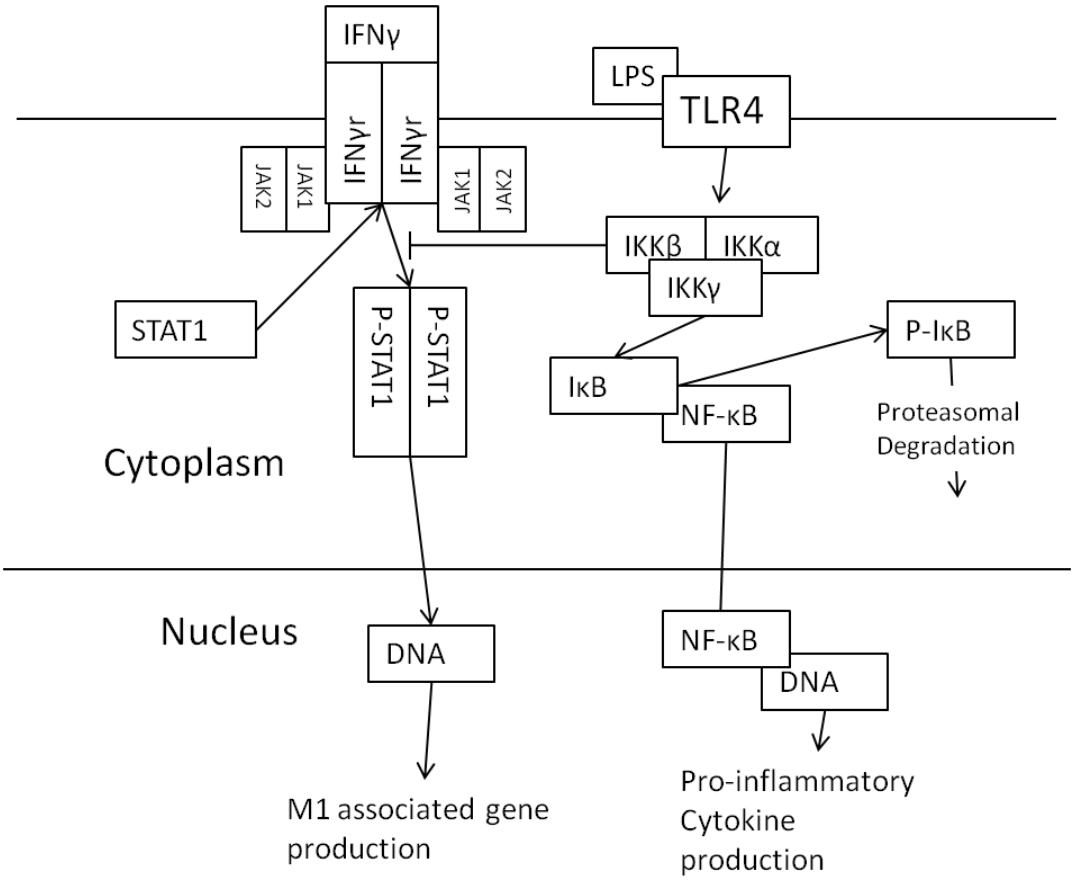

Figure 1.4. Crosstalk between the NF-κB and IFNγ-STAT1 cascade. Evidence exists that IKKβ prevents STAT1 from being phosphorylated. It has been hypothesized that this exists in part to eventually dampen a potent inflammatory response. We will address the effect the AZM has upon IKKβ activation, leading to the prevention of the IFNγ-STAT1 cascade.

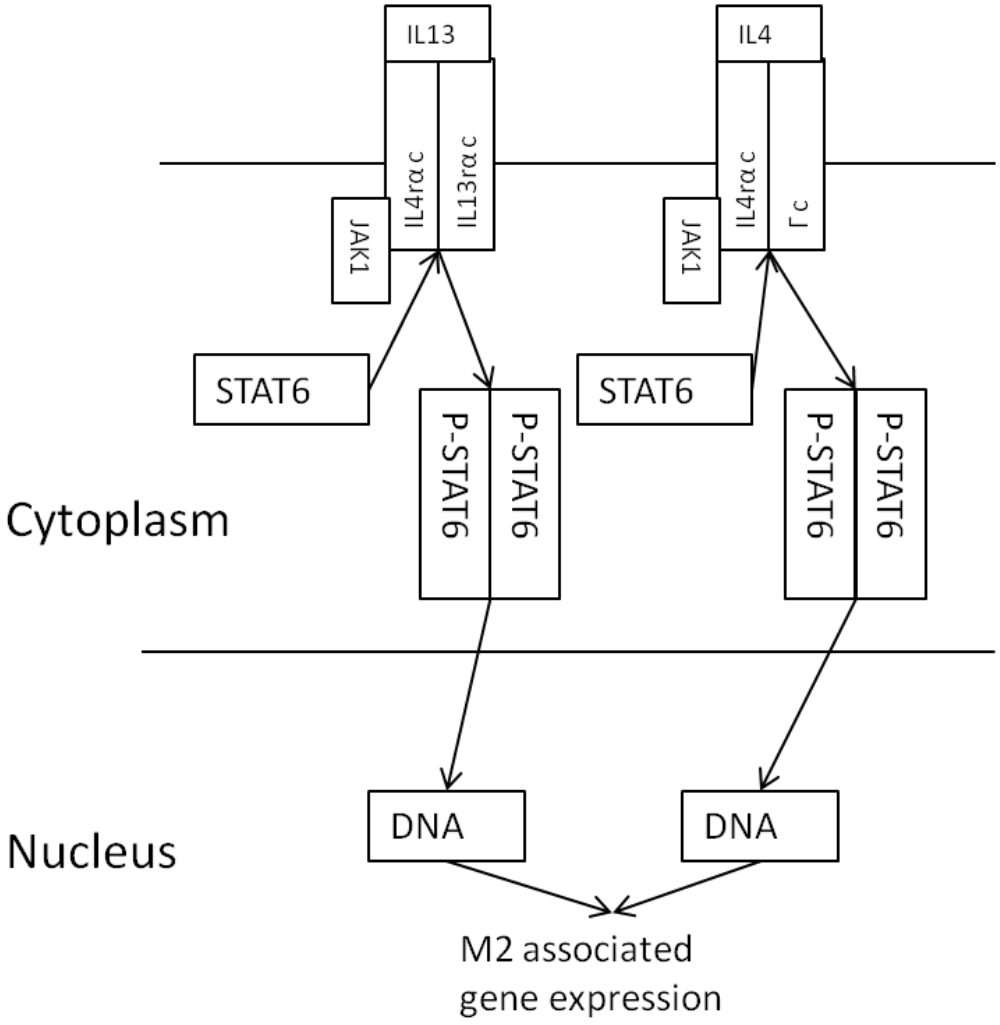

Figure 1.5. The IL4/IL13 signaling cascade. IL4 binds to dimers of the IL4rα chain and the common cytokine gamma chain. IL13 binds to dimers of the IL4rα chain and the IL13rα chain. JAK1is then recruited to the intracellular portion of the receptor. This leads to recruitment and phosphorylation of STAT6. P-STAT6 then dimerizes and translocates to the nucleus, leading to the transcription of genes associated with the M2 phenotype.

Chapter 2: Azithromycin alters interactions between macrophages and other cell types

A. Introduction

Chapter overview

To build upon previously generated data from our laboratory, we expanded our investigation of the impact of AZM exposure, this time in a series of in vitro experiments designed to test the impact the drug has upon macrophage function. While our previous work has described the ability of AZM to affect changes in macrophage polarization to an M2-like phenotype we still have little knowledge as to the functional abilities of cells treated with the drug [63, 75]. Because of the role that M2 cells play in orchestrating tissue remodeling and fibrosis in damaged lungs [2], we set out to investigate the interplay between AZM polarized macrophages and fibroblasts. This was done to determine more about the phenotype of AZM polarized macrophages, and the mechanisms by which macrophages interact with cells that produce fibrotic proteins. We hypothesized that AZM polarized macrophages would interact with fibroblasts in a co-culture system resulting in increased fibrogenesis.

Macrophage polarization: a brief overview

Macrophages are polarized to either the M1 or the M2 phenotype primarily by cytokines produced from T cells [1-3]. Polarization to the M1 phenotype requires signaling from the Th1 derived cytokine IFNγ, as well as a bacterial signal such as LPS. The M2 phenotype requires signaling from IL4 and IL13, which are produced primarily from Th2 polarized T cells [3]. It is important to note that this polarization is not terminal, unlike T cells. If an M1 macrophage is exposed to IL4/13, it can be shifted to the M2 phenotype, and vice versa.

Historically, when describing macrophages, it has been the classically activated, or M1 phenotype that has been described. M1 macrophages are phagocytic, and produce reactive oxygen species such as nitric oxide (NO). This

allows these cells to rapidly and effectively internalize and destroy infectious pathogens [35]. Macrophages are polarized to the M1 phenotype primarily from Th1 T cell produced IFNγ [76, 77]. M1 macrophages additionally initiate inflammation by producing inflammatory cytokines including TNFα, IL12, IL1 and IL6 that draw other inflammatory cell types to the site of an acute infection [34, 36]. Classically activated macrophages additionally upregulate adhesion molecules such as CCR7 that allow macrophages that have internalized bacteria to then relocate to the lymph nodes, allowing presentation to the rest of the immune system [3]. Both the influx of inflammatory cells, as well as the oxidative burst caused by M1 macrophages leads to tissue damage, which over time adversely effects lung function [37].

The host response to these bacteria is, in normal circumstances, under tight control and regulation. However, the damage and destruction caused by both pathogens and the immune system's response to that damage then requires considerable repair [78]. This repair is in part orchestrated by M2 macrophages [2]. These macrophages are both anti-inflammatory and profibrotic. The M2 macrophage pattern of gene expression increases during the regulatory phase of an acute infection in part to produce anti-inflammatory cytokines to prevent excessive damage [79]. M2 macrophages additionally produce the precursors to fibrotic proteins such as polyamines, leading to repair, fibrosis, and scarring [38]. These polyamines precursors are produced primarily from arginase dependent catabolism of arginine to ornithine [80]. M2 macrophages additionally upregulate expression of transforming growth factor beta (TGFβ). During fibrotic lung diseases, increased TGFβ signaling results in chemotaxis of macrophages and fibroblasts to the site of damage, secretion of growth factors, fibroblast proliferation, and production of extracellular matrix molecules by fibroblasts [69, 81].

Transforming growth factor beta

Transforming growth factor beta (TGFβ) exists in three different isoforms, TGFβ 1, 2, and 3. Among these, TGFβ 1 is the best characterized [81-83]. It is

thought that all three isoforms exert similar effects [83]. TGFβ is secreted in an inactive form from cells including macrophages, and is then attached to the extracellular matrix. TGFβ activation plays a vital role in the generation of the fibrotic molecules of the extracellular matrix, including fibronectin and collagen [84]. It can then be cleaved to its active form by a variety of enzymes, including elastases and metalloproteases [82]. Cells secrete large amounts of inactive TGFβ, to allow the body to allow quick activation of the protein and facilitate cell proliferation and fibrogenesis [82]. The secretion of inactive TGFβ, followed by its eventual activation, allows the rapid marshalling of a large amount of activated TGFβ in the face of a strong inflammatory response [82, 83].

Macrophage polarization by azithromycin

Our group has previously shown that AZM is able to polarize macrophages to a phenotype resembling that of alternatively activated cells. We have demonstrated this by assessing surface expression of markers of macrophage polarization, functional proteins produced by each type of cell, and the cytokine production profile [63]. What we do not know, however, is if AZM is polarizing macrophages to the M2 phenotype, or to a novel phenotype that contains unique characteristics. This possibility would explain in part why AZM benefits patients with CF. At first glance, one might assume that shifting macrophage gene expression to the pro-fibrotic M2 phenotype would be detrimental for these patients. More cells with the pro-fibrotic M2 phenotype could conceivably lead to increased scarring and fibrosis in the lungs of these patients. If this was the case, we would expect AZM treatment to worsen the functional decline for these patients. Instead, as noted in Chapter 1, it has been shown that AZM modestly benefits patients with CF [16-18, 20].

We posit that by shifting the balance of macrophage polarization during an acute flare away from the pro-inflammatory M1 phenotype and towards the anti-inflammatory, pro-fibrotic M2 phenotype which will inflict less damage. A decrease in the damage associated with acute infection would then require less repair, and a resultant decrease in remodeling and fibrosis formation. This is

especially true in the situation of CF, as the immune response in these patients is exaggerated [32, 45]. By decreasing the amount of pro-inflammatory M1 macrophages in the lungs of these patients, AZM may be altering the "set point" for an acute flare of the disease. That is, treatment with AZM may be preventing an overly zealous immune response from initially occurring, while allowing the immune system to still respond to the infection in a productive manner.

Data from our lab and others support this notion. In our mouse model of Pseudomonas infection, when AZM induces an M2 phenotype to predominate, neutrophil influx is blunted and peribronchiolar inflammation is lessened. We additionally found greater macrophage influx into the lungs of these mice. The cells that infiltrate into the lungs of these mice additionally produce fewer inflammatory cytokines and more anti-inflammatory cytokines [75]. Herbert et. al. have shown the importance of M2 macrophages in infections with *Schistosoma mansoni*. They found that infected $LysM^{cre}IL4r\alpha^{-/flox}$ mice, which lack IL4 and IL13 signaling on their macrophages, displayed 100% mortality, as compared to wild-type controls, in which upwards of 75% survived the infection. They determined that this increased mortality was due almost entirely to an overly zealous immune response, characterized by NOS2 overexpression and impaired egg expulsion [85]. Pesce et. al. found similar results with *Schistosoma mansoni*. Intriguingly, however, they also found similar results with mice lacking arginase 1 expression in their macrophages. They surmise that this is due to arginase 1 depleting arginine, leading to a blunting of the CD4+ T cell response. The addition of exogenous arginine similarly led to increased mortality, due primarily to the recovery of the CD4+ T cell response in these mice [86].

Finally, AZM may be polarizing macrophages to a novel phenotype that is anti-inflammatory, while not playing a role in fibrogenesis. In these experiments we set out to determine if the phenotype of AZM polarized macrophages leads to increased production of fibrotic proteins in a co-culture system with fibroblasts. An increase in fibrogenesis in this system would suggest that AZM-polarized macrophages and IL4/13-polarized macrophages function similarly. A greater

understanding of the interplay between AZM-treated macrophages and fibroblasts may lead to a greater understanding of the benefits of AZM treatment.

Production of fibrotic proteins and macrophages

Alternatively activated macrophages produce cytokines and other effector proteins that lead to increased production of fibrotic proteins, including TGFβ, fibronectin, and collagen in the lungs [3]. TGFβ signaling results in down-regulation of the molecules that degrade the extracellular matrix, including the matrix metalloproteases [81]. High expression of TGFβ has also been associated with a decline in lung function in patients with CF [87]. Fibronectin and collagen production is also upregulated, both in the macrophages as well as the other cells present in the lung parenchyma. This results from byproducts of arginase metabolism [80]. The enzyme arginase converts arginine to ornithine and urea. Ornithine is a precursor to polyamines, which are, in turn, precursors to matrix proteins including collagen [46, 88]. There is also considerable evidence suggesting that M2 macrophages themselves produce fibronectin [89]. This fibronectin, once produced by either macrophages or fibroblasts, is incorporated into the extracellular matrix, and provides strength and support to the remodeled tissue [89]. We can thus test for the presence of fibrotic proteins *in vitro* as we culture macrophages and fibroblasts together as a functional surrogate, and determine whether AZM treatment results in a macrophage that is pro-fibrotic. We hypothesized that AZM polarized macrophages would increase the production of fibronectin in a co-culture with fibroblasts. We aimed to determine the effect of AZM polarized macrophages on fibrogenesis by other cell types.

B. Detailed methods

Co-culture of macrophages and fibroblasts

The mouse cell lines NIH/3T3 and J774A.1 (ATCC, Manassas, VA) were used for all co-culture experiments. The NIH/3T3 line (ATCC #CRL-1568) is a fibroblast cell line originally obtained from embryonic cultures of NIH Swiss mice

[90]. The J774 (J774A.1, ATCC #TIB-67) cell line is an immortalized macrophage cell line derived from BALB/cN adult mice [91]. Cells were grown in RPMI 1640 media (Invitrogen, Carlsbad, CA), supplemented with 5% fetal calf serum and $2x10^{-5}$M 2-mercaptoethanol at 37°C and 5% CO_2. On day 0 of the experiment, NIH/3T3 cells were added to 6 well plates at a density of 2.5 X 10^5 cells/ml, and allowed to incubate overnight. The media was removed the next morning and replaced with 5 milliliters of new medium along with 5 X 10^4 J774 cells/1ml, and again allowed to incubate overnight. The next morning, cells were stimulated by adding interferon-γ (R&D systems, Minneapolis, MN) (IFNγ) (100ng/mL) and 2.5 X 10^5 *P. aeruginosa*, of the strain PA39018, a non-biofilm producing strain obtained from ATCC (Manassas, VA). To study the effects of the drug, designated wells additionally received 30μM AZM (Sigma Aldrich, St. Louis, MO) (AZM). Some experiments additionally utilized a blocking antibody to TGFβ at a concentration of 0.5μg/ml (R&D Systems, Minneapolis, MN). Cells were incubated and harvested after 0, 6, 12, 24, 48, and 72 hours. At these time points, cells were scraped and centrifuged, and 1mL of media was saved for TGFβ analysis. Cells were washed, enumerated with trypan blue staining to assess viability, and aliquots were taken for the arginase activity assay and qRT-PCR. Supernatants and cell lysates were frozen at -80°C for later analysis, including arginase activity and fibronectin quantification. Cell lysates were suspended in either 150μl of RIPA buffer with Roche Mini-tablet protease inhibitor cocktail, or in RNAlater (Applied Biosystems, Foster City, CA).

Quantification of arginase activity

Arginase activity was assessed via the protocols first described by Corraliza et. al. [92]. This reaction assesses the concentration of urea in the culture supernatant. Urea is a byproduct of the reaction converting arginine to ornithine, and directly correlates to the concentration of arginase present. Briefly, 12.5 μL of 10mM $MnCl_2$ in 50mM Tris HCl was added to 12.5 μL of cell lysates. The arginase enzyme was activated by incubating the samples at 55°C for 10 minutes. A 0.5M arginine solution was then added, and the samples were

incubated at 37°C. The reaction was terminated by the addition of 400 µL of an acid solution consisting of H_2SO_4, H_3PO_4, and water at a ratio of 1:3:7. Alpha-Isonitrosopropiophenone (9% w/v) dissolved in 100% ethanol was added, and the mixture was then heated at 95°C for 45 minutes. All chemicals were purchased from Sigma Aldrich (St. Louis, MO). Optical density was assessed utilizing an ELx808-I microplate reader and a 490 nM filter (Bio-Tek instruments, Winooski, VT). Readings were compared to a standard curve of known urea concentrations, and then were then normalized both to protein concentration and to cell counts. The values for arginase activity shown in this research are expressed in terms of units of arginase activity. One unit of arginase activity is responsible for the catalysis of 1 µmole of L-arginine to ornithine and urea per minute at a pH of 9.5 at 37°C.

Fibronectin protein quantification

Cell culture supernatants were analyzed and the fibronectin concentrations quantified by indirect ELISA. Samples were diluted in coating buffer and incubated at 4°C overnight for adherence to the ELISA plate. Wells were blocked, then incubated with an antibody specific to MMP-9 (Abcam, Cambridge, MA), followed by an anti-rabbit HRP conjugated secondary antibody. Wells were analyzed by OD reading at 450nm, using OptEIA detection reagents (BD,). Readings were compared to a standard curve using MMP-9 or fibronectin recombinant protein.

Surface marker expression

Cells were incubated with fluorescently-labeled monoclonal antibodies to both identify macrophages and detect surface receptors indicative of alternative activation. Antibodies specific for mouse mannose receptor (MR) (Serotec, Raleigh, NC), and CD11b (BD bioscience, San Jose, CA) were used. The cells were washed before and after antibody incubation with azide-containing buffer. Cells were analyzed by flow cytometry using a BD LSRII Flow Cytometer System (BD Biosciences, San Jose, CA) under the direction of a dedicated operator.

Fifty-thousand events per sample were routinely collected, and data was analyzed using FlowJo software package (Tree Star, Ashland, OR).

qRT-PCR

RNA was isolated using RNeasy mini kits (QIAGEN, Valencia, CA). Isolated RNA was quantified using a Nanodrop 2000 (Thermo Fisher Scientific, Wilmington, DE). Reverse transcription was performed on equal amounts of RNA utilizing Taqman Reverse Transcriptase Reagents (Applied Biosystems, Foster City, CA) according to manufacturer's protocols. Quantitative real-time PCR was initiated utilizing Taqman gene expression arrays for murine TGF-β1 and GAPDH using an ABI Prism 7000 (Applied Biosystems, Foster City, CA).

Preparation of *P. aeruginosa* impregnated agarose beads and mouse infection

To ensure a viable infection, *P. aeruginosa* of the biofilm producing strain M57-15 was impregnated in agarose beads. Bead preparation was an adaptation of previously described methods [93, 94]. In the absence of agarose beads, mice are able to quickly clear infections with *P. aeruginosa*. Impregnation in agarose beads allows for a more chronic, stable infection, and leads to greater cellular infiltration and weight loss in these animals [94]. In brief, *P. aeruginosa* was first grown to late log or early stationary phase in TSB. The organism was then added to a 2% agarose solution in PBS. This solution was then combined with warm mineral oil, and quickly cooled. The beads were then washed twice in solutions of deoxycholic acid to remove the mineral oil, followed by 6 washes with PBS. Beads were resuspended in PBS, and an aliquot was collected, homogenized, and plated on TSB agar plates to determine the number of viable bacteria in the beads.

Tissue processing and cell phenotyping

Lungs were minced in RPMI and digested in 50U/ml DNase (Sigma Aldrich, St. Louis, MO) and 1mg/ml collagenase A (Sigma Aldrich, St. Louis,

MO). After incubation for 1 hour, cells were pushed through a mesh screen. Red blood cells were lysed using a hypotonic salt solution. Cells were washed twice, enumerated, and transferred to 5ml round bottom polystyrene tubes for flow cytometry analysis. Aliquots of cells were collected and lysed in RIPA buffer to protect protein in the samples. These cells were then frozen at -80° C for later analysis. An additional aliquot was incubated at 37°C with 5% CO_2 for 2 hours with 50ng/ml phorbol 12-myristate 13-acetate (PMA) and 1µg/ml ionomycin, followed by 2 hours with 10 µg/ml brefeldin A to stimulate production of intracellular cytokines for flow cytometry analysis.

Cells were stained for flow cytometry for markers of general cell phenotype, as well as markers of macrophage phenotype and both inflammatory and anti-inflammatory cytokines. Three different flow cytometry panels were assessed for each type of mouse. The first panel for the C57bl/6 mice consisted of CD11b-PECy5 (Serotec, Raleigh, NC), a marker found on macrophages, GR1-PECy7, a marker of neutrophils, MR-PE, a marker of M2 macrophages (Serotec, Raleigh, NC), CD80-FITC, a marker of M1 macrophages, and biotinylated I-A[b] MHC II, a protein that is increased in expression with classical macrophage activation. Panel 2 consisted of CD11b-APC, CD11c-PECy7 (BD Bioscience, San Jose, CA), a marker of resident macrophages and dendritic cells, CD4-PECy5, a marker of CD4+ T-cells, GR1-FITC, and CD19-PE, a marker of B-cells. Panel 3 consisted of CD11b-PEcy5, CD11c-PECy7, TNFα-FITC, biotinylated TGFβ, and IL10-PE. Secondary staining was performed when appropriate utilizing a streptavadin conjugated to APC. All antibodies were purchased from BD bioscience (San Jose, CA), unless otherwise stated. Cells were analyzed with utilizing a FACSCaliber Flow Cytometer (BD Biosciences, San Jose, CA) with a dedicated operator. Greater than 50 thousand events per sample were routinely examined. Flow cytometry analysis was performed utilizing FlowJo (Treestar, Ashland, OR).

Statistical analysis

Results are reported as mean ± SD and compared using GraphPad Prism (GraphPad Software, La Jolla, CA). A repeated measures ANOVA with Tukey's multiple comparison test were utilized for time courses. For some data, T-tests were used to compare means between groups. Non-linear regression utilized the least squares method for fit. Differences in survival were assessed utilizing a log-rank (Mantel-Cox) test. Unless otherwise stated, significance was deemed to be a p value <0.05.

C. Results and discussion

Azithromycin increases markers of the M2 phenotype in the presence of *P. aeruginosa* when macrophages are co-cultured with fibroblasts

We first assessed markers of M2 activation in the co-culture system, to ensure that AZM was able to achieve this polarization in the presence of both a second cell type, as well as in the presence of a live *P. aeruginosa*, as opposed to bacterial LPS [63]. We measured arginase activity in the lysates from co-cultured cells over time stimulated with the live organism in the presence of IFNγ as described in the Methods section (Figure 2.1). We found that arginase activity was significantly higher in the cells treated with AZM, as compared to the cells that did not receive AZM after 24, 48, and 72 hours in culture. Arginase concentrations decreased as expected when the organism was introduced, as this shifts macrophages into a pro-inflammatory state. AZM exposure appeared to cause stabilization in production, so that by 24 hours the concentration of arginase rebounded to a significantly higher level than the control wells. We next assessed the impact of AZM upon the numbers of cells expressing both CD11b and MR. Cells positive for CD11b represent the macrophage cell line, as fibroblasts are negative for this surface protein, and MR is a representative protein with a trend towards upregulated expression during alternative polarization (Figure 2.2). In concordance with the increases observed in arginase activity, we found that cells treated with AZM displayed increased MR expression at 24, 48, and 72 hours. Both the arginase and mannose receptor data suggest that AZM is also able to polarize macrophages toward an M2-like

phenotype in the presence of viable *P.aeruginosa*, and the fibroblast cell line. This confirmation allowed us to move forward with the co-culture experiments confident that AZM is affecting the changes that we have observed previously in J774 cultures.

Azithromycin increases TGFβ activation

We first assessed the concentration of activated TGFβ in the lysates from our co-culture system (Figure. 2.3 A.). The assay that we utilized non-specifically measures activation of all 3 isoforms. Here we found that after 24 and 48 hours of culture with *P. aeruginosa* in the presence of IFNγ, there was a marked increase in the amount of active TGFβ found in the supernatants when AZM was present ($p<0.05$ and $p<0.01$, respectively). We then assessed the ratio of activated TGFβ to total TGFβ in the system (Figure. 2.3 B). We found that the ratio was higher in the cells that were treated with AZM as compared to cells that did not receive AZM at 24 hours ($p<0.05$). Intriguingly, in the cells that received IFN and LPS there were essentially no differences in the active TGFβ to total TGFβ ratio across the various timepoints. It was only in the cells treated with AZM that we observed a marked increase in TGFβ activation. We finally assessed TGFβ-1 gene expression via quantitative real-time PCR (Figure. 2.3 C) over time after *P. aeruginosa* stimulation. While we observed a marked up-regulation in TGFβ gene expression in both the IFN and IFN+AZM groups after 6 hours, there was then a down-regulation of TGFβ gene expression in both groups. There was less of a decrease in TGFβ-1 gene expression in the cells that received AZM, as compared to the cells that did not receive AZM, although neither individual timepoint differences nor differences of the entire curve were statistically significant.

This data suggests that AZM exerts a considerable effect on TGFβ activation in our co-culture system. We additionally observed trends towards increased TGFβ-1 gene expression in the co-culture system in cells treated with AZM. While the exact mechanism by which TGFβ activation in our co-culture system is increased is yet unknown, we have hypothesized that AZM may be

increasing expression of enzymes that activate TGFβ. The matrix metalloproteases (MMPs) are molecules that play an important role in extracellular matrix homeostasis by cleaving the proteins in the extracellular matrix facilitating matrix turnover. As part of the facilitation of this turnover, MMP-9 additionally plays a role in the cleavage and activation of matrix bound TGFβ, leading to new fibrogenesis [95]. Indeed, work done by others in our laboratory has shown that AZM up-regulates expression of MMP 9, and therefore we have hypothesized that this up-regulation is responsible, at least in part, for increased TGFβ activation. While others have shown that the production of inactive TGFβ is upregulated in M2 macrophages, we did not observe significant differences, only trends in gene expression of TGFβ-1. Three possibilities present themselves. First, we may not have had adequate power to detect significant differences. Second, we only assessed production of TGFβ-1, and did not assess gene expression of any other TGFβ isoforms. Had we assessed these other isoforms, we may have detected significant differences in gene expression with AZM treatment. Finally, AZM appears to not be increasing TGFβ gene expression in our macrophages. This would represent a difference between macrophages polarized to the M2 phenotype via IL4/13 and macrophages polarized to the M2 phenotype via AZM. In IL4/13 dependent M2 macrophage polarization, TGFβ production is upregulated [38].

Azithromycin results in increased fibronectin production in co-cultured macrophages and fibroblasts

We then assessed the concentration of the fibrotic protein fibronectin in the co-culture system (Figure 2.4). Fibronectin is secreted by macrophages and fibroblasts, and we would expect expression to be increased with the addition of AZM [81]. This is in fact what we observed. After culturing cells in the presence of IFNγ and *P. aeruginosa*, significantly higher fibronectin concentrations were measured in the cell lysates at 12 and 24 hours with the addition of AZM ($p<0.01$, 0.05, respectively). Separate controls utilizing only J774 and NIH/3T3 were additionally utilized to confirm that changes in fibronectin expression was due to

effects between the two cell types, instead of AZM directly causing fibrogenesis (Figure 2.4 B., C.). This suggests that macrophages polarized to the M2 phenotype via AZM lead to increased fibronectin production, both from the macrophages and the fibroblasts in the co-culture system. We surmise that this occurs for two reasons. First, we believe that AZM stimulated macrophages are increasing their production of inactive TGFβ. This is confirmed by our qRT-PCR data showing that at our later timepoints there is more TGFβ-1 mRNA in conditions treated with AZM. Others have found similar findings with different co-culture systems [54]. Second, we believe that the AZM treated macrophages are additionally upregulating metalloproteases including MMP, leading to increased activation of the inactive TGFβ in the extracellular matrix. The combination of increased TGFβ production and increased activation of the TGFβ that is produced is responsible for increased fibrogenesis by the fibroblasts in the co-culture system.

The increase in fibronectin concentration that we found suggests that AZM polarized macrophages function in a manner similar to M2 macrophages. We have previously shown that AZM polarized macrophages display surface markers and functional proteins consistent with the M2 phenotype [63]. Here we demonstrate that AZM polarized macrophages exert a similar effect on fibroblasts and fibrogenesis as has been reported by others [55, 96]. This further supports the notion that AZM polarized macrophages function in a similar manner to that of M2 cells, rather than a novel phenotype.

Blockade of TGFβ activity eliminates azithromycin dependent fibronectin expression in co-cultured macrophages and fibroblasts.

We finally repeated these experiments additionally utilizing a blocking antibody to TGFβ. Addition of the blocking antibody eliminated the differences in fibronectin concentrations in the cell lysates between conditions treated with AZM and those that did not receive AZM (Figure 2.5). This further mechanistically narrows the mechanism by which AZM treatment of macrophages results in increased fibrogenesis. It appears that increased activation of macrophage-

derived TGFβ is responsible for the increases in fibroblast derived fibrogenesis in the co-culture system.

Azithromycin results in increased survival in C57bl/6 mice infected with *P. aeruginosa*

We next assessed the role of AZM in C57bl/6 mice infected with *P. aeruginosa*. We wanted to assess the importance of this AZM dependent macrophage polarization in the context of a complete immune response, to further the work done in our *in vitro* system. We examined the effect of AZM on weight loss, survival, and bacterial colony counts in our C57bl/6 mice that were treated with AZM. We first assessed weight loss between mice that did or did not receive AZM (figure Figure 2.6 A.). Infected mice lost weight consistently over the first 3 days after infection, after which time weight was regained over the remainder of the study period. Statistically significant weight loss was noted in both infected groups of mice as compared to a sham-infection control group on days 1 through 3. No statistically significant difference was observed as a result of AZM treatment between groups of infected animals, although the mice treated with AZM displayed a non-significant trend of gaining weight back more quickly around day 7 post-infection. We then assessed differences in survival for animals infected with *P. aeruginosa* incorporated into agarose beads that did or did not receive AZM (Figure 2.6 B.). This data represents pooled data from multiple iterations of our infections. We found that mice treated with AZM had a significantly higher rate of survival compared to mice that did not receive the drug ($p=0.0195$). Only a small amount of our AZM treated animals died or had to be sacrificed early in accordance with our protocol. In animals that did not receive AZM, however, we observed a death rate approaching 50%. Finally, we assessed the number of bacteria present in the lungs of these animals (Figure 2.6 C.). Importantly, we found no differences in the number of bacteria in the lungs of the mice between the two groups. The bacterial burden, in fact, did not differ at any timepoint examined during any experiment performed, suggesting that AZM does not exert an effect on bacterial clearance in this infection model.

Azithromycin increases monocyte influx and decreases neutrophils influx

We then assessed the of the characteristics of cellular influx in both the alveolar space (lavages) and lung digest samples in mice infected with *P. aeruginosa* incorporated into agarose beads, to determine if AZM treatment had an effect. In the lung digests, we found a trend towards an increase in the number of cells present in the lungs of animals treated with AZM at day 14 of the experiment (p=0.067) (figure 2.7 A.) [75]. Expression of the protein CD11b was evaluated as a marker of monocytes that were elicited into the lungs post-infection. The marker is highly expressed on infiltrating macrophages. We found significantly more CD11b+ cells in the lung lavages on day 7 post-infection (p=0.006), indicating an increase in the number of infiltrating monocytes present in the lungs of these mice (figure 2.7 B.). Finally, we found that AZM treatment resulted in decreases in the numbers of neutrophils present in the lungs of these animals, both in the lung digest at day 7 (p=0.002) (figure 2.7 A.) and a trend towards a decrease in the numbers of neutrophils present in the lung lavage samples. The number of $CD4^+$ T cells in the lung parenchyma increased similarly through day 7, but by day 14 there was a significantly higher number of $CD4^+$ T cells in the mice treated with AZM (p<0.001). Similarly, the number of $CD4^+$ T cells that infiltrated the alveolar space was higher in mice treated with AZM on day 7 post-infection (p=0.004). This data shows that AZM appears to be altering the types of cellular influx present in the lungs of these mice.

Azithromycin shifts macrophage polarization in the lungs to the M2 phenotype

Because $CD11b^+$ cells displayed differences in migration characteristics with AZM exposure, we analyzed the activation characteristics of these cells. (Figure 2.8 A.) [75]. When examining the surface protein expression of cells that were CD11b+GR1- (monocytes), MR expression was consistently increased in the AZM treatment group on day 7 post-infection (p=0.003). Conversely, expression of the classical activation marker CD80 was decreased in the cells in the lung digest in mice receiving AZM (p=0.002). Other surface receptors

including CD23, CCR7, and MHC II were up-regulated post-infection on $CD11b^{+}Gr\text{-}1^{-}$ cells in a similar manner between the treatment groups. We additionally observed increased arginase expression in the mice that received AZM on day 7 of the experiment ($p<0.001$) (Figure 2.8 B.). This data further confirms the findings that we have previously observed *in vitro* concerning the ability of AZM to polarize macrophages to an alternative-like phenotype.

Azithromycin alters the influx of inflammatory cells to the lungs of C57bl/6 mice

Patients with chronic inflammatory lung conditions who are infected with *P. aeruginosa* are susceptible to the development of inflammation and fibrosis surrounding the small airways. To determine the extent to which AZM affected the damage to the lung parenchyma, histology sections were prepared from lungs isolated at each timepoint. Evaluation using H&E staining revealed inflammatory changes in both AZM-treated and -untreated groups at days 3 and 7 post-infection. Day 7 sections from AZM-treated animals were suggestive however of a decreased amount of interstitial inflammation surrounding diseased bronchioles (Fig. 2.9). In addition, on day 7 post-infection a systematic examination of the sections showed that inflammatory cells surrounding bronchioles mainly consisted of monocytic cells in mice that received AZM, as opposed to the neutrophil-dominated infiltrates in the control group (Figure 2.9). This finding corresponds to the flow cytometry data presented, and in addition confirms that a majority of the $CD11b^{+}GR1^{+}$ cells induced by AZM treatment were macrophages.

D. Conclusions

General conclusions

Here we present data showing that AZM increases arginase activity and MR expression on macrophages when co-cultured with fibroblasts and stimulated with live *P. aeruginosa*. While we expected to observe these changes based on our previous data, this work proves that this polarization occurs in a similar

manner when using either LPS or live bacteria. We further observed significant increases in fibronectin levels in the co-culture system in cells that were treated with AZM. The increases in TGFβ activation we observed, as well as the trend towards increases in TGFβ-1 gene expression suggest that AZM polarized macrophages result in increased fibrogenesis by fibroblasts in the co-culture system. As part of this work, we have also shown that AZM additionally upregulates proteins that activate TGFβ, including MMP-9. We hypothesize that the increase in TGFβ that we observe is due at least in part to upregulation of MMP9 by macrophages. We believe that this upregulation then results in increased activation of TGFβ, leading to increases in fibrogenesis from the fibroblasts in the co-culture system. Other work in our laboratory has also assessed MMP9 expression in the co-culture system with the addition of the TGFβ blocking antibody. As expected, the addition of the TGFβ blocking antibody exerted no effect on MMP9 expression, showing that the effects of TGFβ in the system are focused on fibrogenesis. This data will be presented in a future graduate dissertation. We cannot, however, eliminate the possibility that AZM may be altering other activators of TGFβ, including plasmin, cathepsin D, or calpain [83].

We further found that AZM exerted considerable effects on macrophage polarization and survival in our C57bl/6 mouse infection model. We found that on day 7 of the infection there was a marked shift in macrophage polarization towards the M2 phenotype in mice treated with AZM, and that mice treated with AZM were significantly less likely to die from their *P. aeruginosa* pneumonia. This shows the significance of macrophage polarization in the response to pulmonary *P. aeruginosa* infections. We hypothesize that this improvement is due to a blunting of the initial potent inflammatory response that occurs in the context of infection with *P. aeruginosa*.

Limitations

The system that we utilized is, by its very nature limited. Our co-culture system was designed to approximate the processes that occur in the lungs

during an acute infection. Extrapolations are difficult to make to *in vivo* systems, as well as to project the clinical relevance of the findings to apply to human therapies. With this limitation in mind, however, we still believe that there are considerable comparisons that can be made between the two systems.

The utilization of live bacteria in some of these experiments also complicates the data. The number of bacteria present in our wells greatly increases over the course of the experiment. At the later timepoints the number of bacteria overwhelms the cells in the culture, leading to widescale death of cells in the system. This may be influencing the results that we see at our later timepoints. Importantly however, the presence of AZM did not alter the growth of the bacteria or the rate of cell death between groups.

In our *in vivo* experiments, we additionally were unable to collect any data from mice who died or were sacrificed according to protocol. The absence of these animals may be skewing the data that we collect. That is, we are unable to determine the phenotype and extent of infiltrating cells into the lungs of the animals that have died. This may result in us observing differences that were not there, or missing significant differences between the two treatment groups.

In chapters three and four we will further examine the importance of AZM dependent M2 polarization *in vivo*. We will examine the importance of M2 macrophage polarization with mice with *P. aeruginosa* pneumonia, as well as in humans with CF.

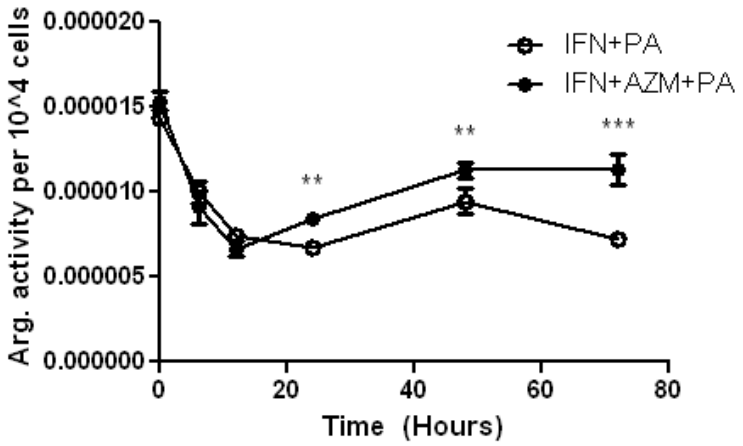

Figure 2.1. Arginase activity in co-culture treated with 30 μM AZM and *P. aeruginosa*. NIH/3T3 were cultured overnight in RPMI + 5% FCS at 37°C with 5% CO_2. The next morning J774 cells were added, and the cells were incubated together overnight. The next morning and IFNγ, *P. aeruginosa* (PA), and AZM were added. Cells were harvested at 0, 6, 12, 24, and 48 hours, and cell lysates were utilized for the arginase activity. Graph shows arginase activity, a measurement of arginase concentrations, in the lysates preparations. Data shows mean ±SD, with each sample run in triplicate. Data were analyzed by two-way ANOVA with a Bonferroni's post-test. ** indicates a p value of < 0.01. *** indicates a p value of < 0.001. Data representative of three replicates.

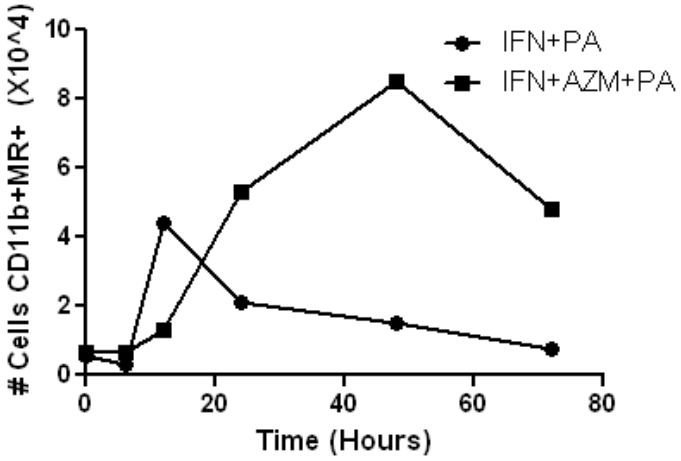

Figure 2.2. Alternatively activated macrophages in a co-culture system treated with AZM and *P. aeruginosa*. NIH/3T3 were cultured overnight in RPMI +5 % FCS at 37°C with 5% CO_2. The next morning J774 cells were added, and the cells were incubated together overnight. The next morning IFNγ, *P. aeruginosa* (PA), and AZM were added. Cells were harvested at 0, 6, 12, 24, 48, and 72 hours, and cell lysates were utilized for the arginase activity. Macrophages were analyzed by flow cytometry for surface expression of mannose receptor. Data were analyzed by two-way ANOVA with a Bonferroni's post-test. ** indicates a p value of < 0.01. Data representative of two replicates.

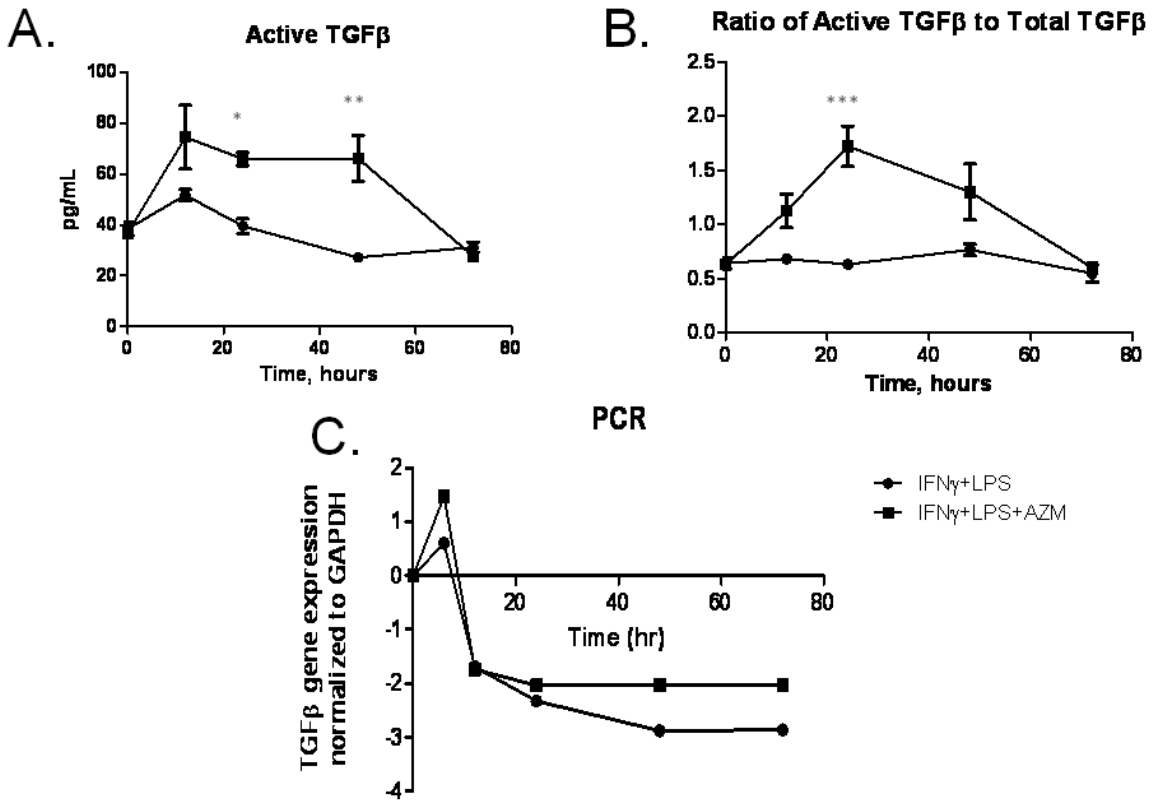

Figure 2.3. TGFβ expression in a co-culture system. NIH/3T3 were cultured overnight in RPMI + 5 % FCS at 37°C with 5% CO_2. The next morning J774 cells were added, and the cells were incubated together overnight. The next morning and IFNγ, LPS, and AZM were added. Cells were harvested at 0, 6, 12, 24, and 48 hours, and cell lysates were collected. Panel (A) Activated TGF-β concentrations in the culture supernatant as measured by $TGF\beta_1$ E_{max} ImmunoAssay System. (B) Ratios of active over total TGF-β were normalized to time zero. (C) PCR analysis of TGF-β mRNA was normalized to GAPDH expression in each sample, and then normalized to expression of TGF-β at time zero. Data were significant to a p value < 0.05. All data were analyzed with two-way ANOVA with Bonferroni's post-test. * equals p value < 0.05, ** p value < 0.01, *** p value < 0.001. Data representative of three replicates.

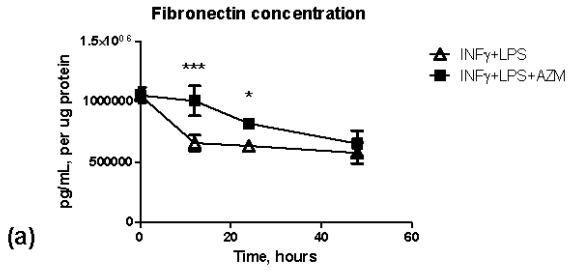

(a)

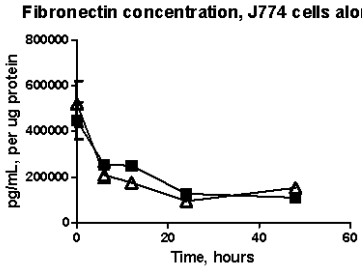

(b)

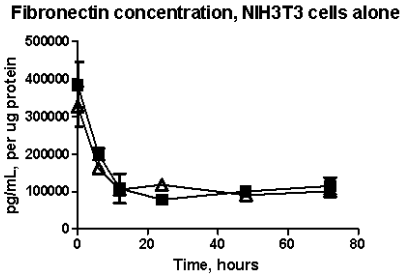

(c)

Figure 2.4. Fibronectin expression in the co-culture system. (A) NIH/3T3 were cultured overnight in RPMI + 5% FCS at 37°C with 5% CO_2. The next morning J774 cells were added, and the cells were incubated together overnight. The next morning and lFNγ, *P. aeruginosa* (PA), and AZM were added. Cells were harvested at 0, 6, 12, 24, and 48 hours, and cell lysates were utilized for the arginase activity. (B) Fibronectin concentrations with just J774 cells, (C) Fibronectin concentrations with just NIH/3T3 cells. Fibronectin concentration in the cell lysate was determined by indirect ELISA. Data represents mean ± SD. *** equals a p value <0.001 while * equals a p value < 0.05. Results were normalized to µg protein in each sample. Data representative of three replicates.

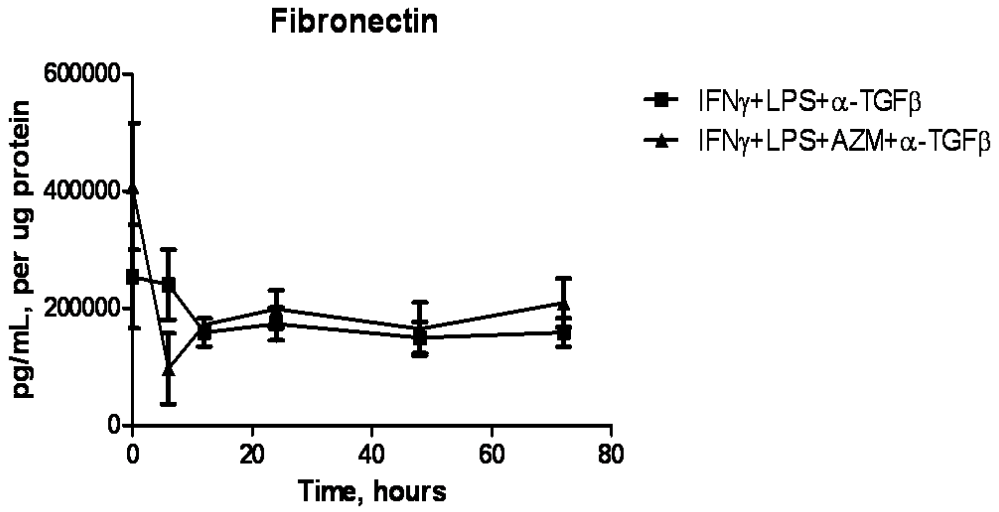

Figure 2.5. Fibronectin expression in the co-culture system in the presence of a TGFβ blocking antibody. NIH/3T3 were cultured overnight in RPMI + 5% FCS at 37°C with 5% CO_2. The next morning J774 cells were added, and the cells were incubated together overnight. The next morning and IFNγ, *P. aeruginosa* (PA), AZM, and a blocking antibody to activated TGFβ were added at a concentration of 5μg/ml. Cells were harvested at 0, 6, 12, 24, and 48 hours, and cell lysates were utilized for the arginase activity. Fibronectin concentration in the cell lysate was determined by indirect ELISA. Results were normalized to μg protein in each sample. Data representative of three replicates.

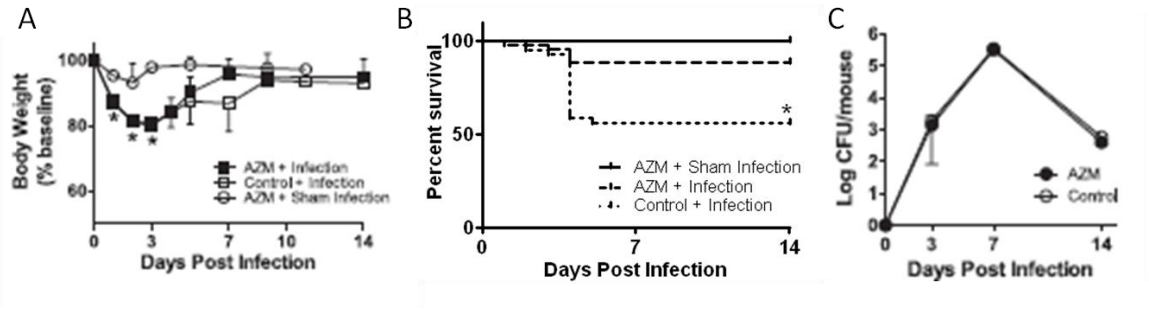

Figure 2.6. Weight loss, survival, and infection burden over time in C57bl/6 mice. Mice were infected with *P. aeruginosa* impregnated agarose beads, and received either 3.2 mg AZM daily or vehicle control beginning 4 days before infection. One group of mice additionally received AZM, but only a sham infection. 4 mice were sacrificed at each timepoint (A) percent weight loss from baseline. (B) Percent survival from multiple pooled replicates of the experiment. (C) Number of bacteria present in the lungs of these mice. Significant differences ($p<0.05$) are indicated (*), and are representative of the results for multiple experiments.

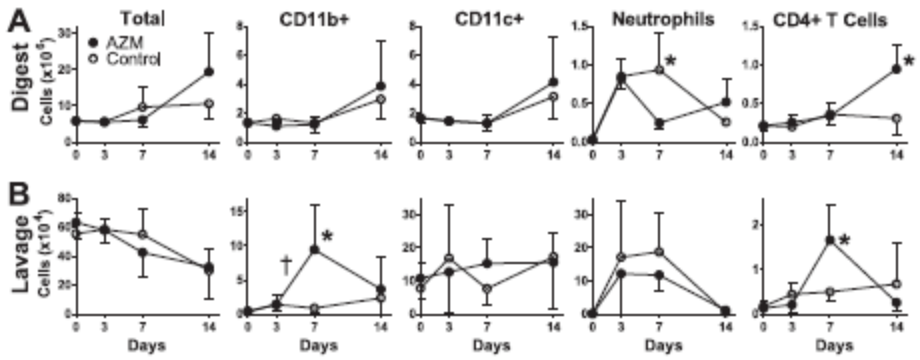

Figure 2.7. Immune cell infiltration into lungs of *P. aeruginosa* infected mice treated with AZM. Mice were infected with agarose beads containing between 10^5 and 10^6 *P. aeruginosa*. Immune cell subtypes were quantified by flow cytometry in the (A) lung digest or (B) lung lavage. Panels represent total cells, CD11b+ cells (infiltrating macrophages) (non-lymphocyte gate), CD11c+ cells (resident macrophages) (non-lymphocyte gate), neutrophils and infiltrating monocytes (CD11b-GR1+), and CD4+ T cells (lymphocyte gate). Mean values ± SD are depicted. Significant differences ($p<0.05$) are shown for differences between groups at the same time point (*), and between groups when all animals were taken into account across time points (†)

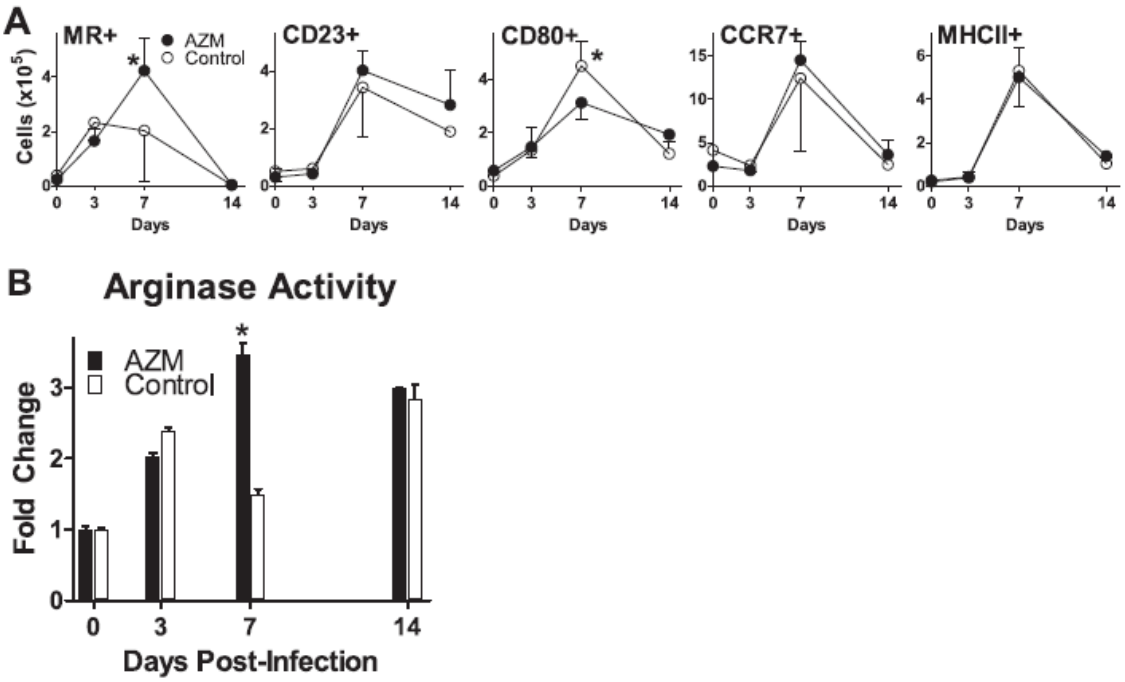

Figure 2.8. Characteristics of macrophage activation status in AZM treated C57bl/6 mice infected with *P. aeruginosa*. (A) Surface staining via flow cytometry of markers of M2 activation (MR, CD23), or M1 activation (CD80, CCR7, and MHC II) on cells that were CD11b+. (B) Fold increase from baseline in arginase activity. Samples from each mouse group were pooled and run in triplicate. Mean values ± SD are depicted, and samples were deemed statistically significant with a $p<0.05$ (*)

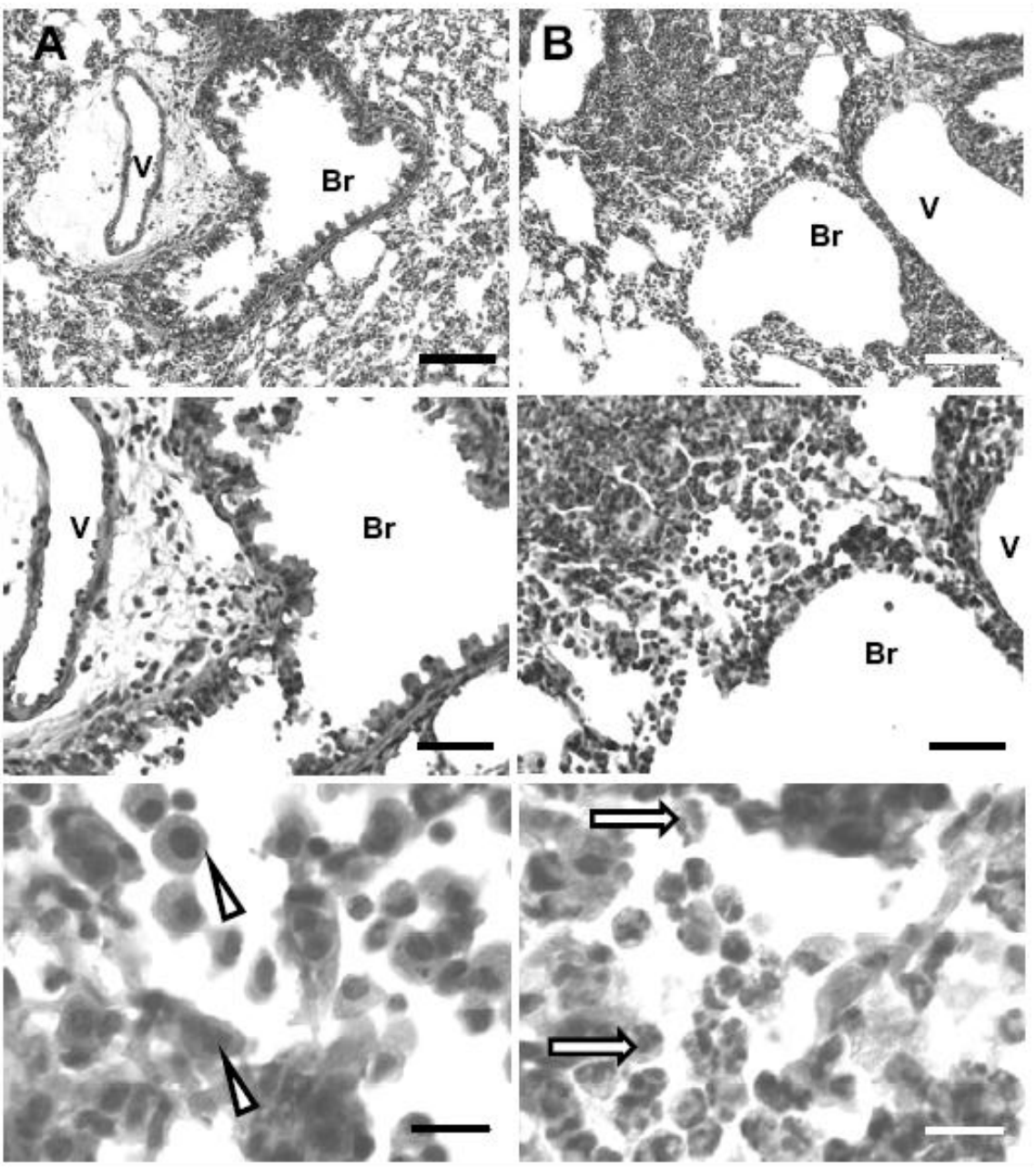

Figure 2.9. Lung sections from mice which are day 7 post *P. aeruginosa*. H & E stains of lung sections that received (A) AZM or (B) vehicle control. Magnification increases from top to bottom, with bars representing 50, 25, and 12.5 µm, respectively. Pictures represent a predominately monocytic cellular infiltration into the lung parenchyma in AZM-treated animals (triangular pointers), while in control mice the inflammatory response is dominated by neutrophils (arrows). Br=bronchiole, V=venule.

Chapter 3: Mechanistic investigations into the anti-inflammatory effects of azithromycin

A. Introduction

Chapter overview

We next investigated aspects of the mechanism by which AZM polarizes macrophages to the M2 phenotype, and the importance of this polarization in the host response to *P. aeruginosa* infection. The mechanism by which AZM affects the shift in macrophage polarization to an M2-like phenotype is as yet unknown. It has previously been shown that AZM decreases the activation of NF-κB signaling [74, 97]. NF-κB has been shown to play an important part in both the innate and adaptive immune system, leading to inflammation and cell death [7, 98]. Activation of NF-κB leads to the up-regulation of a wide variety of pro-inflammatory molecules including the cytokines IL-6, IL1-β, and TNFα; and enzymes including iNOS and COX-2 [7]. Some have hypothesized that by inhibiting activation of NF-κB, AZM decreases the net inflammatory response to pathogens in CF [74, 97]. It has been shown that through this mechanism of NF-κB inhibition, AZM decreases the production of pro-inflammatory cytokines [97]. Cheung et. al. utilized a cell line with a stably expressed reporter gene and found that the IC_{50} for AZM in the system was approximately 56μM [74]. Cigana et. al. observed that AZM exerted similar effects with DNA binding to NF-κB in CFTR deficient cell lines. They additionally found that AZM treated cells produce less TNFα [97]. While these hypotheses may help to explain the beneficial effects of AZM in patients with CF, it does not by itself explain a mechanism by which AZM is able to polarize macrophages away from the M1 phenotype, and towards the M2 phenotype. We hypothesized that AZM achieves this via inhibition of STAT1 through cross-talk from NF-κB signaling mediators.

To extend our cell culture experiments, we assessed the ability of AZM to alter macrophage phenotype in mice. Specifically, we were interested in assessing the ability of AZM to polarize macrophages to an alternatively

activated phenotype *in vivo*, and whether this polarization occurs independent of the traditional mechanisms necessary to achieve M2 polarization. As shown in Chapter 2, AZM can polarize macrophages to an alternatively activated phenotype in C57Bl/6 mice infected with *P. aeruginosa*. The drug alters the cellular influx into the lung parenchyma and alveolar space during acute infection to a more monocytic, and less neutrophilic profile, and controls the inflammatory response observed [75]. We were curious if we would see a similar effect in mice that lack the IL4rα chain, which are unable to polarize to an M2 phenotype via IL4 or IL13 signaling. Several groups (including our own studies) have demonstrated the impact that AZM exerts upon cytokine expression [37, 63, 99, 100]. However, due to data presented below in the first half of this chapter concerning AZM's effect on IKKβ activation, we believe that cell signaling mechanisms are altered such that the effects of the drug are independent of the downstream effects of cytokines. It would be reasonable to surmise that the ability of AZM to polarize macrophages is due to alterations in cytokine production, or to effects on T cells. However, we have shown *in vitro* that AZM exerts direct effects on macrophages, rather than on the milieu of cytokines in the lungs [63]. In the second half of this chapter, we will address the hypothesis that azithromcyin polarizes macrophages to an M2 phenotype independent of IL4rα function.

Cell signaling and macrophage polarization: A brief overview

Macrophages are polarized to one of the two traditional phenotypes via signaling from three distinct pathways. M1 activation requires signaling from both the IFNγ and TLR4 signaling cascades. IFNγ dependent signaling results in phosphorylation and dimerization of STAT1. These dimers then translocate to the nucleus of the cell, and induce inflammatory gene expression [4, 5]. In M1 activation, this signaling pathway synergizes with the NF-κB pathway, leading to the up-regulation of pro-inflammatory molecules. The NF-κB pathway begins with LPS binding to TLR4. This binding leads to phosphorylation of the IKK complex, including phosphorylation of IKKβ. Activation of IKKβ leads to the

phosphorylation, ubiquitination, and the destruction of IκB. The destruction of IκB, which sequesters NF-κB, then allows NF-κB to translocate to the nucleus of the cell. This then results in up-regulation of pro-inflammatory cytokines such as IL6, IL1β, and TNFα. Additionally, pro-inflammatory molecules including iNOS and COX-2 are up-regulated [6-8].

Alternative polarization utilizes a different signaling pathway for its activation. M2 polarization begins with the binding of either IL4 or IL13 to their respective receptors. Interestingly, both the IL4r and the IL13r utilize, in part, the same receptor subchain, the IL4rα chain. Activation of either the IL4r or the IL13r results in phosphoryaltion and dimerization of STAT6. Upon activation, STAT6 then translocates to the nucleus of the cell and up-regulates genes associated with anti-inflammatory processes and the M2 phenotype [69-73]. Many groups report being able to polarize macrophages to the M2 phenotype only by stimulating with either IL4 or IL13 [1, 34]. In our lab, we additionally utilize stimulation from LPS to polarize macrophages to the M2 phenotype. We use this method because we learned that AZM is unable to polarize macrophages to the M2 phenotype in inactive macrophages. Signaling from both IFNγ and LPS is required to be able to achieve this polarization to the M2 phenotype with AZM. This characteristic of AZM provides basis of support for our hypothesis that the mechanism of the drug's ability to polarize cells lies in its interference with these signaling cascades.

IL4rα chain KO mice

We utilized the mouse strain Balb/c-*Il4ra*^{tm1Sz}/J (IL4rαKO) for these experiments. These mice are on a Balb/c background, and lack the IL4rα chain on all cell types. They have been shown to display a decreased Th2 response, and have a markedly impaired Th2 polarization in response to infections with a wide variety of pathogens [101-103]. Most of the work performed with these mice has examined their ability to respond to pathogens that induce a robust Th2 response, most notably parasites. The IL4rαKO mice are less able to clear infections with the parasite *Brugia malayi*, an organism in which a strong Th2

response is necessary for clearance [102]. Similar responses have been shown in experiments utilizing the parasite *Nippostrongylus brasiliensis*, suggesting that IL4 and the IL4rα chain play an important role in the ability of the body to generate a robust Th2 response [101]. The role of IL4rα signaling has not been studied in the response to infection with extracellular bacteria.

B. Methods

Isolation and *ex vivo* stimulation of splenocytes from IL4rαKO mice

Mice were humanely sacrificed and spleens were collected in RPMI + 5% fetal calf serum (FCS) (Invitrogen, San Diego, CA). Spleens were homogenized by pushing them through a mesh screen. Following homogenization, red blood cells were lysed with a hypotonic lysis buffer consisting of 0.15M ammonium chloride, 10mM potassium bicarbonate, and 0.1mM EDTA (ACK). Cells were then washed twice with PBS and enumerated. Cells were allowed to adhere on T75 flasks overnight in RPMI + 5% FCS. The next morning, the media was discarded, and adherent cells were washed with PBS and scraped to enrich the population to primarily consist of macrophages.

Cells were cultured in 24 well plates at a concentration of $4x10^5$ cells per well in 2ml of RPMI + 5% FCS. Cells were then treated with IFNγ (20ng/ml), IL4 (10ng/ml), IL13 (10ng/ml), both IL4 and IL13, or both IFN and AZM (60μM) overnight at 37°C with 5% CO_2. The next morning 50ng/ml of LPS was added to each well. Cells were then cultured for 6 hours. Cells were scraped, washed with PBS, and lysed in RIPA buffer consisting of 50mM Tris-HCl, 150mM NaCl, 1% (v/v) triton X-100, 1% (w/v) sodium deoxycholate, 0.1% sodium dodecyl sulfate, and 4mM EDTA (Sigma Aldrich, St. Louis, MO). Protein concentrations were quantified utilizing the Pierce BCA reaction kit (Rockford, IL).

Stimulation of a macrophage cell line with cytokines

The mouse macrophage cell line J774A.1 (ATCC, Manassas, VA) was utilized for our cell culture experiments. Cells were plated in 6 well plates at a

concentration of $2.5x10^6$ cells/5 ml of RPMI + 5% FCS. Wells were treated with 20ng/ml IFN, 10ng/ml each of IL4 and IL13, or both 20ng/ml IFN and 60μM AZM to receive a robust polarization to the M2 phenotype. Some wells were additionally treated with the IKKβ inhibitor IKK-16 (Tocris Bioscience, St. Louis, MO). IKK-16 is a kinase inhibitor that prevents the phosphorylation and activation of IKKβ [104]. IKK-16 has also been shown to decrease TNF-α dependent upregulation of adhesion molecules, and to decrease LPS dependent TNF-α release in mice, showing that it exerts a significant effect on IKKβ signaling [104]. Cells were then incubated overnight at 37°C with 5% CO_2. The next morning 50ng/ml LPS was added to all wells, and the cells were incubated for 24 hours. Cells were scraped, washed with PBS, enumerated, and lysed in 0.1% (v/v) triton X-100. Protein concentrations were quantified utilizing the Pierce BCA reaction kit. An aliquot of the media supernatant was collected and frozen at -80°C for additional analysis.

Quantification of arginase activity

Arginase activity was assessed via the protocols first described by Corraliza et. al., and is reported here as a surrogate measurement to the amount of arginase present [92]. For detailed methods please refer to chapter two. In brief, samples were incubated with arginine, the reaction was terminated, and a detection reagent was added to the samples. One unit of arginase activity is responsible for the catalysis of 1 μmole of L-arginine to ornithine and urea at a pH of 9.5 at 37°C.

Quantification of Nitrite Concentration

Nitrite concentrations in cell culture supernatants were additionally obtained for some experiments. When produced from NOS2, nitric oxide (NO) is quickly degraded into nitrite and nitrate at roughly equivalent rates. These NO breakdown products are then relatively stable in the supernatants. Nitrite concentrations were obtained via the griess reaction [105]. In brief, a solution of 1% sulfanilamide in 5% phosphoric acid was mixed with a solution of 0.1% N-(1-

napthyl)-ethylenediamine dihydrochloride. The resulting solution was then mixed with an equivalent volume of cell culture supernatant. The samples were run in triplicate on a microplate reader at 490nM. Absorbance was compared to a standard curve of known nitrite concentration.

Preparation of *P. aeruginosa* impregnated agarose beads and mouse infection

To ensure a viable infection, *P. aeruginosa* of the biofilm producing strain M57-15 was impregnated in agarose beads. Bead preparation was an adaptation of previously described methods [93, 94]. In the absence of agarose beads, mice are able to quickly clear infections with *P. aeruginosa*. Impregnation in agarose beads allows for a more chronic, stable infection, and leads to greater cellular infiltration and weight loss in these animals [94]. In brief, *P. aeruginosa* was first grown to late log or early stationary phase in TSB. The organism was then added to a 2% agarose solution in PBS. This solution was then combined with warm mineral oil, and quickly cooled. The beads were then washed twice in solutions of deoxycholic acid to remove the mineral oil, followed by 6 washes with PBS. Beads were resuspended in PBS, and an aliquot was collected, homogenized, and plated on TSB agar plates to determine the number of viable bacteria in the beads. Considerable variability exists with the beads between infections, resulting in variability between infections.

Dosing and Infection of IL4rαKO mice

Azithromycin tablets (Pliva, Zagreb, Croatia) were triturated and suspended in 2% methylcellulose. Six to eight week old mice were housed in the DLAR facility at the Biopharmacy Building at the University of Kentucky under pathogen free conditions. The treatment group received 3.2mg (approximately 160mg/kg) of AZM daily via oral gavage, while the control group received only methylcellulose. This AZM dose is high in comparison to the doses of AZM that are used in humans, where doses in the range of 3-4 mg/kg/day are commonly utilized in these patients. This was done in order to increase the likelihood that

macrophages would be polarized to the M2 phenotype in these mice. Preliminary experiments *in vitro* have shown that this dose will shift the response toward an M2-like dominant phenotype in the lungs of these mice [63]. Thus, at this dose we were confident that intracellular concentrations of the drug would be adequate. Mice have metabolism rates that are many fold higher than found in humans, producing difficulties in interspecies scaling of drug dosing in such studies [106, 107]. AZM is primarily found intracellularly due to its partitioning characteristics, with extremely low serum concentrations [108], therefore equating serum concentrations in mice to those found in humans would mean little. Because this weakens our ability to extrapolate these results to predict clinical relevance, the importance of our translational studies (Chapter 4) is heightened. As an antibiotic, AZM functions by binding to the ribosome of bacteria, preventing bacterial synthesis. It is conceivable that AZM exerts beneficial effects in subjects with CF by altering protein synthesis of molecules involved in the degradation of IKKβ, or other molecules.

Mice were sedated and infected intratracheally with 100µl of PBS containing *P. aeruginosa* agarose beads. The goal was to target the mice with an infection of $2x10^5$ bacteria. Because of variability inherent in our preparation methods, and because we do not know the actual inoculum of the bead preparation until the day after infection, in these experiments mice received between $1.6x10^5$ and $1.2x10^6$ CFU of bacteria. After infection, mice were transferred to a BSL 2 room. Mice were weighed daily, and humanely sacrificed at various post-infection timepoints. Lung lavages were performed and first washes were collected. Subsequently, lungs were collected and the left lower lobe of the lung was fixed in formalin for later sectioning on a Shandon cryotome (Thermo Scientific, Waltham, MA). The remainder of the lung tissue was placed in RPMI + 5% FCS for additional processing. This study and all procedures were approved by IACUC.

Adoptive Transfer

Adoptive transfer methodologies were utilized to develop genetic chimeras. The number of cells and timing of transfer were chosen based upon preliminary experiments and data from others showing the ability of adoptively transferred monocytes to abrogate inflammation-mediated pathology [51]. Bone marrow-derived monocytes and T cells from spleens of mice were purified using antibody cocktails with magnetic bead technologies (StemCell Technologies). Mice were anesthetized, and $1x10^6$ T cells and/or $1x10^6$ monocytes were infected retro-orbitally 1 day prior to being infected with *P. aeruginosa*.

Immunohistochemistry of mouse lung

After harvest, the left lower lobe of the mouse lung was placed in formalin for at least two hours, then transferred to a 20% sucrose solution for cryopreservation. Samples were then embedded in Tissue-Tek O.C.T. compound (Sakura Finetek, Torrance, CA), and frozen at -80°C. Embedded samples were then sectioned at 10μm on a Cryotome (Thermo Scientific, Waltham, MA), and stored at -20°C until staining.

The O.C.T. compound was washed off of the sections with PBS with 0.2% Triton X-100 (PB-X). Slides were blocked utilizing using a blocking buffer consisting of 5% normal goat serum and 5% bovine serum albumin in PB-X overnight at 4°C. Slides were incubated first with an antibody for arginase-1, followed by three washes with PB-X. A FITC labeled goat anti-rabbit antibody was then added and incubated for 1 hour at room temperature. The process was then repeated utilizing an antibody for NOS2, and a Texas red labeled secondary antibody.

Tissue Processing and Cell Phenotyping

Lungs were collected and processed for flow cytometry in the same manner as in chapter 2. Three different flow cytometry panels were assessed for each type of mouse. The first panel for the IL4rαKO mice consisted of CD11b-PECy5 (Serotec, Raleigh, NC), a marker found on macrophages, GR1-PECy7, a marker of neutrophils, MR-PE, a marker of M2 macrophages (Serotec, Raleigh,

NC), CD80-FITC, a marker of M1 macrophages, and biotinylated I-A[d] MHC II, a protein that is increased in expression with classical macrophage activation. Panel 2 consisted of CD11b-APC, CD11c-PECy7 (BD Bioscience, San Jose, CA), a marker of resident macrophages and dendritic cells, CD4-PECy5, a marker of CD4+ T-cells, GR1-FITC, and CD19-PE, a marker of B-cells. Panel 3 consisted of CD11b-PEcy5, CD11c-PECy7, TNFα-FITC, biotinylated TGFβ, and IL10-PE. Secondary staining was performed when appropriate utilizing a streptavadin conjugated to APC. All antibodies were purchased from BD bioscience (San Jose, CA), unless otherwise stated. Cells were analyzed with utilizing a FACSCaliber Flow Cytometer (BD Biosciences, San Jose, CA) with a dedicated operator. Greater than 50 thousand events per sample were routinely examined. Flow cytometry analysis was performed utilizing FlowJo (Treestar, Ashland, OR).

Statistical Analysis

Statistical analysis was performed utilizing Graphpad Prism (GraphPad software, La Jolla, CA). Comparisons between groups were made via one way ANOVA with Tukey's multiple comparison test for ratio level data, and by Fisher's Exact test for nominal data. A repeated measures ANOVA with Tukey's multiple comparison test were utilized for time courses. For some data, T-tests were used to compare means between groups. Non-linear regression utilized the least squares method for fit. Differences in survival were assessed utilizing a log-rank (Mantel-Cox) test. Unless otherwise stated, significance was deemed to be a p value <0.05.

C. Results and discussion

1. Alteration of macrophage polarization with azithromycin is IKKβ dependent

Azithromycin decreases NF-κB activation, while increasing IKKβ activation

We first assessed select proteins in the NF-κB signaling cascade to determine the effect that the presence of AZM has upon their activation (Figure 3.1). We treated cells with IFN, AZM, and LPS, and collected cell lysates at various timepoints. We found that treatment with AZM resulted in increased levels of the inactive isoform of NF-κB (p105), and decreased levels of the active isoform (p50) NF-κB present in the cells, particularly between 5 and 30 minutes after the addition of LPS. Congruent with these results, IκB expression was increased by AZM. LPS causes IκB activation to decrease, as IκB binds to NF-κB, keeping it inactive and preventing it from entering the nucleus to promote inflammatory gene expression. Treatment with the drug caused IκB to reappear earlier in the cell lysates (15 minutes after stimulation), whereas IκB was not detected in the control samples until the 60 minute mark. However, we additionally discovered that AZM treatment resulted in increased levels of IKKβ present in the cells. This was surprising, because increased activation of IKKβ should result in an increased NF-κB activation, which was not the case. The bottom portion of Figure 3.1 shows the effect of increasing AZM concentration upon IKKβ activation at 10 minutes after the addition of LPS (the point in time at which there is the most difference in NF-κB activation affected by the drug). IKKβ is dramatically increased at this timepoint at the 5, 10, and 15μM concentrations of AZM as compared to the zero drug lane. These results suggest that the inhibition of NF-κB activation by AZM occurs in the pathway downstream of IKKβ (discussed below). This data provided us with evidence suggesting that AZM polarizes macrophages to the M2 phenotype in part via crosstalk between IKKβ and the STAT1 signaling [68].

Inhibition of IKKβ activation prevents azithromycin from polarizing macrophages to the M2 phenotype

We then set out to determine whether AZM exerts its effect in part via the activation of IKKβ. Fong et. al. have previously shown that activation of IKKβ prevented polarization to the classically activated phenotype [68]. Using a genetically engineered mouse strain that caused tissue-specific over-expression

of IKKβ, this group showed that over-expression of the protein caused an inhibition of M1 macrophage activation along with a blunting of inflammation associated with Streptococcal pneumonia [68]. We treated cells with cytokines and AZM to polarize to either the M1 or M2 phenotype, as well as with 100 nM IKK-16, a competitive inhibitor of IKKβ (Figure 3.2). The compound displays the high affinity for IKKβ, with an IC_{50} of 40nM. At higher concentrations, it can also inhibit the activation of the entire IKK complex as well [104]. We found that treatment with IKK-16 had no effect on arginase activity in cells treated with IL4/13 plus LPS (the M2 control condition). In cells incubated with AZM, however, treatment with IKK-16 decreased arginase activity to similar levels of cells that were not exposed to the drug. This suggests that inhibition of IKKβ prevents AZM from polarizing macrophages to the alternatively activated phenotype, and strongly supports the conclusion that AZM shifts the macrophage polarization balance through its effects on IKKβ.

We then assessed gene expression for arginase I in cells that were treated with IKK-16. Cells were stimulated similarly to in the previous experiment, except that a concentration of 50nM IKK-16 was utilized to allow the potential for AZM to overcome this inhibition. We found that in the presence of the inhibitor, gene expression for ARG1 was significantly decreased in cells that were treated with AZM (Figure 3.3) ($P<0.05$). Interestingly, there was a trend towards a decrease in ARG1 gene expression for wells treated with IL4/13 and IKK-16, when compared to just the IL4/13 group ($p=0.115$). This data further suggests that AZM's ability to induce expression of ARG1, an important gene in M2 activation, is dependent on its ability to activate IKKβ.

Finally, we assessed whether increasing inhibition of IKKβ prevented AZM increases in arginase production (Figure 3.4). We treated cells either with IFNγ, 60μM AZM and LPS, or IL4/13 and LPS. Cells were additionally exposed to increasing concentrations of IKK-16, to further assess the effect of IKKβ inhibition on AZM-dependent M2 activation. We found, as expected, that inhibition of IKKβ had little effect on IL4/13 dependent arginase production. Up to the highest

concentration studied, 200nM, IKK-16 did not significantly lower arginase activity. Interestingly, however, we found that in AZM treated cells, inhibition of IKKβ by IKK-16 greatly inhibited arginase activity in a concentration-dependent manner. This further suggests that AZM alters macrophage polarization via IKKβ dependent mechanisms.

Increasing azithromycin concentrations overwhelms IKKβ inhibition

We next examined the effect of AZM concentration in the presence of IKKβ inhibition on the shift of cells to the M2 phenotype (Figure 3.5). As expected, we found that in cells that were not treated with IKK-16, AZM treatment resulted in a dose-dependent effect on arginase activity. When we treated cells with 12.5nM IKK-16, we found that AZM was still able to increase arginase activity in the cells. We did observe, however, that treatment with IKK-16 shifted the dose-response curve to the right, showing that the inhibition caused by IKKβ can be overcome by increasing concentrations of AZM. Increases in arginase activity by AZM were completely ablated in the presence of with the 25nM IKK-16. Unfortunately, we were not able to treat cells with AZM concentrations higher than those we utilized due to toxicity to the J774 cells. This data suggests that AZM achieves its effect on macrophage polarization, at least in part, via activation of IKKβ and further pinpoints the molecular target of the anti-inflammatory effects of AZM. Due to toxicity associated with very high concentrations of AZM, we were not able to reach the plateau at which AZM maximally increases arginase activity with these cells, and were thus unable to fully determine the EC_{50}.

We then assessed changes in nitrite concentration with increasing concentrations of AZM (Figure 3.6). Nitrite concentrations in cell supernatants serve as a counterpoint to arginase activity in cells. Nitrite is a stable breakdown product of NO, and high levels of nitrite in cell supernatants suggest a net M1 polarization. We anticipated that AZM would be unable to decrease nitrite concentration in cells treated with IKK-16. In the absence of IKKβ inhibition, treatment with AZM resulted in decreased supernatant nitrite concentrations.

Surprisingly, however, we found that we still observed decreases in nitrite concentrations as we increased AZM concentration with our cells that were treated with IKK-16. While it was somewhat surprising that we did not observe an increase in nitrite concentrations with IKKβ inhibition, corresponding to a decrease in arginase activity that we observed, these findings can still be explained. IKKβ, as previously stated, plays an important role in multiple signaling cascades. Inhibiting IKKβ activation results in decreased NF-κB activation. This results in decreased activation of the M1 phenotype, and explains why we did not see increases in nitrite concentration in our cells treated with IKK-16. This underscores the complexity present in cell signaling. It also suggests that the effects reported by other groups on cytokine production could also be independent of the drug's impact on macrophage polarization. Indeed, IKKβ appears to be exerting two roles in macrophages, both a pro-inflammatory role via activation of NF-κB activation, and an immunoregulatory role via STAT1 inhibition. This signaling protein may be affecting a balance function in order to control inflammation in this setting: as classical macrophage activation occurs along with inflammation, the NF-κB pathway could then participate in the regulation of STAT1 signaling over time.

In summary, the changes in arginase activity that we observed by shifting AZM and IKK-16 concentrations suggests that AZM exerts its effects on macrophage polarization via IKKβ dependent mechanisms. A greater understanding of these interactions and the cellular targets of AZM may lead to future drug targets that would allow clinicians to alter inflammation without the need to place patients on antibiotics for an extended amount of time, which leads to increases in antimicrobial resistance.

2. Azithromycin polarizes macrophages to the M2 phenotype independent of IL4rα function

IL4rαKO mouse splenocytes can be polarized to the M2 phenotype with azithromycin

We then set out to determine whether AZM's ability to polarize macrophages to the M2 phenotype is dependent on IL4/IL13 signaling. While we have been able to show that AZM dependent M2 polarization requires IKKβ, we were curious to determine if the drug signals through the IL4r and IL13r [2, 3]. First, we conducted a series of ex vivo experiments for which we collected splenocytes from both Balb/C and IL4rαKO mice and exposed them to LPS, cytokines, and AZM in a similar manner as described above. Figure 3.7 shows arginase activity normalized to viable cell count for cells stimulated with LPS for 6 hours. We found that cells from KO animals treated with IFNγ plus LPS plus AZM displayed increased arginase activity compared to all of the other conditions that we tested. However, arginase concentrations were significantly lower than those produced in the WT cells. This suggests that AZM may be functioning in part by priming macrophage polarization to the M2 phenotype, at which point cytokines produced by these cells then shift more macrophages to the M2 phenotype. As expected, IL4, IL13, or both cytokines together had little effect on arginase production in the KO cells. The up-regulation in arginase activity that was induced via AZM treatment in cells that are otherwise unable to be polarized to the M2 phenotype suggests that AZM exerts its effect via IL4 and IL13 independent mechanisms.

IL4rαKO mice are more susceptible to infection with *P. aeruginosa* than their parent strain

We were additionally interested to determine how mice with a deficient ability to generate alternatively activated macrophages were able to respond to infections with bacterial pathogens. We utilized the IL4rαKO in part to answer this question. In addition to the IL4rαKO mice, we utilized 2 other strains of mice to help to assess this question, the Balb/c and C57bl/6 strains. The Balb/C and C57bl/6 strains have extremely different cytokine profiles during infections, and resultingly respond to these infections very differently. C57bl/6 mice display high levels of IFNγ and low levels of IL4. Their macrophages additionally express high levels of iNOS, and low levels of the enzyme arginase [46]. Balb/c mice,

however, have more of a Th2-dominant response. They in general produce high levels of IL4, low levels of IFNγ, and express lower levels of the protein iNOS as well as high levels of the enzyme arginase 1 [46]. Interestingly, when mice are infected intratracheally with bacteria, the Th2 polarization present in the Balb/c strain of mice is traditionally associated with better outcomes to the infection [46], with the mice being more likely to survive. In fact, lung damage and fibrosis are readily induced by infection with *P. aeruginosa* in C57Bl/6 mice, but BALB/c mice are immune to this pathology [109-111].

Because of the differences in response of the inbred strains, we infected C57bl/6, Balb/c and IL4rαKO intranasally with *P. aeruginosa* at various inoculums, and assessed survival (Figure 3.8). Intranasal inoculations were utilized primarily to ensure a potent acute infection. As we expected, C57bl/6 mice were susceptible to infection with *P. aeruginosa*, while Balb/c mice were resistant, as it took an extremely high inoculum of 10^{10} CFU to cause appreciable mortality. Interestingly, however, while their parent strain is resistant to intranasal infection with *P. aeruginosa*, the IL4rαKO strain was much more susceptible to infection with *P. aeruginosa*. Indeed, the survival curve for the IL4rαKO mice more closely resembles the C57bl/6 strain than the Balb/c strain, suggesting that alternative macrophage activation through IL4rα may be partly responsible for the innocuous inflammatory response observed in the Balb/c strain.

We next examined histology for the three different strains of mice, and found marked differences. Balb/c mice showed diffuse cellular infiltrations throughout the lungs (Figure 3.9 A.). The cellular infiltrates in C57bl/6 were primarily concentrated along the edges of small airways (Figure 3.9 B.). The lungs of the IL4rαKO mice displayed cellular infiltrates that, while somewhat diffuse, were more concentrated along the airways than those of their parent strain (Figure 3.9 C.). This finding could have clinical relevance, due to the fact that *P. aeruginosa* infection in patients with CF primarily causes a peribronchiolar inflammation and damage. This again shows that the IL4rαKO mice more closely

resemble the *P. aeruginosa* susceptible C57bl/6 strain, and suggests that alternatively activated macrophages play an important role in the ability of mice to blunt the damaging inflammatory response associated with *P. aeruginosa* infection.

We additionally examined differences in surface protein expression and cytokine production in IL4rα KO mice. Mice were sacrificed 6 days after infection with between 3.8 x 10^4-3 x 10^5 CFU of *P. aeruginosa* incorporated into agarose bead, and lung digest samples underwent surface staining as well as intracellular cytokine staining, and analyzed by flow cytometry. We first assessed the expression of surface markers of macrophages (CD11b), T cells (CD4), and neutrophils (approximated by GR-1 expression) (Figure 3.10 A.) and compared the results to the WT strain. While we did not observe significant differences, we found trends that IL4rαKO mice displayed fewer CD4+ T cells (p=0.203), and more GR1+ cells (p=0.110). We then assessed expression of surface markers of macrophage polarization and compared the results between the two strains (Figure 3.10 B.). Encouragingly, we found that IL4rαKO mice displayed significantly fewer cells expressing the M2 markers MR (p=0.047) and CD23 (p=0.043), while observing no differences in surface expression of the M1 marker CCR7 between the strains. Finally, we assessed intracellular expression of pro- and anti-inflammatory cytokines including TNFα, TGFβ and IL10 (Figure 3.10 C.). We found a trend towards a decrease in the number of cells producing TNFα (p=0.109). We additionally found no differences in the numbers of cells expressing the anti-inflammatory cytokines TGFβ and IL10, although there was a trend towards a significant difference in the latter (p=0.063). These phenotypic differences suggest the importance of control of macrophage activation via the IL4 and IL13 receptors, and the role of these macrophages in the response to *P. aeruginosa* infections.

To this point, we have described how the absence of IL4rα function results in impaired survival and increased inflammation in mice infected with *P. aeruginosa*. This suggests that M2 macrophages play an important role in the

response to *P. aeruginosa* in the lungs of these mice. We believe that the lack of M2 macrophage polarization results in an overly zealous inflammatory response that causes excessive damage, thereby increasing morbidity and mortality.

IL4rαKO mice adoptively transferred with cells from Balb/c mice display IL4rα+ cells in their lungs

A confounding factor in using this genetically engineered strain of mouse is that not only are macrophages devoid of IL4rα—this defect is also present among T lymphocytes. Therefore, to address this issue, we utilized an adoptive transfer approach to restore normal IL4rα expression in these cell types. We set out to compare the response to *P. aeruginosa* pneumonia among IL4rαKO mice that received adoptive transfer of either normal T cells only, or both normal T cells and monocytes. In order to validate the transfer of cells, we first confirmed that WT cells adoptively transferred into IL4rαKO mice would migrate to the lungs in response to infection. On the day before infection, IL4rαKO mice were adoptively transferred with both monocytes and T cells, or with only T cells from Balb/c mice, as described above. The IL4rαKO mice have deficient IL4rα KO function on all of their cells, including T cells. Mice were then infected intratracheally with *P. aeruginosa*-incorporated agarose beads, and sacrificed at various time points. Cells were collected and stained for CD11b, GR1, CD4, and IL4rα. We first assessed the presence of the IL4rα chain on macrophages, defined as cells being CD11b+ as well as GR1-. As expected, we found macrophages expressing the IL4rα chain in mice that received both macrophages and T cells, whereas IL4rα expression was absent in the group receiving normal T cells only (Figure 3.11). Interestingly, we first began to see this difference at 7 days post infection. This resembles our previous studies in C57bl/6 mice, showing that the influx of cells into the lungs of mice is most pronounced at 7 days post infection. When we assessed the presence of the IL4rα chain on T cells that had been adoptively transferred, we found significant amounts of T cells that expressed the ILr4α chain in both of the groups. This data shows that we are able to effectively adoptively transfer cells with normal

IL4rα chain function to mice lacking the IL4rα chain. This allows us to assess the importance of IL4rα chain signaling specifically associated with macrophages in the context of pulmonary infections with *P. aeruginosa*.

Impact of Adoptive Transfer on Weight Loss and Survival

We assessed survival and weight loss in our IL4rαKO mice that had been adoptively transferred with cells from Balb/c mice. We pooled survival data from 3 replicate experiments to determine whether there was a difference between the groups. We first found that there was no difference in survival between animals that received both macrophages and T cells, as compared to animals that only received T cells (p=0.0939) (Figure 3.12 A.). We also found no differences in weight loss between the two groups at any specific timepoint, or in total over time (p=0.3147) (Figure 3.12 B.). It is important to note, however, that we observed few fatalities in these experiments. This may be due to the initial inoculula that we utilized being too low for the mice. Additionally, with the addition of normal T cells to these mice, these cells may allow for better control of the inflammatory response.

Effect of adoptive transfer on cellular influx into lungs of IL4rα KO mice

We next examined the cellular infiltrates of infected IL4rαKO mice that underwent adoptive transfer of either WT macrophages and T cells or only T cells (Figure 3.13). We observed a decrease in the numbers of infiltrating macrophages on day 7 post-infection (p=0.04) (CD11b+CD11c-GR1-) in mice that received both M and T cells, compared to mice that received only T cells. We did not, however, observe any differences in the amounts of the more alveolar subset of cells in the lungs, designated as CD11b-CD11c+GR1-. Importantly, mice that only received T cells and monocytes displayed dramatically greater neutrophil influx (as approximated by the number of GR1+ cells) in the lungs than mice that received T cells, peaking around day 7 post-infection. This suggests that M2 macrophages play an important role in decreasing the neutrophilic response in acute infections with *P aeruginosa*

pneumonia. This is an important finding, as dysregulated inflammation characteristic of patients with CF is primarily neutrophil driven, as presented in detail in Chapter 1. We also observed a decrease in CD4+ T cells in mice that received macrophages capable of M2 polarization. Although adoptive transfer changed the influx of immune cells over time in the lungs, in general it did not bring the values to the levels observed in the WT strain.

Ability of azithromycin to rescue mice infected with *P. aeruginosa* that lack IL4rα responses

We demonstrated in Chapter 2 that AZM can blunt inflammation and improve lung damage and survival in C57Bl/6 mice infected with *P. aeruginosa*. Data presented in this chapter suggests that the converse is also true: that the absence of alternative macrophage activation (i.e. absence of IL4rα signaling) worsens neutrophil-driven pulmonary inflammation associated with this infection. To apply these results to our mechanistic investigation of the drug, we next assessed the ability of AZM to induce alternative macrophage activation in IL4rαKO mice, and whether this will blunt the excessive inflammation associated with *P. aeruginosa* infection in this strain. IL4rαKO mice were infected with agarose beads containing between 5.5×10^4 and 1.5×10^5 *P. aeruginosa* for these experiments. Beginning 4 days before infection mice were dosed with 3.2mg AZM per day, and mice sacrificed at various timepoints for analysis.

We first assessed the numbers of bacteria present in the lungs of KO mice that had been infected with *P. aeruginosa* beads. In the past, we have observed that treatment with AZM exerted no effects on bacterial colony counts in Balb/c mice that had been infected with *P.aeruginosa* [75]. Here, we found similar results. We found no differences in bacterial CFU at any of the three timepoints that we collected (Figure 3.14). We then assessed the percentage of weight loss from day 0 in our KO animals (Figure 3.15). Here we found no differences in weight loss between the KO animals that received AZM as animals that did not receive AZM ($p=0.0649$ by 2-way ANOVA). These findings mimic those that we observed with our adoptive transfer.

Azithromycin shifts cells in the lung to the M2 phenotype in IL4rαKO mice

We next assessed the phenotype of cells in both the lung lavage and lung digests of the IL4rαKO mice infected with *P. aeruginosa* for markers of M1 and M2 activation via flow cytometry. We found a non-significant trend towards increased expression of the M2 marker mannose receptor on cells in the lung lavages of mice treated with AZM (Figure 3.16 A.). We additionally observed trends towards increased MR expression in the percentages of cells in the lung lavage of the mice, which became statistically significant at day 14 ($p<0.05$) (Figure 3.16 C.). Intriguingly, we did not observe differences in mannose receptor expression in the lung digests, both when assessing the total number of cells positive for both CD11b and MR, as well as when we compared the percentages of cells in the digest that were CD11b+ that also expressed MR (Figure 3.16 B., D.). It is possible that the large amount bacterial antigen in the lungs of these mice was able to overwhelm the ability of AZM to alter macrophage to the M2 phenotype.

We next assessed surface expression of CD80, a marker of M1 activation. Here we found few differences between the two groups, and in fact observed a slight increase in both the number and percent of cells expression CD11b that also expressed CD80 (Figure 3.17 A., C.). Again, we observed no differences between the two groups in the lung digest (Figure 3.17 B., D.). It is important to note, however, the very large percentages of cells, especially in the lung lavage, that were positive for CD80 across all of the time points. This again suggests that in IL4rαKO animals there is strong inflammatory response to bacteria. In a mouse with normal IL4rα function we would expect this inflammatory response to be dampened by M2 macrophages that were activated via traditional mechanisms. In the IL4rαKO mice, however, there may be less of a shift away from an M1 macrophage polarization, even in the presence of AZM. Again, this could be a matter that the large amount of bacterial signaling that is present in the lungs of these mice is overwhelming the ability of AZM to help achieve a shift to the M2 phenotype.

We then plotted the ratio of cells that had CD80 surface expression to that of cells that had MR surface expression, the results of which can be seen in figure 3.18. In the lung lavage we observed that the ratio of cells that expressed either CD80 or MR at day 0, 4, and 7 (Figure 3.18 A.). Interestingly, however, at day 14 we observed an increase in the ratio of CD80 positive cells to MR+ cells. This increase was significantly higher in mice that did not receive AZM as compared to mice that received AZM. By day 14, mice had essentially cleared the bacteria, and were in the process of recovering from the infection. It is only after the infection had been cleared that we are able to observe significant differences in the CD80/MR ratio, suggesting that AZM is able to shift macrophage polarization in these mice towards the M2 phenotype. We observed similar findings in the lung digest (Figure 3.18 B.), although rather than observing essentially no changes in the ratio across days 0, 4, and 7, we saw a trend towards a gradual, non-significant increase in the ratio of CD80/MR positive cells. Again, we observed that at day 14 a significantly higher CD80/MR ratio in mice that did not receive AZM when compared to mice that did receive AZM.

Azithromycin alters influx of inflammatory cell types in IL4rαKO mice

We then assessed the ability of AZM to alter cellular influx to the lungs of mice during infection with *P. aeruginosa*. We have previously shown that in C57bl/6 mice treatment with AZM increases the influx of CD11b+ cells, and decreases the influx of neutrophils in the lungs [75]. Here we observed similar findings in our KO animals. In the lung digests, we found a significant increase in the ratio of CD11b+ cells (representing infiltrating macrophages) to neutrophils (CD11b- GR1+) at day 7 in the lung digest (Figure 3.19 B.). Unfortunately, the large variability in the lung lavage data on day 7 made it impossible to observe any differences in cell influx (Figure 3.19. A.). The large difference at day 7 in the lung digest, however, suggests that AZM is altering the types of cells that influx into the lungs of mice during an acute infection with *P. aeruginosa* independent of IL4 and IL13 dependent mechanisms.

We also examined lung histology from the mice at various timepoints, to visually assess the types of cells that infiltrate into the lungs (Figure 3.20). On day 0, we found few cells in the lungs, and the cells that we did see were mononuclear, and appeared to be monocytes and macrophages. On day 4 we observed many more cells in the lungs of the mice. While in both the AZM and non-AZM treated animals we observed more neutrophils (as determined by the appearance of the nuclei of the cells), it appears that there were fewer neutrophils in the mice treated with AZM than in the animals that did not receive AZM. On day 7, we observed similar trends, although the differences between the AZM treated animals and the animals that did not receive AZM was not very large. By day 14 the infection is essentially resolved, and we observed many fewer cells in the lungs of the animals at this point in time. We also did not observe major differences in the types of cells present in the lungs of the animals at this timepoint.

Azithromycin treated IL4rαKO mice display shifts in arginase 1 and NOS2 localization

We additionally assessed the localization of two of the prototypical proteins of macrophage polarization, NOS2 for M1 macrophages, and arginase 1 for M2 macrophages. While we did not observe large differences in total arginase activity in our IL4rαKO mice that we treated with AZM (Figure 3.21), we found profound differences in the relative location of arginase in the lungs of these animals when employing IHC. On day 14 post-infection with 1.5×10^5 CFU of *P. aeruginosa* incorporated into agarose beads, we found that animals that had not received AZM displayed expression of both NOS2 and arginase 1 (Figure 3.22). Animals that did receive AZM, however, expressed markedly less NOS2 protein. Interestingly, we found a marked up-regulation of arginase 1 protein in the animals treated with AZM. This increase was most pronounced in the areas around the small airways of these mice, as compared to the rest of their lungs. This is the typical location of *P. aeruginosa* infection, and is additionally the area affected most severely in CF pathogenesis. This suggests

that AZM is able to polarize macrophages away from the M1 phenotype (as determined via NOS2 protein expression). It also appears that AZM treatment is increasing M2 polarization in the lungs of these animals, to a certain extent in the entire lung, but to a greater extent around the airways. This suggests that AZM, in addition to the effects that it exerts on macrophage polarization, is affecting trafficking of macrophages in the lungs of these animals. In fact, it appears that AZM is causing M2 macrophages to concentrate in the peribronchiolar areas around the airways.

It is unknown what the impact of this effect may be. First, it is possible that these M2 macrophages would result in increased fibrosis and scarring in the airways around the lung. Second, the marked decrease in NOS2 protein expression in mice treated with AZM suggests that there may likely be less total damage in the lungs of these animals to recover from. In that case, it may be that even though we found markers consistent with M2 macrophages around the airways of these mice, airway damage may not necessitate repair and remodeling to a significant extent.

D. Conclusions

General Conclusions

Here we have shown data suggesting that AZM polarizes macrophages to the M2 phenotype via IKKβ-dependent, and IL4rα-independent mechanisms. Others have shown that IKKβ prevents activation of STAT1 in myeloid cells [68]. We showed that treating cells with an inhibitor of IKKβ activation prevents AZM from polarizing macrophages to the M2 phenotype. We additionally showed that with certain degrees of IKKβ inhibition, increasing AZM concentration was able to overwhelm this inhibition. This suggests that AZM is somehow causing the activation of IKKβ, and that this activation is at least in part responsible for polarization away from the M1 phenotype, and towards the M2 phenotype for these macrophages. We additionally showed, utilizing cells stimulated *ex vivo* from IL4rαKO mice,that AZM is still able to shift macrophages to the M2

phenotype, even in the absence of signaling via the traditional methods necessary for M2 polarization.

This data suggests future targets for investigation into the exact molecular site where AZM is exerting anti-inflammatory effects. Future work targeting these molecules may allow for the creation of novel therapeutics that include the beneficial immunomodulatory effects of AZM, without the anti-infective properties. This would result in the avoidance of inducing antimicrobial resistance that results from long term treatment with an antibiotic. Antibiotic resistance is a growing problem, and it has been shown that long-term macrolide treatment greatly increases resistance to those medications [17]. While we were not able to find an exact target and mechanism by which AZM alters macrophage phenotype, we were able to considerably narrow the field of targets. Namely, by showing that inhibition of IKKβ prevents AZM based M2 polarization, it suggests that activation IKKβ plays an important role in this activation. We hypothesize that this is due to inhibition of the STAT1 cascade similar to what Fong et. al. have previously shown [68]. The Fong article suggests an interaction between the two important cell signaling mechanisms in macrophages. They surmise that this interaction exists to down-regulate the inflammatory response in cells. We believe that AZM polarizes macrophages to the M2 phenotype via this mechanism.

Additionally, we were able to show that AZM dependent M2 activation is independent of IL4 and IL13 function, suggesting that it does not depend on the traditional mechanisms associated with M2 activation. This eliminates one prospective mechanism for AZM dependent activation, and further supports our previous finding that AZM shifts macrophage polarization to an M2 phenotype in the presence M1 stimulation conditions.

We additionally showed that AZM is able to exert many of the effects *in vivo* that it was able to exert *in vitro*, even in mice lacking IL4rα signaling. AZM increased the number and percentages of cells in the lung lavage expressing MR. When mice had cleared the infection on Day 14 of the experiment, we

observed a shift towards expression of the M2 marker MR, and a shift away from the M1 marker CD80. In the absence of an intrinsic M2 response to blunt the initial inflammatory response to pulmonary infection with *P. aeruginosa*, AZM was unable to affect a major phenotypic shift in macrophages *in vivo*. As the infection begins to clear, however, and the infectious burden falls in the lungs, it appears that AZM is able to exert a more major effect on the macrophage phenotype in the lungs of these animals.

Limitations

It was initially difficult for us to make comparisons between the three initial mouse strains that we utilized (C57,bl6, Balb/c, and the IL4rαKO mice). As previously stated, the IL4rαKO mice are on a Balb/c background. The Balb/c strain is traditionally thought to be resistant to pulmonary infection with Pseudomonas, especially compared to the C57bl/6 strain which is susceptible to severe acute pulmonary damage induced by Pseudomonas infection [46, 47]. This means that our KO mice are on a background for a strain that is resistant to pulmonary infections. While this allows us to make some interesting observations (e.g. that a defect in IL4rα signaling shifts the phenotype from a pulmonary infection resistant strain to a pulmonary infection susceptible strain), it does make comparisons between groups difficult. Namely, it is difficult to compare these mice to their parent strain, since a bacterial inoculum that would kill an IL4rαKO or C57bl/6 mouse is easily cleared by a Balb/c mouse. With that in mind, however, we were still able to make interesting observations with the IK4raKO mice on the background that we have them.

There is variation between the flow cytometry assessment of the types of cells present in the lungs of these mice, and the visual inspection of the cells via histology. Namely, we observed our largest differences in the ratio of macrophages to neutrophils at day 7 via our flow cytometry analysis, and in our visual analysis of the lungs the largest difference appears to have been on day 4. It is important to note that while the lung lavage and lung digest samples represent cells from the entire lungs of the animals, the histology sections

represent only a thin slice of the lungs. This means that the histology results may not be fully representative of the rest of the lungs of the animal. Regardless of the specific day that we observed the largest difference in the macrophage to neutrophil ratio in the lungs of these mice, the consistent trend between the two groups is that AZM treated animals displayed a more monocytic, and less neutrophilic influx into their lungs in the context of a bacterial pneumonia.

We additionally had considerable variation in our mouse experiments in regards to our infections of IL4rαKO animals. The infection model that we use for our mice is extremely complex and results in considerable variation, both between individual mice that are infected, as well as between experiments. The *P. aeruginosa* agarose beads are extremely difficult to make, and variability in bead production makes it difficult to target the same inter-experiment dose. This results in difficulty comparing replicates of infections. Additionally, there is difficulty in ensuring that all mice receive the same amounts of bacteria in their intratracheal inoculation. This may explain some of the considerable variability that we observed with our flow cytometry and other data from our mice. Instead of the intratracheal infection approach that our lab utilizes for the infections, others first tracheotomize the animals for the infection [112]. That approach, however, has considerable trauma associated with it, leading to alterations in the immune response. We believe that these alterations make the infection approach that we utilize to be more appropriate, as we see fewer alterations in the immune response. Due to the nature of our infection model, and the ease in which mice are able to clear pulmonary infections with *P. aeruginosa*, we are forced to utilize this model, with all of the benefits and difficulties entailed to it. Finally, we cannot eliminate the possibility that AZM is exerting effects on other cells, including neutrophils T cells, and epithelial cells. These effects on other cells may be responsible in part for the beneficial effects seen with AZM.

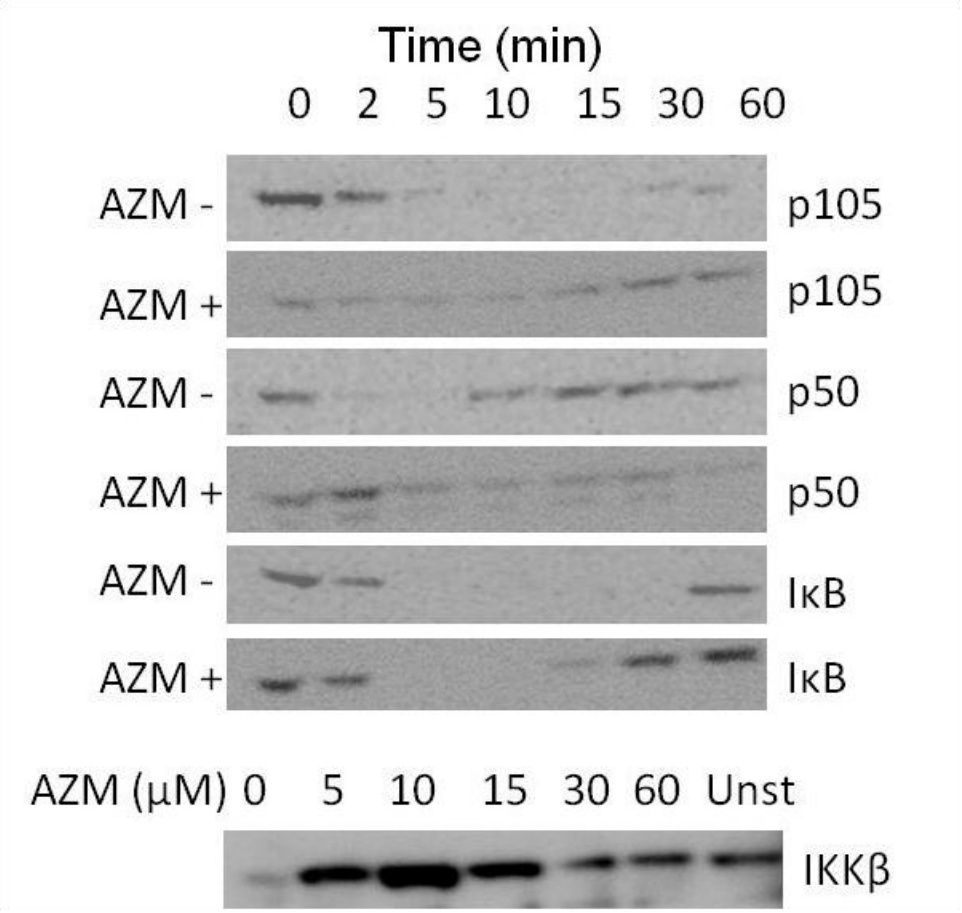

Figure 3.1. Western blots of proteins in the NF-κB cascade. J774 cells were stimulated with IFN, LPS and 30 μM AZM for variable amounts of time at 37°C with 5% CO_2. Lysates were probed for proteins in the NF-κB cascade, including inactive NF-κB (p105), active NF-κB (p50), and IκB. Cells were then stimulated for 10 minutes for IFN, LPS, and variable concentrations of AZM, and probed for IKKβ. 10 minutes were utilized for IKKβ experiments due to large differences in NF-κB activation observed in the samples.

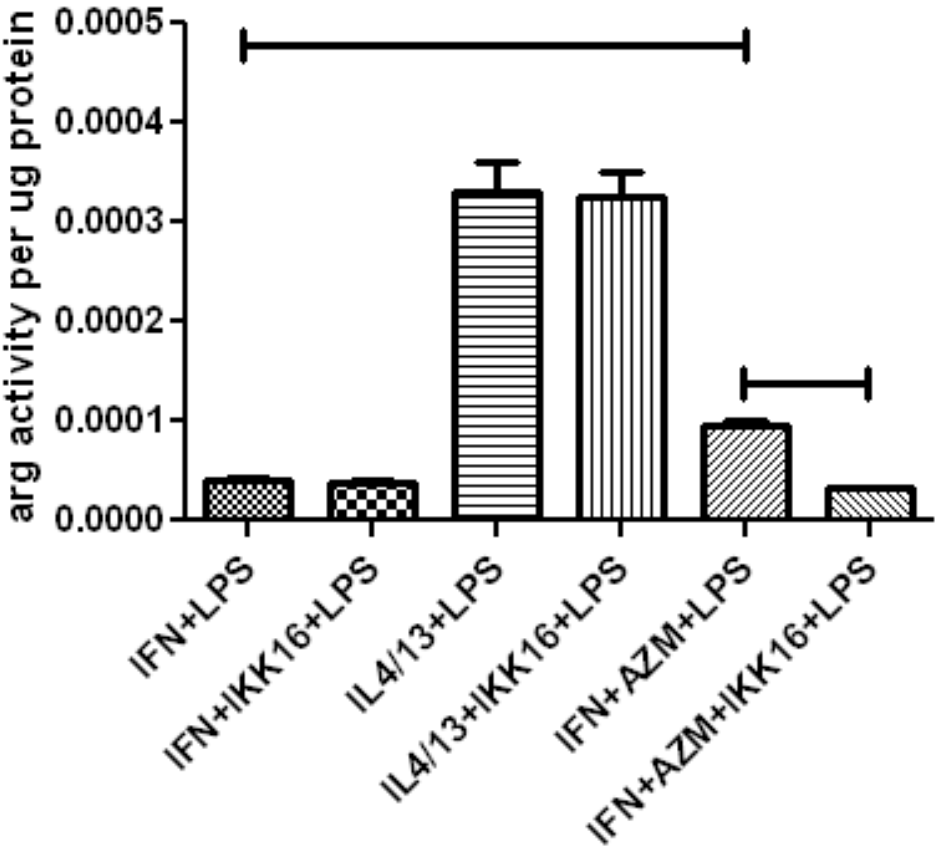

Figure 3.2. Arginase activity in the presence of an IKKβ inhibitor. J774 cells were stimulated overnight with IFN, IL4/13, 30 μM AZM, and 100nM of the IKKβ inhibitor IKK-16 at 37°C with 5% CO_2. Cells were then stimulated with LPS for 24 hours. Cells were then lysed, and lysates were utilized for the arginase assay. Statistical analysis was performed with a one way ANOVA with Tukey's multiple comparison test. Arginase samples were run in triplicate, and data represents mean ± SD. Data representative of 3 replicates. Data deemed statistically significant with $P<0.05$

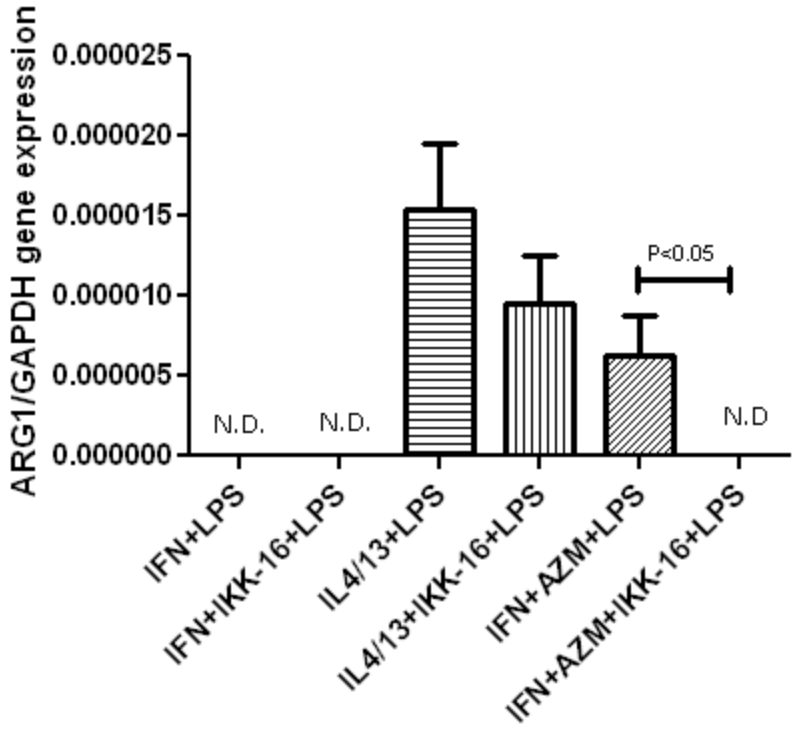

Figure 3.3. Arginase 1 gene expression in the presence of an IKKβ inhibitor. J774 cells were stimulated overnight with IFN, IL4/13, 30 μM AZM, and 50 nM of the IKKβ inhibitor IKK-16. Cells were then stimulated with LPS for 24 hours at 37°C with 5% CO_2. Cells were preserved in RNAlater, mRNA was isolated, and qRT-PCR was performed on each sample in triplicate. Statistical analysis was performed via T-tests for related samples. Data represents mean ± SD. Data representative of 2 replicates.

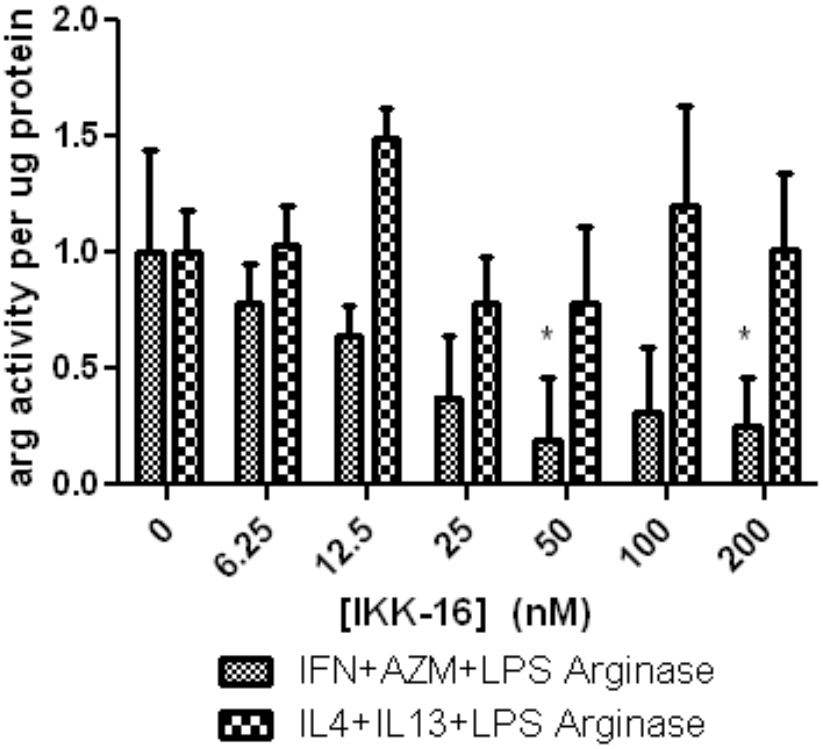

Figure 3.4. Arginase activity with increasing concentrations of an IKKβ inhibitor. J774 cells were stimulated overnight with IFN and 30 μM AZM or IL4/13. Cells were also treated with increasing concentrations of IKK-16. Cells were then stimulated with LPS for 24 hours at 37°C with 5% CO_2. Cells were lysed, and lysates were utilized for the arginase assay. Results were normalized to conditions with no IKK-16. * represent significant decreases from baseline assessed via ANOVA. Arginase samples were run in triplicate, and data represents mean ± SD.

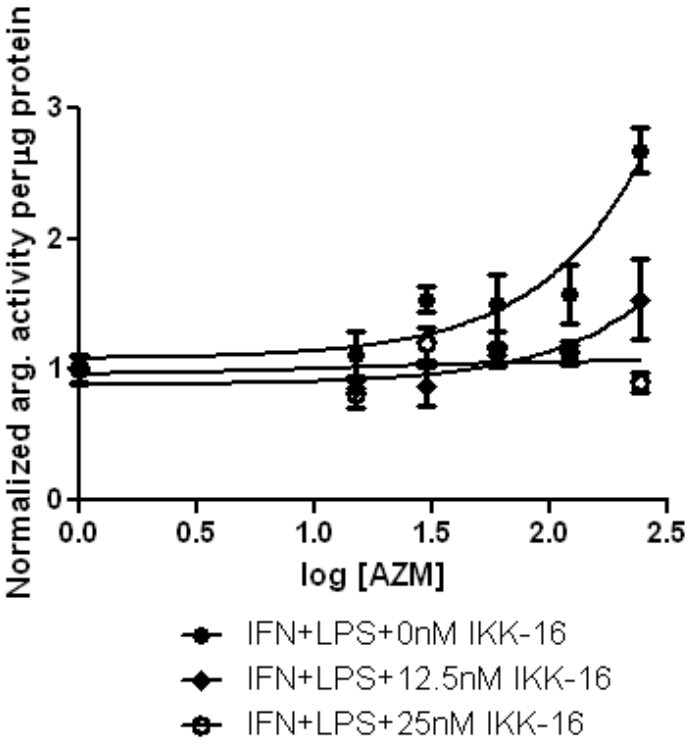

Figure 3.5. Arginase activity with increasing concentrations of AZM. J774 cells were stimulated overnight with IFN, IL4/13, IKK-16, and variable concentrations of AZM. Cells were then stimulated with LPS for 24 hours at 37°C with 5% CO_2. Arginase samples were run in triplicate, and data represents mean ± SD. Results were normalized to conditions with no AZM. Non-linear regression of data was fit utilizing a log(agonist) vs. three parameter response in Graphpad Prism. Data representative of three replicates.

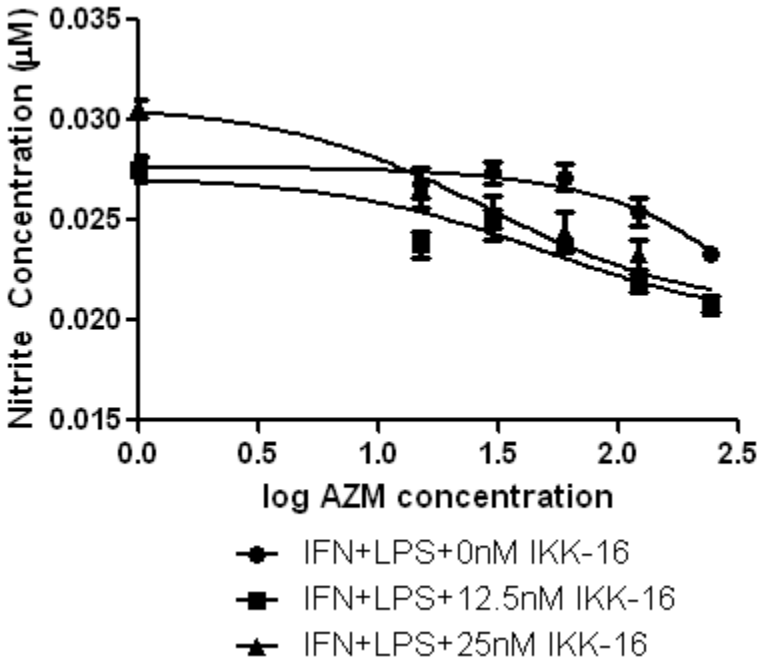

Figure 3.6. Nitrite concentration with increasing concentrations of AZM. J774 cells were stimulated overnight with IFN, IL4/13, IKK-16, and variable concentrations of AZM. Cells were then stimulated with LPS for 24 hours at 37°C with 5% CO_2. Samples were run in triplicate, and data represents mean ± SD. Non-linear regression of data was fit utilizing a log(agonist) vs. three parameter response in Graphpad Prism. Data representative of three replicates

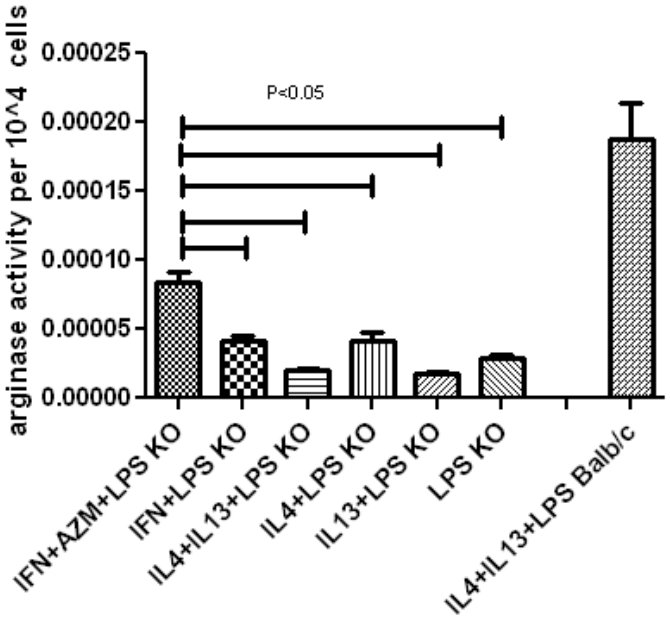

Figure 3.7. Arginase activity in *ex vivo* stimulated mouse splenocytes. Splenocytes were collected and stimulated overnight with IFN, IFN+AZM, IL4, IL13, IL4/13, or no cytokines at 37°C with 5% CO_2. Cells were then treated for 6 hours with LPS. Lysates were collected, and the arginase assay was performed on the lysates. Each sample was run in triplicate. Statistical analysis was performed via one way ANOVA with Dunnett's multiple comparison test. Samples were compared to the IFN+AZM+LPS group. Differences were deemed significant with a $p<0.05$.

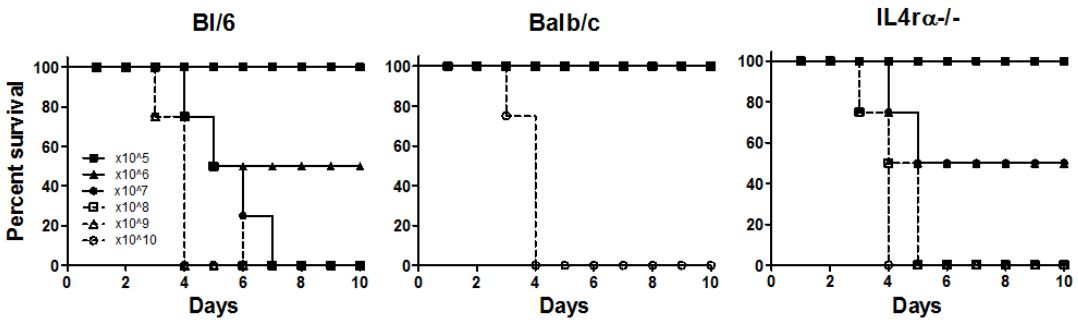

Figure 3.8. Survival curves with increasing inocula of *P. aeruginosa* in C57bl/6, Balb/c, and IL4rαKO mice. Mice were infected intranasally with between 10^5 and 10^{10} *P. aeruginosa*, and monitored over time.

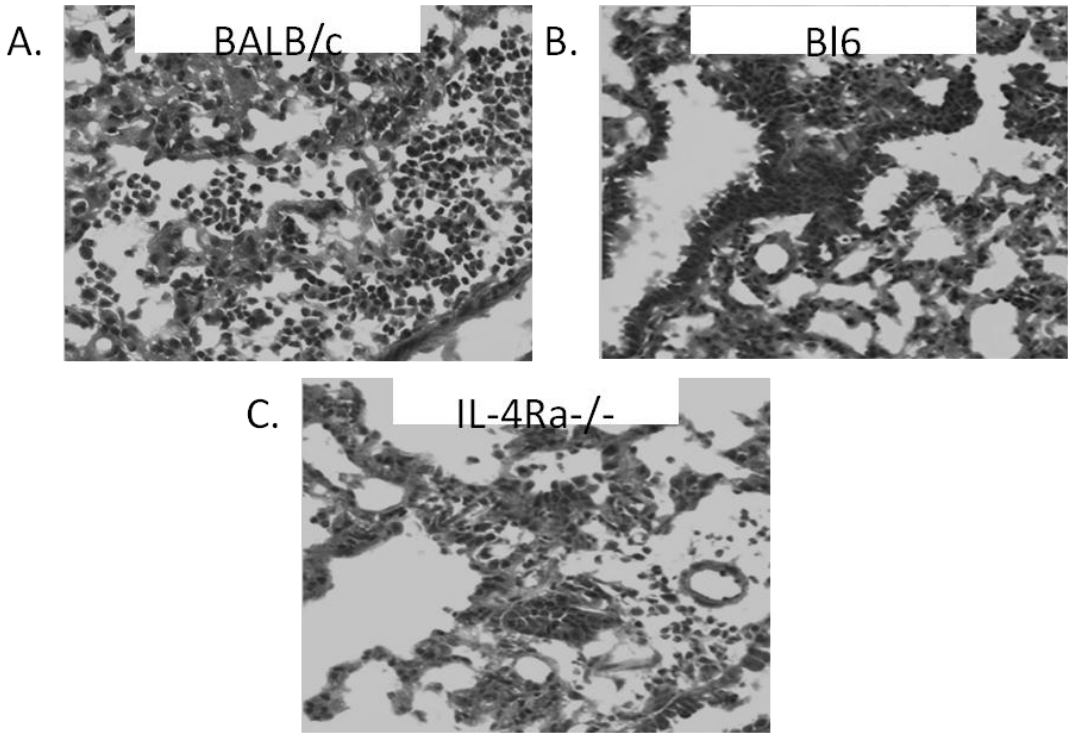

Figure 3.9. Lung sections from mice infected with *P.aeruginosa*. Lung sections were collected, and H & E staining was performed on the lung sections. Sections are from mice that were of the strain (A) Balb/c; (B) C57bl/6; (C) IL4rα KO. Balb/c mice displayed diffuse cellular infiltrations throughout the lung section, while in C57bl/6 mice cells are concentrated along the small airways. Cellular infiltrates in the IL4rα KO mice more closely resemble the C57bl/6 mice than those of Balb/c. Pictures representative from multiple pictures/mouse.

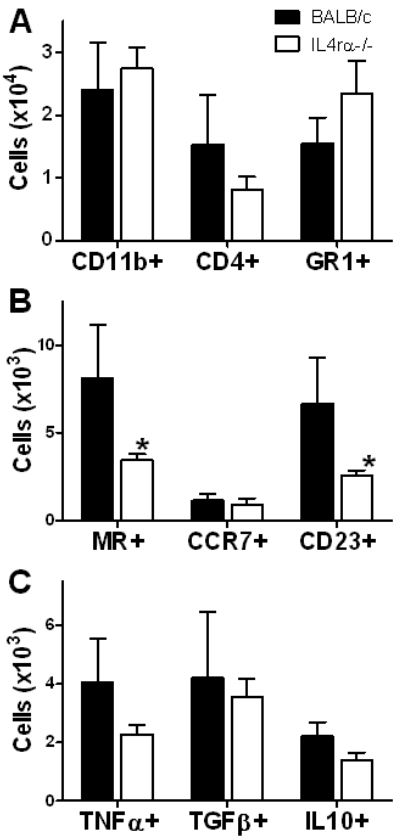

Figure 3.10. Phenotype of cells collected from either Balb/c or IL4rα mice. Lungs were collected, and lung digests were stained for flow cytometry. Panel (A) cells positive for CD11b (macrophages), CD4 (T cells), or GR1 (neutrophils and inflammatory monocytes); (B) The subset of CD11b positive cells positive for MR, CCR7, CD23; (C) subset of CD11b positive cells intracellularly expressing TNFα, TGFβ and IL10. Data represents mean number of cells expressing the surface markers ± SD, and are from 4 mice/group.

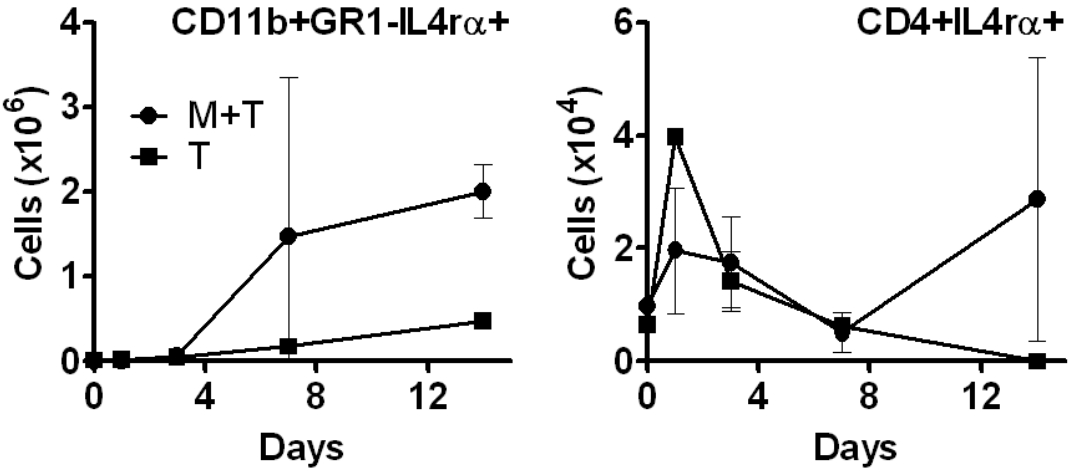

Figure 3.11. Adoptive transfer into IL4rα KO mice. Bone marrow derived monocytes and T cells (M + T) from spleens, or just T cells (T) of Balb/c mice were isolated and adoptively transferred into IL4rα KO mice on day -4 before the experiment. On day 0, mice were intratracheally infected with agarose beads containing 5 x 10^5 *P. aeruginosa*. Surface receptor expression in the lung digest samples were assessed via flow cytometry. Cell counts are depicted for the CD11b+GR1-IL4rα+ and the CD4+IL4rα+ subsets of cells. Data represents mean ± SD for 4 mice/group.

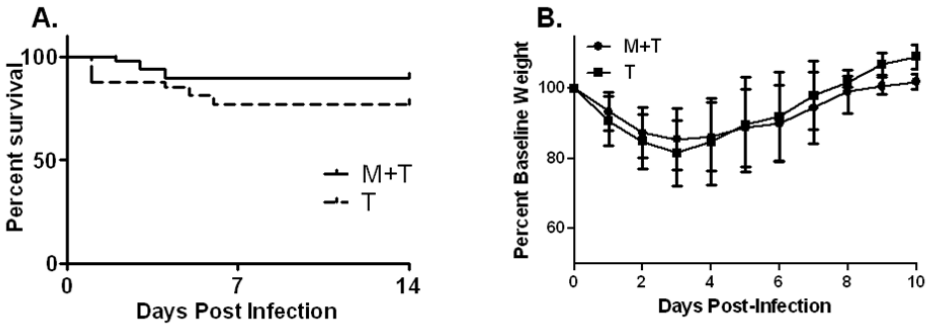

Figure 3.12. Survival and weight loss with adoptively transferred mice. IL4rαKO mice were adoptively transferred with either macrophages and T cells (M + T), or just T cells from Balb/c mice on day -4 of the experiment. On day 0, mice were infected with agarose beads containing *P. aeruginosa*. Data is pooled from 3 replicates of the experiments. Panel (A) represents percent survival between the two groups; (B) weight loss normalized to day 0. Data represents mean ± SD. Experiment began with 16 mice/group

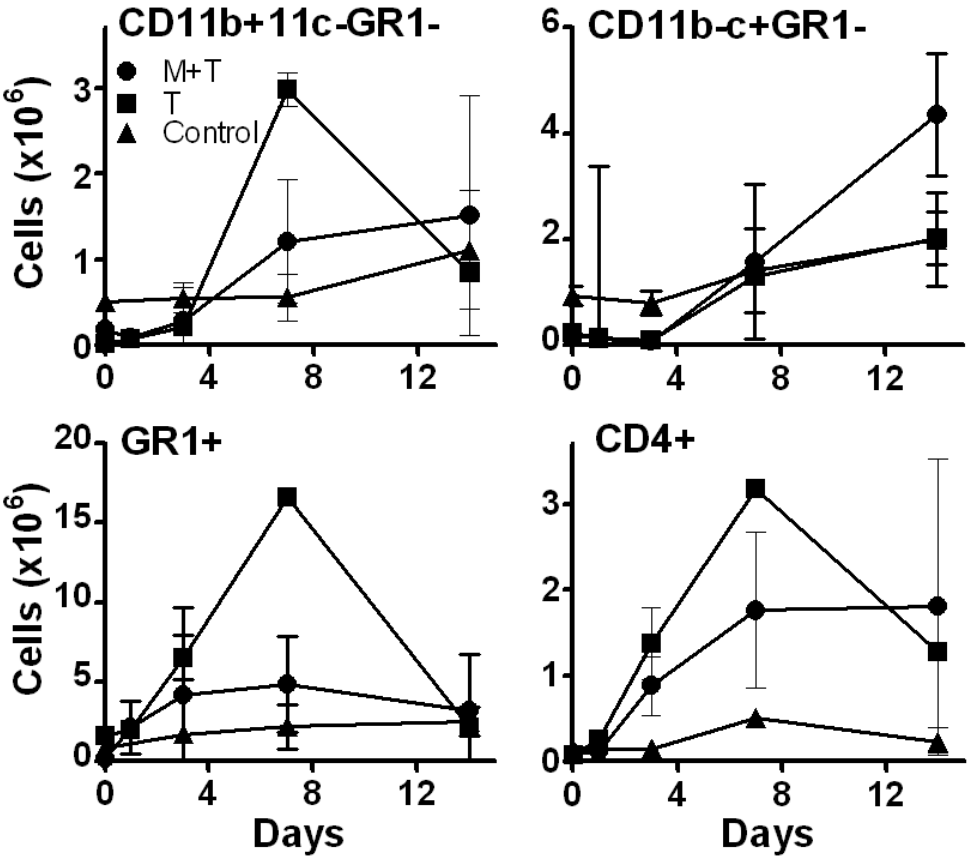

Figure 3.13. Phenotype of cells in lungs of adoptively transferred mice. Cells from Balb/c mice were adoptively transferred to IL4rαKO mice on day -1, and infected with agarose beads containing *P. aeruginosa*. Balb/c animals were utilized as a control. Cell phenotypes were assessed via flow cytometry. Panels represent post infection lung digest cell counts for CD11b+CD11c-GR1- (infiltrating macrophages), CD11b-CD11c+GR1- (resident macrophages), GR1+ (neutrophils), and CD4+ (T cells). Data represents mean ± SD with 4 mice/group.

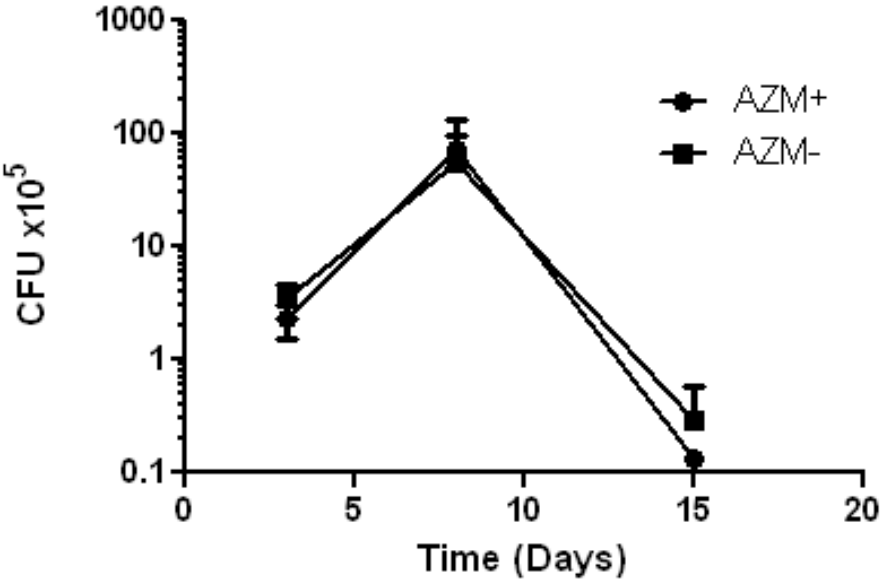

Figure 3.14. Bacterial CFU in IL4rαKO mice treated with AZM. Beginning four days before infection, mice received either 3.2 mg AZM daily, or vehicle control beginning 4 days before infection, and continuing throughout the infection. Mice were then infected intratracheally with 5.5 x 10^4 bacteria, and monitored over time. Lungs were collected, and a portion were homogenized and plated to determine the numbers of viable *P. aeruginosa*. Data represents mean ± SD with 4 mice/group.

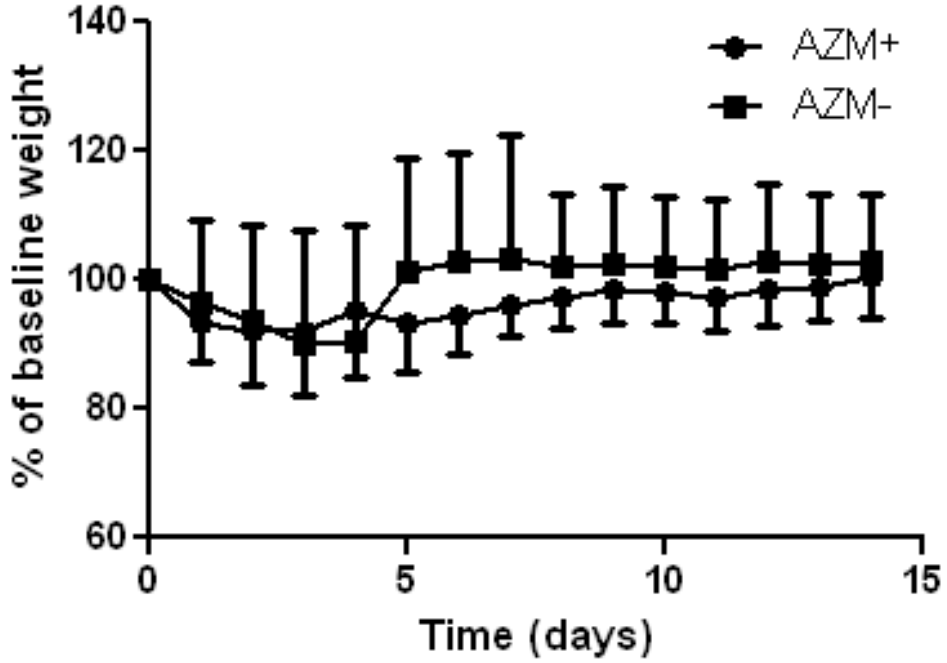

Figure 3.15. Weight loss in IL4rαKO mice treated with AZM. Mice were treated with 3.2 mg AZM or vehicle control daily beginning 4 days before infection with agarose beads containing 1.5 x 10^5 *P. aeruginosa*. Data shown is normalized to percent weight from day 0. Data represents mean ± SD, and is representative of two experiments.

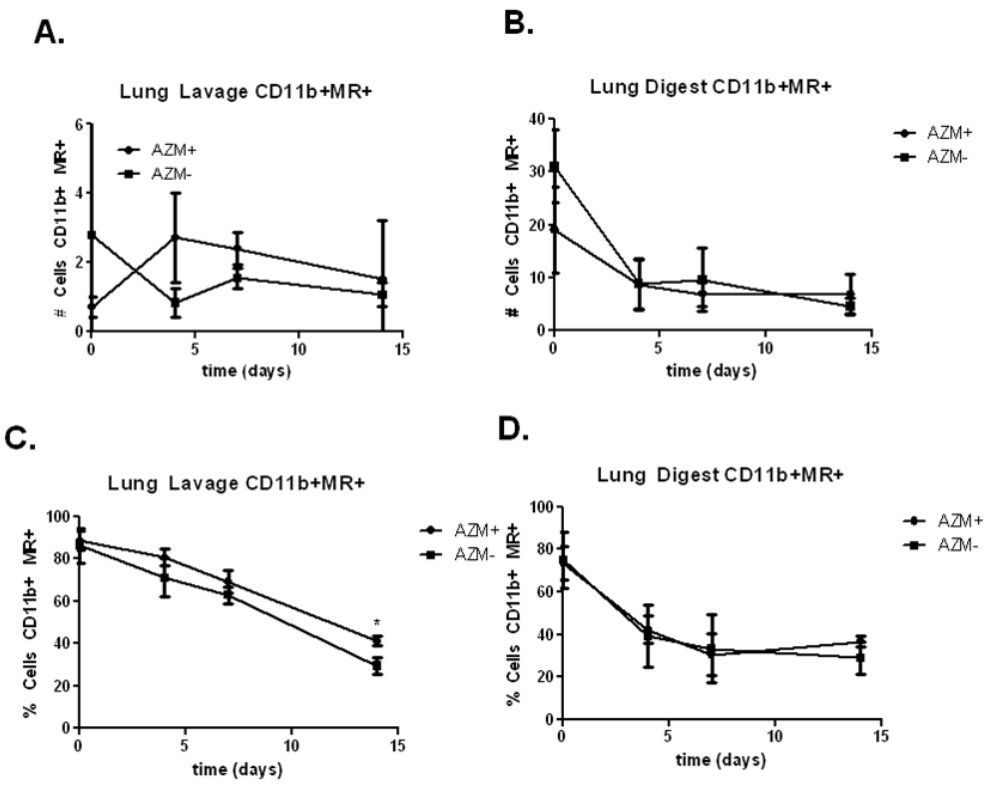

Figure 3.16. Counts and percentages of CD11b+MR+ cells in the lungs of lL4rαKO mice treated with AZM . Mice were treated with AZM or vehicle control beginning 4 days before infection with agarose beads containing 1.5 x 10^5 *P. aeruginosa*. Cell phenotypes were assessed via flow cytometry. Panels (A) and (B) represent the number of cells positive for CD11b which also expressed MR in the (A) lung lavage; (B) lung digest. Panels (C) and (D) represent the percentage of CD11b+ cells also expressing MR in the (C) lung lavage; (D) lung digest. Data represents mean ± SD from 4 mice/group. Statistical analysis was performed utilizing repeated measures ANOVA with Bonferroni's post test. Data is representative of two experiments.

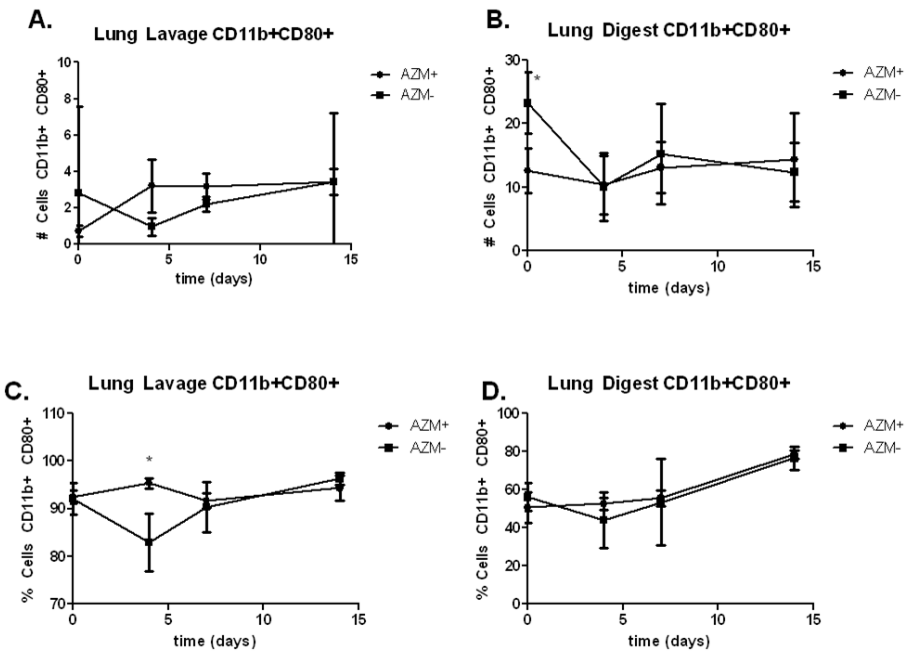

Figure 3.17. Counts and percentages of CD11b+CD80+ cells in the lungs of IL4rαKO mice treated with AZM. Mice were treated with 3.2 mg AZM or vehicle control beginning 4 days before infection with agarose beads containing 1.5 x 10^5 *P. aeruginosa*. Cell phenotypes were determined via flow cytometry. Panels (A) and (B) represent the number of cells positive for CD11b which also expressed CD80 in the (A) lung lavage; (B) lung digest. Panels (C) and (D) represent the percentage of CD11b+ cells also expressing CD80 in the (C) lung lavage; (D) lung digest. Data represents mean ± SD from 4 mice/group. Statistical analysis was performed utilizing repeated measures ANOVA with Bonferroni's post test. Data is representative of two experiments.

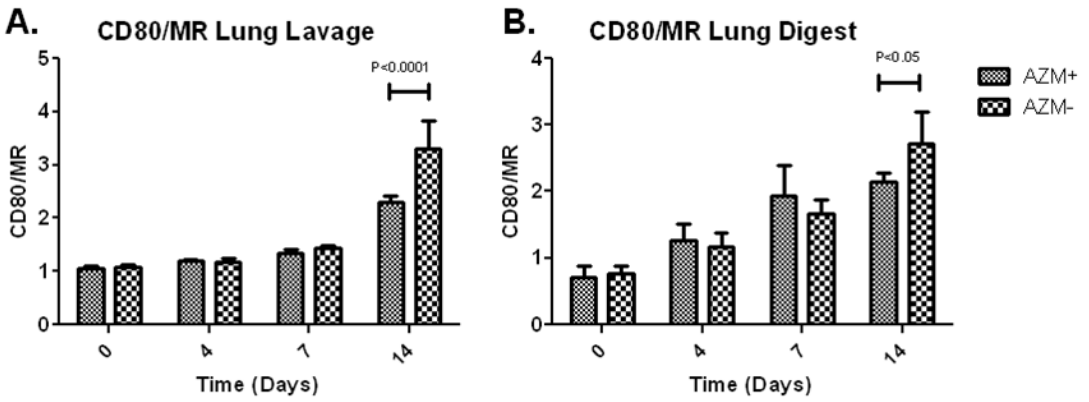

Figure 3.18. Ratio of CD80 to MR positive cells in lungs of IL4rαKO mice treated with AZM. Mice were treated with 3.2 mg AZM or vehicle control daily beginning 4 days before infection with agarose beads containing 1.5 x 10^5 *P. aeruginosa*. The number of CD11b+ cells expressing CD80 were divided by the number of CD11b+ cells expressing MR. Number of cells positive for various surface markers were determined via flow cytometry. Data represents mean ± SD from from 4 mice/group. Statistical analysis was performed utilizing repeated measures ANOVA with Bonferroni's post test. Assessing differences in ratios was utilized to determine subtle differences in net macrophage polarization.

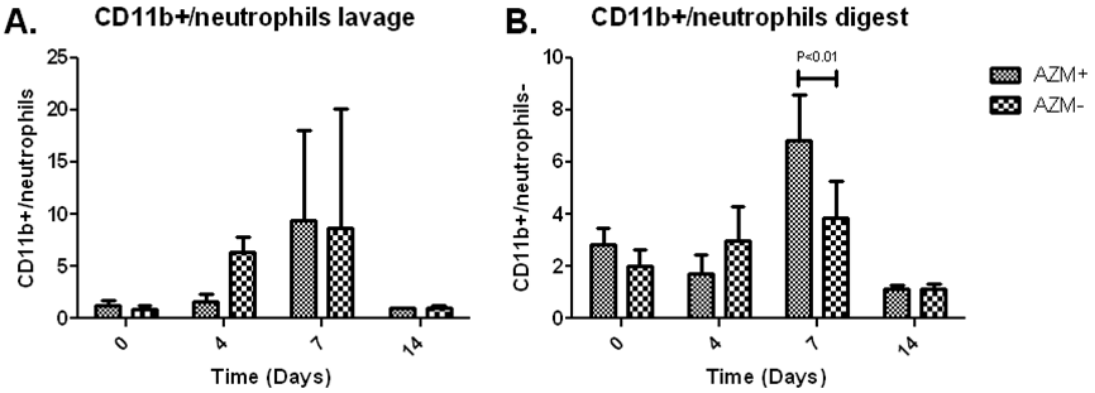

Figure 3.19. Ratio of CD11b+ cells to neutrophils in lungs of IL4rαKO mice. Mice were treated with 3.2 mg AZM or vehicle control daily beginning 4 days before infection with agarose beads containing 1.5 x 10^5 *P. aeruginosa*. The number of CD11b+GR1- cells were divided by the number of CD11b-GR1+ cells. Number of cells positive for various surface markers were determined via flow cytometry. Data represents mean ± SD from from 4 mice/group. Statistical analysis was performed utilizing repeated measures ANOVA with Bonferroni's post test.

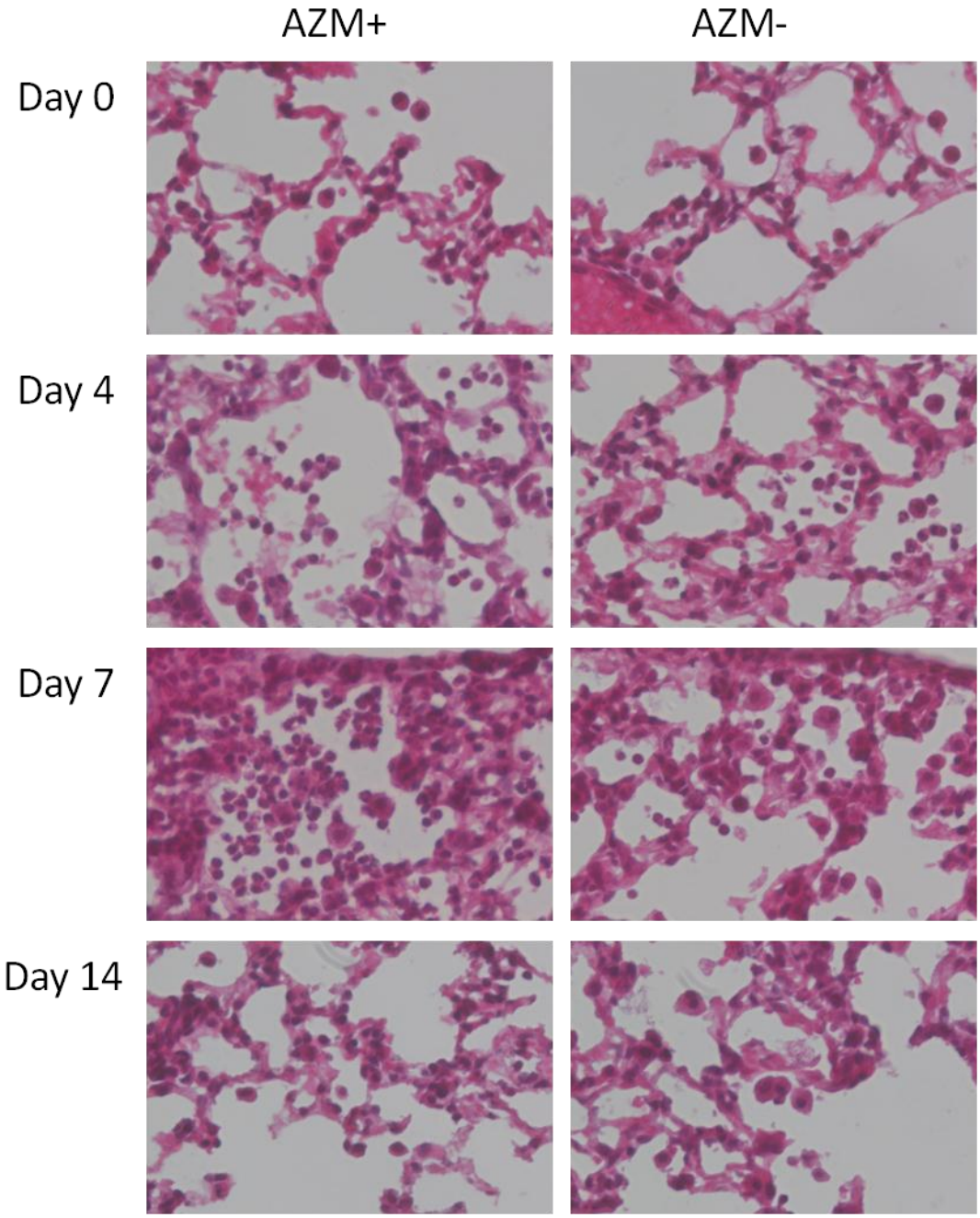

Figure 3.20. Lung sections of IL4rαKO mice treated with AZM. Mice were treated with 3.2 mg AZM daily beginning 4 days before infection with agarose beads containing *P. aeruginosa*. Lung sections were stained with H & E. Columns represent mice that did or did not receive AZM, while rows show the various days in which sections were collected.

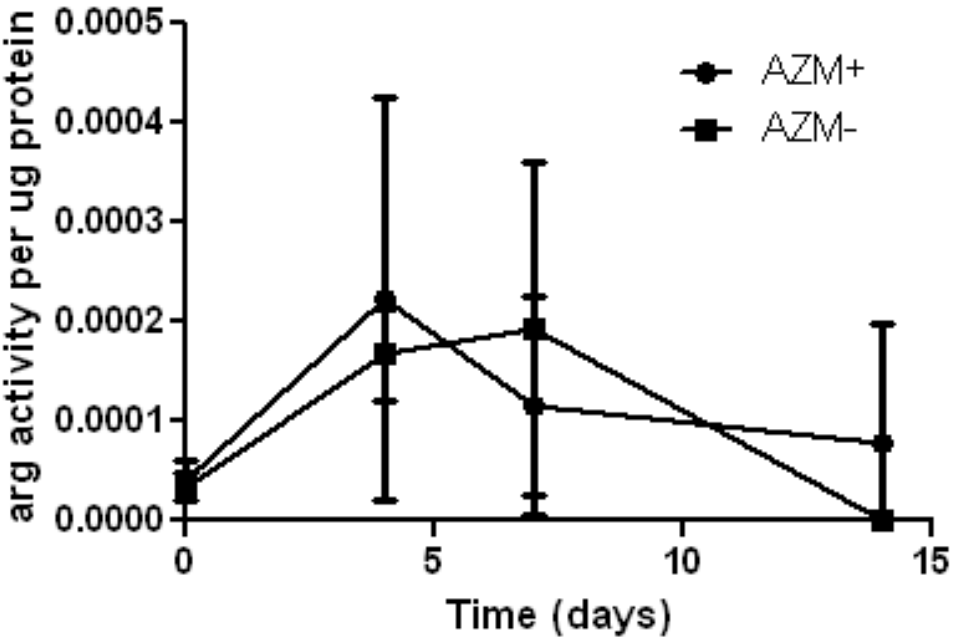

Figure 3.21. Arginase activity in IL4rαKO mice treated with AZM. Mice were treated with either 3.2 mg AZM or a vehicle control daily beginning 4 days before infection with agarose beads containing 1.5 x 10^5 *P. aeruginosa*. Lung digests were collected, lysed in RIPA buffer, and analyzed with the arginase assay. Data represents mean ± SD with four mice/group, and is representative of two experiments.

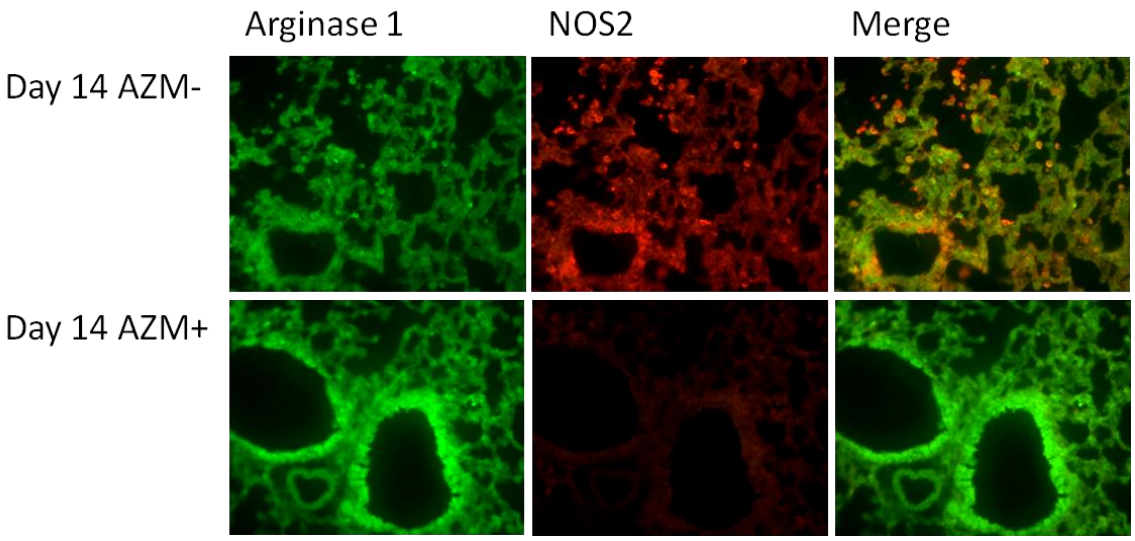

Figure 3.22. Arginase 1 and iNOS localization in IL4rαKO mice treated with AZM. Lung sections from mice 14 days post infection with agarose beads containing 1.5 x 10^5 *P. aeruginosa* were stained with primary antibodies to both arginase 1 and iNOS, with either FITC or texas red secondary staining. Panels represent arginase 1 localization, iNOS localization, and merged data, from left to right. Data representative of multiple pictures from one mouse/group. Other timepoints displayed similar results (data not shown).

Chapter 4. Correlation of macrophage-associated gene expression to clinical characteristics in patients with cystic fibrosis

A. Introduction

Chapter overview

To conclude this work we characterized the impact of chronic AZM therapy on macrophage gene expression and markers of inflammation in the lungs of patients with CF, as well as the relationship between macrophage polarization and lung function in these patients. While it has previously been shown that AZM improves markers of clinical function in patients with CF, we were interested in determining whether AZM alters macrophage phenotype in patients with stable CF, to extend our earlier findings both *in vitro* and utilizing our mouse infection model [16, 18, 20]. The data presented to this point was generated in cells and animals with functional CFTR protein, a difference that could potentially lead to difficulty in extrapolating that data to humans. To assess the impact of AZM therapy on macrophage phenotype in patients with CF, we collected sputum samples from patients at both the pediatric and adult Cystic Fibrosis clinics at the Kentucky Clinic, isolated mRNA from the cells, and correlated the gene expression to the patient's clinical status. We were primarily interested in assessing gene expression in patients who were stable in their disease. This was to assess the effect of AZM on macrophage polarization while minimizing confounding factors associated with acute infection and flare of the disease, and the changes in gene expression and cellular influx that results. We hypothesized that M2 macrophage polarization would be correlated to declines in lung function in patients with CF and that AZM therapy would additionally polarize macrophages to the M2 phenotype.

Cystic Fibrosis: a brief overview

Defects in the CFTR lead to impaired chloride reabsorption. This results in thick, dehydrated secretions in the lungs of patients with CF [11]. These thickened secretions provide an excellent breeding ground for a wide variety of

bacteria, most notably *P. aeruginosa* [11]. It is exceptionally difficult for patients with CF to clear the bacteria, and over time they are considered to be chronically colonized with the organism. The course of the disease is characterized by repeated flares of inflammation caused by acute infections, followed by repair and recovery. The cycle then repeats, causing a vicious circle of exacerbation, followed by a decline in lung function over time, which then makes it more likely that the patient will have a bacterial flare in the future [113]. These changes in lung function can be tracked in a variety of ways, most notably by assessing the forced expiratory volume in one second (FEV1), specifically the percent of the predicted value for the patient. FEV1 represents the volume of air that a patient can expel from their lungs in 1 second after fully inhaling. This value can then be compared to the expected volumes of a patient with similar age, height, and other physical parameters [114]. FEV1% predicted is commonly used as one of the key parameters in assessing disease progression in patients with CF. While the lungs are the organ in which CF symptoms are the most life-threatening, it also effects many other organ systems in patients, including the pancreas, the digestive tracts, and the reproductive tracts [22, 23]. As one would expect from a disease that affects multiple systems, patients with CF commonly receive large numbers of medications to treat the associated symptoms. This results in a significant number of potential confounding factors in any clinical study, and makes comparisons difficult. For the purposes of this dissertation, we will be focusing on medications that deal with the pulmonary symptoms of CF, as well as any immunomodulatory agents that they may be taking. Previous data from our laboratory has shown that subjects with CF displayed an inverse correlation between parameters of lung function and markers of M2 activation [115]. We found that the negative relationship in MR surface expression was more pronounced in subjects who were not colonized with *P. aeruginosa*, as compared to subjects who were colonized with *P. aeruginosa*. We also found that arginase activity was inversely correlated with lung function in subjects colonized with *P. aeruginosa*, while there was no relationship in subjects who were not colonized with the organism. We also found that these changes were associated with

changes in the Th1/Th2 balance in the lungs of these subjects [115]. While others had previously described the role of the Th1/Th2 polarization in CF, we were the first to assess macrophage polarization in these patients. This research continues our previous work to assess gene markers associated with inflammation, macrophage phenotype, and fibrosis. We hypothesized that inflammatory genes would be associated with improvements in lung function in these patients, and that AZM treatment would be associated with a shift in gene expression towards the M2 phenotype in these patients.

B. Detailed methods

Clinical design

Subjects were recruited from both the pediatric and adult cystic fibrosis clinics at the Kentucky Clinic at the University of Kentucky Chandler Medical Center, during routine clinic visits. For inclusion, patients diagnosed with CF were to be between the ages of 2-50 years, and not be in an acute exacerbation of their disease. This determination was made by the treating pulmonologist. Patients were ineligible to participate in the study if they were experiencing an acute exacerbation of their disease at the time of initial sample collection (e.g. a clinically relevant decline in FEV1% predicted since their previous appointment, or if their disease required hospitalization to treat their symptoms). Additional exclusion criteria included any active infectious process, malnutrition, HIV infection, cancer, or women who were pregnant or breastfeeding. Subjects 18 and older were consented, while the parents of subjects under the age of 18 signed parental consent forms, and the subjects signed assent forms. All patients or their legal guardians additionally signed HIPAA waivers to allow us to perform chart reviews at a later date.

Sample collection

Sputum samples were collected from patients at both the pediatric and adult cystic fibrosis clinics at the Kentucky Clinic. The University of Kentucky

Institutional review board allowed us to collect samples during normal follow up clinic visits. Patients were asked to provide a spontaneous sputum sample during the course of a routine clinic visit. Samples were collected within 30 minutes of lung function tests being performed. Samples were immediately placed on ice and transported to the laboratory, at which time 5 ml of PBS was added, followed by the addition of 5 ml of digestion buffer (0.1% DL-Dithiothreitol [Promega, Madison, WI] + 50 units/ml Deoxyribonuclease I [Sigma Aldrich, St. Louis, MO]). Samples were then incubated for 30 minutes at 37°C, with shaking every 5 minutes to aid in the digestion. After incubation, samples were centrifuged for 7 minutes at 1200 RPM. The incubation process was repeated once if the sample was deemed to still be overly viscous. Cells were enumerated, and aliquots were collected for cytospin and Diff-Quick staining. Cells were placed in RNAlater (Ambion, Austin, TX), and frozen at -80°C for subsequent analysis. Spontaneously provided sputum samples are composed of macrophages, neutrophils, and epithelial cells. Epithelial cell contamination is one of the weaknesses associated with the collection of sputum samples.

RNA isolation

Digested sputum samples were thawed and RNAlater was removed. Cells were lysed utilizing Qiashredders and RNeasy mini-kits (Qiagen, Valencia, CA), and samples were processed according to the provided protocols. Samples were initially lysed in 600ul of buffer RLT, containing guanidinium thiocyanate, and finally suspended in 30ul of nanopure water. RNA was quantified using a Nanodrop 2000 (Thermo Scientific, Wilmington, DE). RNA samples were frozen at -80°C for future analysis.

Generation of cDNA

Reverse Transcription was performed utilizing materials from Applied Biosystems (Foster City, CA). A set amount of isolated mRNA was incubated with a reverse transcriptase cocktail consisting of 5.5 mM magnesium chloride, 500μM deoxy NTP, 2.5μM random hexamers, 0.4U/μL Rnase inhibitor, 1.25U/μL

MultiScribe Reverse Transcriptase, and TAQMAN RT buffer. Incubation conditions were 10 minutes at 25°C, 30 minutes at 48°C, and finally 5 minutes at 95°C. cDNA was frozen at -80°C until ready for quantitative real-time PCR.

Quantitative real-time PCR (qRT-PCR)

qRT-PCR was performed on the samples for a variety of gene markers of M1 and M2 polarization, as well as inflammation and fibrosis. TAQMAN gene probes (Applied Biosystems, Foster City, CA) were used for analysis. A complete list of genes probed for is given in table 4.1. These genes were chosen to allow us to examine the net macrophage polarization, as well as the total inflammatory and fibrotic profile of the cells in the sputum samples. Samples were run in triplicate for each gene. The final volume for each sample was 20µL, consisting of TAQMAN universal PCR MasterMix (Applied Biosystems, Foster City, CA) and TAQMAN gene probes in concentrations suggested by the manufacturers. Samples were run utilizing an ABI 7900 HT fast real time PCR system (Applied Biosystems, Foster City, CA), and the amplification phase of the reaction was run for 50 cycles. The complete cycling parameters can be seen in table 4.2. Gene expression was calculated as 2^-(average C_t gene of interest-average C_t GAPDH).

Statistical analyses

Principal component analysis (PCA) was performed as a method of data reduction utilizing the statistical software package SPSS (IBM, Chicago, IL). PCA allows the creation of new variables comprised of combinations of the previously collected data. These new variables are weighted based off of the correlations between the various genes. The output is designed such that the first newly generated variable (or “component”) explains the highest amount of the total variance between the initial genes; the second component explains the next highest amount of total variance, and so forth. Generated components were deemed to explain a significant amount of the total variance if they had an eigenvalue greater than 1. Additional statistical analysis was performed utilizing

Graphpad Prism (GraphPad software, La Jolla, CA). Comparisons between groups was made via one way ANOVA with Tukey's multiple comparison test for ratio level data, and by Fisher's exact test for nominal data.

C. Results and discussion

Subject demographics

Thirty patients were recruited for the study, with a total of 66 samples collected from September 2009 to December 2010. We collected 30 original samples, 18 first follow-up samples, 12 second follow-up samples, 4 third follow-up samples, and 1 fourth follow-up sample. Subject demographics are shown in Table 4.3. Of particular note is the large percentage of patients that are taking AZM. While not yet considered as standard of care, AZM's use is wide-spread in patients with CF who are chronically colonized with Pseudomonas, a practice that is anticipated to become standard of care in the near future [14]. Additionally we observed that a large number of our subjects were receiving other antibiotics to control their disease progression. This is commonly done by utilizing two antibiotics in an alternating month schedule, to attempt to prevent acute exacerbations of their disease. Treatment with other antibiotics may conceivably be altering macrophage polarization and therefore confounding our results. Interestingly, among our subject population was a higher percentage of individuals who were colonized with *S. aureus* than patients who were colonized with *P. aeruginosa*. This is most likely due to the large amount of patients that we have in the study who are under the age of 18. While *P. aeruginosa* eventually becomes the most significant pathogens in patients with CF, younger patients are more likely to be colonized with *S. aureus* [11]. And, *S. aureus* is considered an emerging pathogen in this patient population, as the incidence of colonization and infection grows [116].

Correlations between macrophage, inflammatory, and fibrotic gene markers

We first assessed whether there were linear correlations between gene markers of macrophage phenotype, and markers of inflammation and fibrosis. While the relationship between macrophage polarization and expression of various inflammatory and fibrotic markers has been established in many disease states, there is no evidence examining gene expression from cells isolated from the lungs of subjects with CF. We first assessed the correlations between all of our gene expression values, to attempt to find significant relationships. We first assessed the correlation between TLR4, a marker of M1 activation, and the inflammatory marker IL1α and the pro-fibrotic marker TGFβ. We found a linear correlation between TLR4 and IL1α gene expression (Figure 4.1 A.) (R^2=0.3901, p<0.0001). This confirms the relationship that others have shown between markers of M1 activation and inflammatory cytokine production. We observed similar findings between TLR4 and TGFβ (Figure 4.1 B.) (R^2=0.5037, p<0.0001). While at first glance it may seem counterintuitive to find a linear relationship between a marker of M1 macrophage activation and an anti-inflammatory, pro-fibrotic marker, it is important to note that when subjects are not in an acute exacerbation of their disease, there is homeostasis that occurs in the lungs of these subjects in a balance of both pro- and anti-inflammatory markers. We also found a linear relationship between gene expression of the pro-inflammatory cytokine TNFα and the fibrotic protein fibronectin (Figure 4.1 C.) (R^2=0.2575, p<0.0001). Much of the reason for damage that occurs in the lungs of patients with CF is due to an overly zealous initial inflammatory response. One of the potential methods by which AZM improves lung function in these subjects is by shifting macrophage polarization from the M1 to the M2 phenotype, and decreasing the amount of damage done by the initial inflammatory response to an infection.

We next examined the relationship between markers of M2 activation and genes associated with fibrosis. We were interested in determining if markers of alternative macrophage polarization correlated with fibrotic markers in our subject population, including subjects taking AZM. We found a linear relationship between CCL-18, and fibronectin gene expression (Figure 4.1 D.) (R^2=0.3341,

$p<0.0001$). We found an extremely strong linear relationship between MR and fibronectin gene expression (Figure 4.1 E.) ($R^2=0.8981$, $p<0.0001$). CCL-18 is upregulated in M2 macrophages, resulting in chemotaxis of T-cells and activated monocytes and dendritic cells [117]. While not surprising, it is encouraging to see that this relationship still holds strong in the lungs of subjects with CF. As we have seen previously, this relationship seemingly suggests that an M2 macrophage polarization may exert a deleterious effect on the lungs of subjects with CF, and seems to imply that AZM is not beneficial in these subjects. Again, however, the other possibility is that AZM is blunting the initial inflammatory response to infections in the lungs of subjects with CF, resulting in less damage to be repaired in the lungs of these subjects. Finally, we found a linear relationship between gene expression of MR and IL10 (Figure 4.1 F.) ($R^2=0.2411$, $p<0.0001$). While not surprising, it is encouraging to observe that gene expression of the anti-inflammatory cytokine IL10 was correlated with gene expression of markers of M2 macrophage activation. We did not observe any other significant relationships for the expression of these genes. This again shows that the M2 macrophages that we observe in subjects with CF are phenotypically similar to M2 macrophages that have been observed by others.

Impact of azithromycin treatment and age on gene expression, clinical parameters

We next assessed the impact of clinical parameters, including treatment with AZM, upon gene expression associated with macrophage polarization. We did this by utilizing data not only from initial visits, but from all subject samples collected. By doing so we were able to increase the power of our analysis. Additionally, it was necessary to do this in order to increase the number of samples from subjects not on AZM. We first examined differences in lung function between subject groups stratified by various parameters. Figure 4.2 A. shows FEV1% predicted for subjects stratified on the basis of AZM therapy at the time of sample collection. We found that FEV1% predicted in patients taking AZM was statistically significantly lower than that of patients who were not

receiving AZM. This is almost certainly due to the fact that as patients advance in their disease progression, they are more likely to be placed upon long-term AZM therapy. Similarly, adult patients displayed significantly decreased FEV1% predicted when compared to pediatric patients (Figure 4.2 B.). Again, this difference is likely due to routine decline in lung functions that occur as patients age. Finally, figure 4.2 C. depicts the impact of stratification by AZM therapy in both age groups individually. Here we can see that most of the differences in FEV1 % predicted observed in the previous two graphs lie within the pediatric subgroup. There were essentially no differences between adult patients receiving or not receiving AZM. However, the low number of samples from adult patients who were not receiving AZM makes comparisons difficult, as the chance of a type II error is high.

We next assessed NOS2 and ARG1 gene expression in our patient populations. NOS2 is widely considered to be one of the prototypical markers of classical macrophage activation [1, 3]. ARG1 is similarly considered to be a marker of M2 activation in mice, there is, however, evidence that it may be a less significant marker of M2 activation in humans [118]. Figure 4.3 A. shows differences in NOS2 gene expression between subjects who either did or did not receive AZM. We found a significantly lower expression of NOS2 in subjects treated with AZM. We observed the opposite trends for ARG1 gene expression, as it was increased in subjects receiving AZM (Figure 4.3 B.). While we did not observe statistically significant differences between the two groups for ARG1 gene expression, this may be due to having insufficient power to detect the differences between the two groups. Due to the time consuming nature of subject recruitment, as well as the expense associated with processing subject samples, we limited ourselves to 30 subjects for this study.

When we separated the samples not only by AZM status, but additionally stratifying subjects by age, additional interesting observations were made. In figure 4.3 C. we can see that the difference in NOS2 gene expression is most pronounced in our pediatric subjects, with almost all of our pediatric subjects

receiving AZM having little to no gene expression of NOS2. When we examined ARG1 gene expression, however, we found that this difference is most pronounced in our adult subject population, and less pronounced in our pediatric population. While we did notice trends in ARG1 gene expression in our adult subjects who were either on or off AZM, we did not observe significant differences. These two findings suggest that AZM is able to polarize macrophages to an alternatively activated phenotype in the sputum samples that we collected. It is important to note that there is a great deal of variability in gene expression between our various samples, which may explain the difficulty that we had to obtain statistical differences between the groups.

We then compared expression of other inflammatory, fibrotic, and M2 genes between subject groups stratified on the basis and AZM treatment. We found a trend towards a decrease in gene expression for the pro-inflammatory cytokine IL1α (Figure 4.4 A.) ($p=0.1241$), suggesting that AZM may be decreasing pro-inflammatory cytokine expression among our subject population. We also found a non-significant decrease in fibronectin gene expression (Figure 4.4 B.) ($p=0.2947$). When we assessed other gene markers for M2 activation, we found no differences in CCL18 gene expression (Figure 4.4 C.), and a slight decrease in MR gene expression (Figure 4.4 D.) ($p=0.0835$). The slight decrease in IL1α gene expression in subjects who were receiving AZM further describes ways that AZM appears to benefit these subjects. More difficult to explain, however, is that we observed no differences in gene expression for CCL18, and even a slight decrease in MR gene expression in subjects treated with AZM. It is possible that this is due more to the types of subjects who are likely to be receiving AZM, e.g. subjects with more severe declines in lung function are more likely to have impaired expression of the genes that we assessed. The small degree of differences that we observed, well above statistical significance, however, makes it difficult to truly assess any differences among these samples.

Finally we assessed gene expression related to the clinical parameters used to measure lung function and disease progression, FEV1 and FVC (forced vital capacity) % predicted. While we did not observe significant correlations among any of the gene expression values and FEV1% predicted, we did find significant linear correlations between FVC % predicted and the inflammatory cytokines IL1α and TNFα (Figure 4.5 A. and figure 4.5 B.). This suggests that declines in lung function are associated with a decrease in gene expression for these pro-inflammatory M1 related cytokines. This can potentially be explained by the shift that occurs over time in the lungs of CF subjects from a Th1 dominant polarization to more of a Th2 polarization. It may also be due to a decline in the number of cells in the lungs of subjects who have been long colonized with bacteria, with a resulting decrease in the mRNA that we were able to collect from the subjects. It may also be due to changes in the profiles of cells that are present in the lungs of the subjects as lung function declines. Interestingly, we also found a linear correlation between FVC % predicted and gene expression of the anti-inflammatory cytokine IL10 (Figure 4.5 C.). This gene is most likely upregulated in order to ensure that the inflammatory response does not become dysregulated. Similarly to the inflammatory cytokines, it may also be a response that as lung function declines in subjects with CF the cells are less robust than they are in subjects with better lung function.

Principal component analysis and gene grouping

To this point, we have been able to make observations in how the expression of certain genes of interest varies among our subjects, and how gene expression indicative of macrophage phenotype polarization relates to markers of inflammation, fibrosis, and clinical indices. However, these previous analyses do not present a robust profile that can correlate a certain macrophage gene expression profile to the clinical parameters (including AZM therapy) of our subject population. In order to determine whether such a description can be purported, we utilized principle component analysis (PCA) to simultaneously examine the expression variability of all genes measured.

An initial round of PCA was performed using the gene data from the initial clinic visit for each subject only. This is because PCA requires independence among all data measurements. All 15 genes of interest were included in the first round of analysis. This first round of PCA created 5 components. The weighting of genes in each component for this analysis shown in Table 4.4. Component 1 accounted for 32% of the total variance of the gene samples, while component 2 accounted for an additional 18% of the total variance. Components 3, 4, and 5 explained an additional 12%, 10%, and 7% of the total variance for these genes, respectively. We found 4 genes with a high weighting in component 1 and a low weighting in component 2. Conversely, we determined that an additional 4 genes were weighted high in component 2, and a low in component 1. These groupings explain genes with expression that vary in a similar manner, showing that these genes are associated with each other.

This is especially interesting when one considers the function of the genes that were grouped together in the process of creating the first 2 components. The genes MMP9, NOS2, TGFB, and TLR4 had high weighting in component 1 and low weighting in component 2. NOS2 and TLR4 both are traditionally associated with the M1 phenotype [3]. CCL18, fibronectin, IL12b, and MR were highly weighted in component 2, and had a low weighting in component 1. CCL18, fibronectin, and MR are traditionally associated with the M2 phenotype [3]. That the gene weightings generally grouped in a manner consistent with either an M1 or M2 activation confirms the validity of utilizing PCA. Component 1 did contain some M2 associated genes, contrariwise component 2 contained some genes traditionally associated with inflammation. It is important to note, however, that the inflammatory profile in the lungs of these patients is dynamic. Anti-inflammatory genes may be up-regulated in the aftermath of an inflammatory flare, and vice versa. Interestingly, arginase 1 was not strongly associated with any of the components. This is consistent with findings from others suggesting that while arginase 1 is an important marker of macrophage polarization in mice, it may be a less important marker in humans [118]. We did, however, find other

markers that are traditionally associated with the M2 phenotype were highly weighted into component 2.

We next performed an additional round of PCA utilizing only the genes that were highly weighted in either component 1 or component 2. The previous round of PCA produced gene weighting that varied similarly among subject samples. The second round was performed to allow us to focus just on the most significant genes that we assessed. The gene weightings from the second round of PCA are presented in figure 4.5. Utilizing the restricted gene set, 2 components were generated. These two components were responsible for 39% and 34% of the total variance among the 8 genes in the restricted gene set, respectively. The weightings from these two components were utilized to generate individual values for each sample. These two generated components were utilized for the next series of analysis.

Subject clinical data stratified via PCA components

We plotted the values for components 1 and 2 for each initial subject visit, as shown in figure 4.6. One of the basic assumptions of PCA is that each component is orthogonal to every other component; that is, there should be no correlations between individual components. This allows us to graph the two components, and determine if individual subjects group together. We found that the subject samples sorted into three distinct groups. There was first a group of subjects that had low values for both component 1 and component 2. It is reasonable to assume that macrophages in these patients were not polarized to either the M1 or M2 phenotype. Next, there was a group of subjects that had a higher value in component 1 than component 2. These patients are considered to have had a macrophage profile that was polarized more toward that of an M1 phenotype. Finally, there was a group of subjects that had a higher value in component 2 than component 1. The macrophage populations of these individuals can be considered to have a net M2 polarization.

We first assessed AZM status in each of the three groups to see if this differed according to macrophage gene expression status. Figure 4.7 A. shows the percentage of patients in each of the three groups that were taking AZM. According to these results, AZM therapy did not influence the gene expression profile as stratified by PCA ($p=0.6465$, Fisher's Exact Test). It is important to note, however, that the percentage of patients taking AZM was extremely high in all three groups. As patient lung function declines, clinicians at the University of Kentucky CF clinics are extremely likely to place the patients on the drug. Due to this, it made it difficult to assess the impact of AZM therapy in this analysis.

Figure 4.7 B. shows the average age of subjects in the three groups. We found that patients with a high PC2 value (M2-biased) were significantly older than patients who were high in PC1 (M1-biased). This is consistent with data in the literature showing that a Th2 polarization increasingly persists in the lungs of patients with CF as they age [32]. This Th2 polarization likely would correlate with an increase in polarization of macrophages to the M2 phenotype, and suggests a possible explanation for why we observed that patients who had higher gene expression of M2 markers were significantly older than patients with high gene expression of M1 markers.

We next compared lung function of subjects in the three groups. Figure 4.8 A. shows that there were no differences in the mean FEV1% predicted between the three groups. Figure 4.8 B. shows the FVC % predicted. Here again we did not observe a difference in this parameter between the three groups. We had initially anticipated that there would be differences between the component 1 high and the component 2 high groups. This data suggests that macrophage phenotype does not correlate to baseline lung disease severity in these patients, as analyzed by this variable reduction process.

We then compared additional antibiotic use among the three groups. Patients with CF are routinely placed on other antibiotics as a means to either treat acute exacerbations or limit their incidence. Figure 4.9 shows non-AZM antibiotic use between the three groups. We first assessed the percentages of

patients receiving oral and IV antibiotics other than AZM for their disease (Figure 4.9 A.). We found that patients that had high values for component 2 were less likely to be taking other antibiotics than patients with low values for both components (Fisher's Exact Test, p=0.0932). We observed a similar trend in patients with high values in component 1 (p=0.0809), but the results were not significant, due in part to the relatively small number of patients in the group. We next assessed the percentages of subjects receiving inhaled tobramycin therapy (Figure 4.9 B.). Inhaled tobramycin is commonly used to control pulmonary infections in patients with CF, most notably for patients colonized with *P. aeruginosa* [14]. We observed similar trends in inhaled tobramycin usage as we did in the non-AZM antibiotic usage in these subjects. Namely, patients with high values for component 2 appeared to be less likely to receive inhaled tobramycin than patients with either high values in component 1 or with low values for both components. There are a few possible explanations for this. First, patients with either polarization to the M1 or M2 phenotype may be innately more stable in their disease, and be less likely to require other antibiotics than patients whose macrophages are inactive. Second, treatment with other antibiotics may be helping to keep bacteria at a state where a robust macrophage response of either phenotype may not be necessary. Unfortunately, due to the nature of the data that we collected for this study, it is impossible to determine which of these two possibilities is the case for our patients with CF.

Lastly, we assessed the bacterial colonization status among our PCA-stratified subject groups. Figure 4.10 presents the percentages of subjects that were colonized with either *P. aeruginosa* or *S. aureus*. Due primarily to the difficulty that CF patients experience in clearing infectious pathogens from their lungs once they have been infected, subjects were deemed to be colonized with one of the two bacteria if the last recorded sputum cultures in their charts showed a positive culture. We did not find statistically significant differences in bacterial colonization between the three groups. One of the initial assumptions of PCA (sample independence) prevented us from utilizing all 66 of our samples, restricting us to just the initial visits for the 30 subjects. The smaller number of

samples likely prevented us from being able to find significant differences between the three groups. The trends that we observed, however, were very intriguing. Most interestingly, subjects with high values in component 2 were more likely to be colonized with *P. aeruginosa*, but less likely to be colonized with *S. aureus*. The reason for these differences in bacterial colonization status is unclear. When considering our population, subjects with high values for component 2 were significantly older than patients with high values for component 1. *P. aeruginosa* becomes the most significant pathogen in patients with CF as they age, with studies suggesting colonization rates in excess of 80% in adult patients [11]. Contrariwise, younger subjects are more likely to be colonized with *S. aureus* [11]. There is also evidence that the microbial infection patterns are changing across the United States in subjects with CF. One of these shifts is a greatly increased rate of colonization (upwards of 20%) with *S. aureus*, especially MRSA [116, 119]. Additionally, evidence exists that the rates of *P. aeruginosa* colonization have been declining in patients with CF, on the order of 5-6% in most patient age ranges over the time span from 1995-2005 [116]. These differences in bacterial colonization rates in patients over time may suggest a possible explanation for the differences seen in the three groups. Another possibility, however, is that the pathogens themselves are playing a role in macrophage polarization, or that different macrophage polarizations may be more beneficial in subjects colonized with one of these two pathogens.

D. Conclusions

General Conclusions

In these experiments we present data suggesting a possible mechanism by which AZM benefits patients with CF. By utilizing PCA, we were able to observe 2 distinct gene groupings consistent with an M1 or an M2 macrophage polarization. By utilizing these two distinct components, we were able to place our subjects into three different groups, and assess clinical parameters for these subjects. Disappointingly, we were not able to determine whether AZM treatment correlated with one or more groups. We believe that this is primarily due to the

high prevalence of subjects receiving AZM in our study. Future consideration of the duration of treatment with AZM for subjects may enhance this analysis. It was also intriguing that we did not observe differences in FEV1 % predicted between the three groups. While we focus on the role of AZM in these subjects, there are also a wide variety of other treatments that these subjects are taking to improve their lung function, both pharmacologic and non-pharmacologic, and the effects of these other treatments may be overwhelming our ability to tease out the effects of AZM. While AZM therapy did not influence the stratification of subjects here based upon macrophage-related gene expression, it has been shown by others in the past to improve parameters in patients with CF [16, 18, 20]. We were, however, able to show gene groupings that are consistent with either an M1 or an M2 macrophage polarization. This suggests that differences in macrophage polarization do exist in these subjects.

It was also interesting to observe the gene groupings in our two principal components. Our first component consisted of MMP9, NOS2, TGFB, and TLR4. NOS2 and TLR4 have traditionally been very strongly associated with the M1 phenotype. MMP9, a metalloprotease, is associated with cleavage of the fibrotic proteins, and can be considered in terms of its role as a marker of remodeling and ECM turnover. While it has been linked to the M1 phenotype in the past, this data further links MMP9 with other M1 associated genes. PCA groups genes with similar variances, and finding MMP9 associated with genes strongly associated with the M1 phenotype strongly suggests that MMP9 gene expression is upregulated as part of the gene expression profile of M1 macrophages. In our second principal component, we found strong weightings for the genes CCL18, fibronectin, IL12b, and MR. CCL18 and MR have traditionally been strongly associated with the M2 phenotype. Finding fibronectin expression to be associated with other M2 associated genes was additionally not particularly surprising. This upregulation in fibronectin expression associated with M2 macrophages could additionally explain why the Th2 phenotype is associated with declining function in subjects with CF as they age.

Most intriguing are the differences that we observed in bacterial colonization status for subjects in the three groups, as well as the differences that we observed in age between the three groups. Subjects with high values for M2 gene markers were significantly older than subjects with high values for M1 gene markers, suggesting a shift towards the M2 phenotype as subjects age. While consistent with observations from others showing a Th2 polarization over time in patients with CF, it was interesting to see that this observation holds true for macrophages as well. Additionally, the differences we observed in bacterial colonization status may illustrate the shifting patterns of bacterial colonization that is occurring in patients with CF. Differences in bacterial colonization may also be driving differences that we observe in macrophage polarization.

At first glance, much of this data seems to suggest that treatment with AZM may be deleterious in many patients. Namely, we showed that in our subject population, pro-inflammatory cytokine gene expression was increased with higher values for lung function. Treatment with AZM results in decreased inflammatory markers as well as an upregulation in a cell type that produces fibrotic proteins. This would seem to suggest that AZM may potentially result in harm in patients with CF. However, we also observed that AZM resulted in decreases in NOS2 gene expression. The M2 shift, therefore, results in a decrease of genes necessary for the oxidative burst to destroy bacteria. This oxidative burst, however, leads to damage in the airway, both during an acute flare of the disease, and during the resting state of the disorder. In light of the beneficial effects that patients with CF have long reported with AZM, another possibility presents itself. By shifting macrophage polarization away from the inflammatory M1 phenotype, and towards the pro-fibrotic M2 phenotype, this may be resulting in less oxidative damage occurring in the lungs of these patients. The decrease in damage may then result in less need for repair from the M2 phenotype, and a resultant decrease in scarring and fibrosis.

Limitations

There are several limitations associated with the data generated here. First, not all patients with CF are able to provide sputum samples. Sputum production becomes more likely as subjects age. Very young patients, as well as patients with mild disease are less likely to be sputum producers. Thus, while our age range for subjects in our study was technically between the ages of 2-50, the youngest subject that we recruited in the study was in fact 8 years old. This also results in our data being skewed towards older, less healthy subjects. This is also in part likely one of the reasons why a large amount of our subjects were on AZM.

Additionally, there is considerable variability in the quality of sputum samples that subjects provide. While sputum samples consist predominately of monocytes, macrophages, and neutrophils, low-quality samples can also have considerable epithelial cell contamination. Some studies exist that suggest that the percentage of epithelial cells in collected sputum samples in patients may range from 20%-50% [120, 121]. Additionally, for gene analysis, having mRNA from a more representative sampling of cells in the lungs might allow us a better picture of the inflammatory and fibrotic state of these subjects.

The ideal method for acquiring cell from the lungs of patients is by bronchoalveolar lavage fluid (BALF). BALF samples are considerably more pure, with a much higher percentage of monocytes and macrophages than sputum samples, and essentially no epithelial cells [122]. This procedure, however, is extremely invasive, requiring specialized training, as well as heavy anesthesia. Additionally, there are risks associated, including fever, pneumonitis, bleeding, and bronchospasm [123]. This results in BAL primarily being perfomed for patients who have been admitted to the hospital for an acute exacerbation of their disease. Since we were interested in the status of patients who were at a baseline state of pulmonary function, we were unable to collect samples in this manner. Ultimately, we felt that the disadvantages of collecting only sputum samples from these patients were outweighed by the advantages of being able to easily collect cells in a minimally invasive manner during a routine clinic visit.

We were additionally surprised to observe that such a large amount of our subjects were taking AZM. From our previous work, we had anticipated that we would have fewer subjects that were taking the drug. In our previous studies we found that only 65% of the subjects were taking AZM [115]. Here, almost 80% of our subjects were being treated with AZM. The high rate of AZM usage in our subjects made it difficult to determine the significance of the impact that the drug may exert on macrophage gene expression. We hope in the future to be able to have subjects stop taking AZM, and compare gene expression in the subjects when they are on AZM to when they are not receiving the agent.

We were unable to record the duration that subjects were taking AZM due to the nature of our chart reviews. It would have been interesting to assess how duration of AZM treatment in our subjects grouped with our principal component analysis, to determine whether duration of AZM treatment was associated with gene expression in our subjects. Additionally, we were unable to take subjects off of AZM for the purposes of our study. We plan to do this in the future.

Gene	Type of Gene	Abbreviation	Product #
Inducible Nitric Oxide Synthase	M1 Marker	NOS2	Hs01075529_m1
Toll-Like Receptor 4	M1 Marker	TLR4	Hs00152939_m1
Arginase 1	M2 marker	ARG1	Hs00163660_m1
Matrix metallopeptidase 9	M2 marker	MMP9	Hs00234579_m1
CCL-18	M2 Marker	CCL18	Hs00268113_m1
Mannose Receptor 1	M2 Marker	MR1	Hs00267207_m1
Arginase II	M2 marker?	ARG2	Hs00982833_m1
Tumor Necrosis Factor alpha	Pro-Inflammatory	TNF	Hs00174128_m1
Interleukin 1α	Pro-Inflammatory	IL1A	Hs00174092_m1
Interleukin 12a	Pro-Inflammatory	IL12A	Hs00168405_m1
Interleukin 12b	Pro-Inflammatory	IL12B	Hs00233688_m1
Interleukin 10	Anti-Inflammatory	IL10	Hs00961622_m1
Transforming Growth Factor beta	Anti-Inflammatory	TGFB1	Hs00998133_m1
Collagen 1A1	Fibrotic Marker	COL1A1	Hs00164004_m1
GAPDH	Housekeeping gene	GAPDH	4333764f

Table 4.1. List of genes utilized for qRT-PCR. Data also includes classification of the role of the gene, the abbreviation utilized throughout this chapter, and the product number.

Temperature (°C)	Duration	Number of Cycles
50	2 minutes	1
95	10 minutes	1
95	15 seconds	50
60	1 minute	

Table 4.2. Cycling parameters utilized for qRT-PCR

Patient Age: median (range)	16 (8, 48)
Percent Male	66%
Percentage under 18	66%
Percentage taking azithromycin	76%
FEV1% predicted: median (range)	55% (23%-116%)
FVC% predicted: median (range)	72% (33%-133%)
Percentage colonized with *P. aeruginosa*	53%
Percentage colonized with *S. aureus*	66%
Percentage receiving other antibiotics	40%
Percentage complaining of shortness of breath	43%

Table 4.3. Demographics of subjects enrolled in the study.

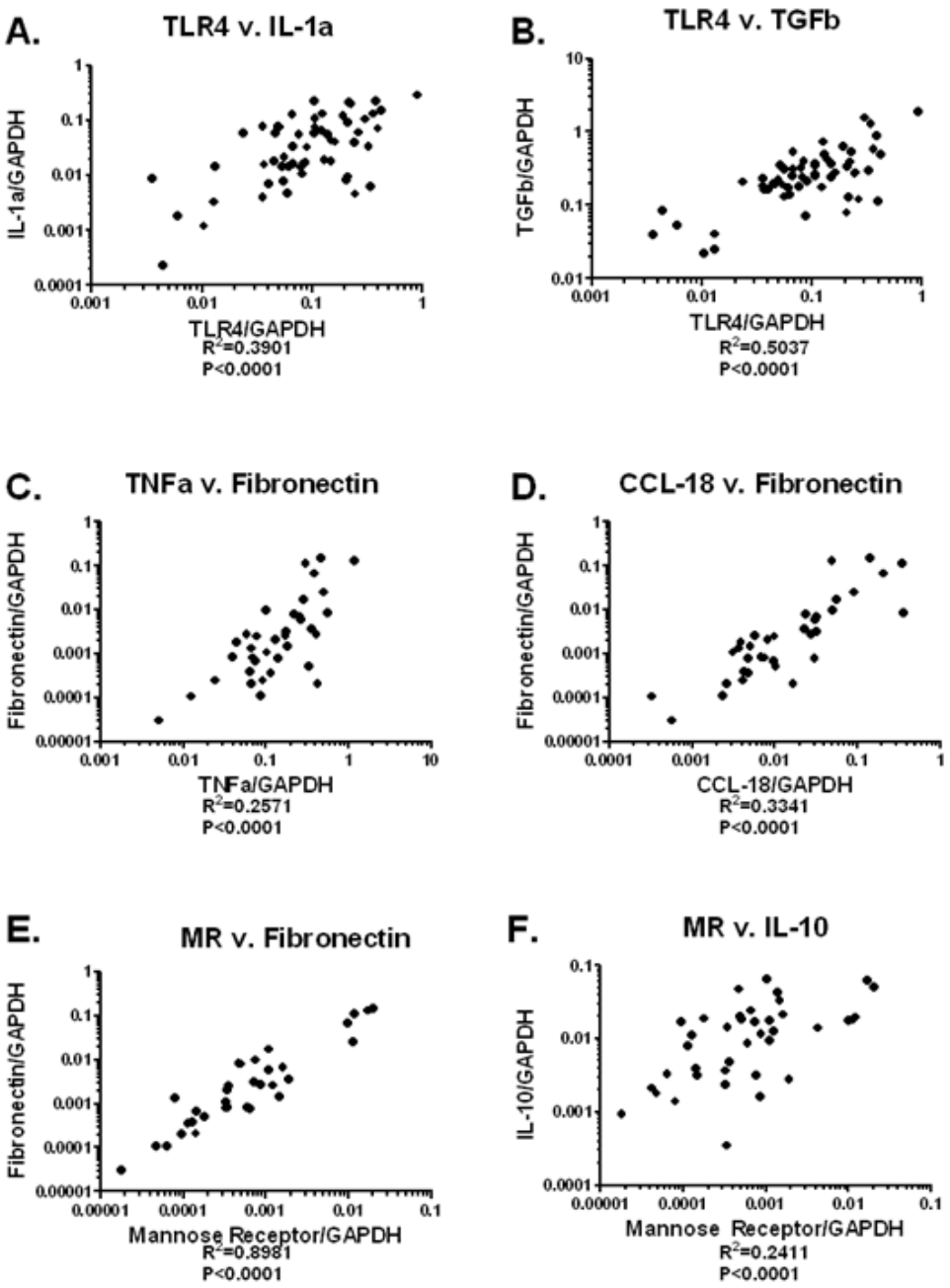

Figure 4.1. Gene expression correlations in sputum samples from subjects with CF. Sputum samples from CF patients were collected, and mRNA was isolated. Gene expression was assessed via qRT-PCR, and values for the genes of interest were normalized to expression of the housekeeping gene GAPDH. Panels represent (A) Correlation between TLR4 and IL1α; (B) TLR4 and TGFβ; (C) TNFα and fibronectin; (D) CCL-18 and fibronectin; (E) MR and fibronectin; and (F) MR and IL10. Gene samples were run in triplicate, and average value for each gene was plotted. R square and p values are listed below each graph. Linear regularity was assessed with Graphpad Prism.

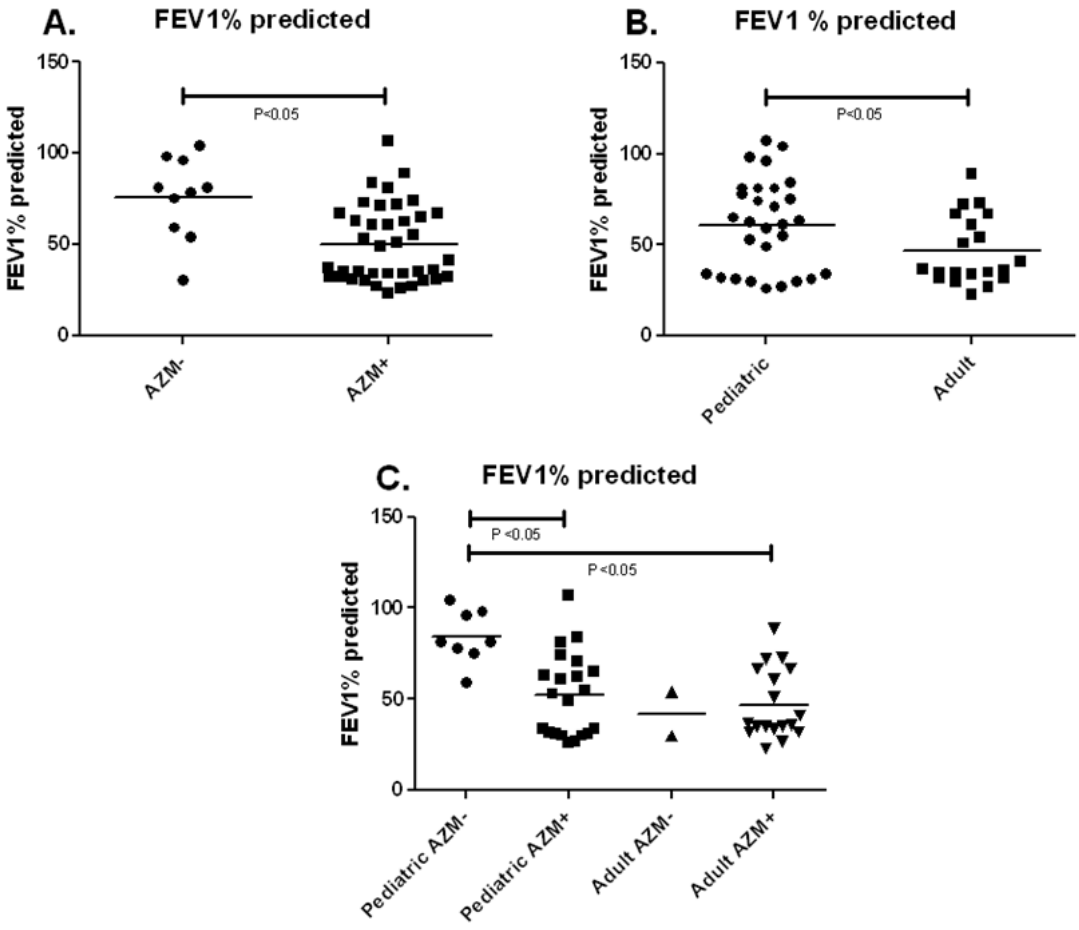

Figure 4.2. FEV1% predicted compared for both subject AZM status and subject age. FEV1 % predicted was compared to (A) AZM usage; (B) subject age; (C) both age and AZM usage. FEV1% predicted was collected from chart review. Statistical analysis was performed via either an unpaired t-test, or a one-way ANOVA with Tukey's multiple comparison test, where appropriate. Differences were deemed to be statistically significant with a p value <0.05

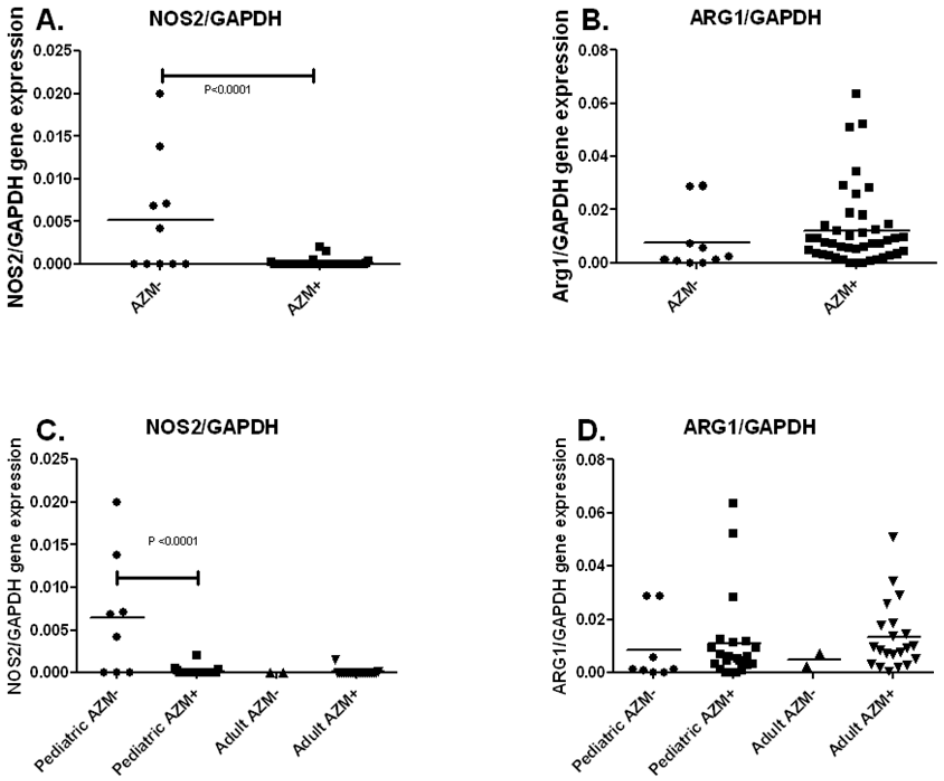

Figure 4.3. Expression of prototypical M1 and M2 genes in subjects receiving AZM. Sputum samples from subjects with CF were collected, and mRNA isolated. Gene expression was assessed via qRT-PCR, and normalized to the housekeeping gene GAPDH. Panels (A) and (B) are stratified to AZM usage, and are compared to either (A) the M1 gene marker NOS2; or (B) the M2 gene marker ARG1. Panels (C) and (D) are stratified with both AZM usage and subject age, and are compared to (C) NOS2; or (D) ARG1. Statistical analysis was performed via either an unpaired t-test, or a one way ANOVA with Tukey's multiple comparison, where appropriate. Differences were deemed statistically significant with a p value <0.05.

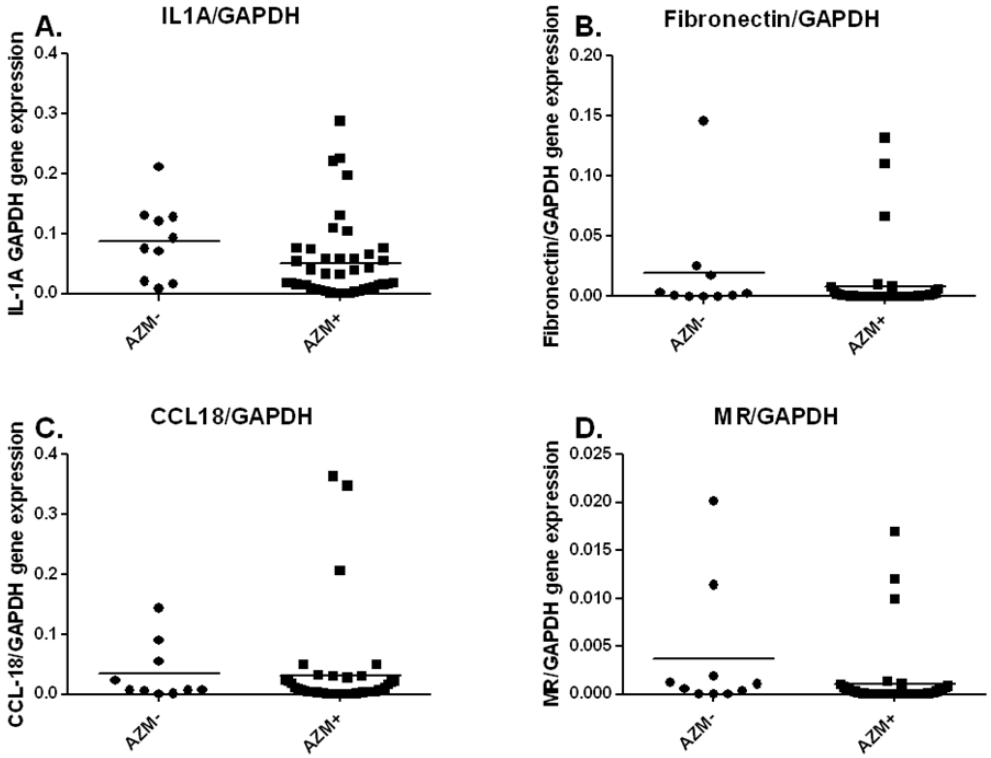

Figure 4.4. Gene expression of M1 and M2 associated genes in subjects with CF. Sputum samples from subjects with CF were collected, and mRNA was isolated. Gene expression was assessed via qRT-PCR, and gene expression was normalized to the housekeeping gene GAPDH. Panels are stratified in terms of AZM usage, and consist of (A) the M1 gene marker IL1-α; (B) the fibrotic gene marker fibronectin; (C) the M2 gene marker CCL18; (D) the M2 gene marker MR. Statistical analysis was performed via an unpaired t-test. Statistically significant differences were not observed between any groups.

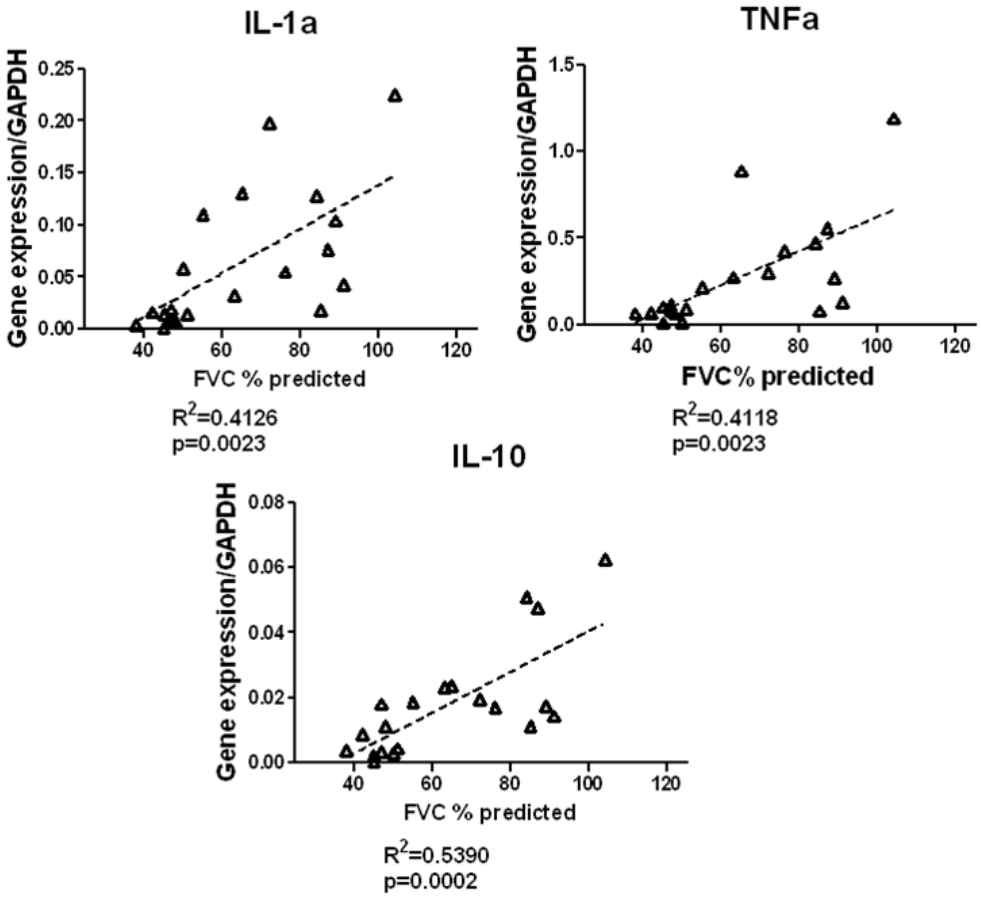

Figure 4.5. Correlation between FVC% predicted and M1 and M2 associated genes. Sputum samples were collected from subjects with CF, and mRNA was isolated. Gene expression was assessed via qRT-PCR and normalized to the housekeeping gene GAPDH. FVC % predicted (determined via chart review) was compared to (A) IL1α; (B) TNFα; (C) IL10. Gene samples were run in triplicate, and average value for each gene was plotted. R square and p values are listed below each graph. Linear regularity was assessed with Graphpad Prism.

	Component				
	1	2	3	4	5
arg1	-.050	-.031	-.496	-.012	-.125
Arg2	.158	.134	-.151	.864	.046
CCL18	.026	.589	.126	-.016	.773
Col1A1	-.130	-.143	.283	-.045	.911
Fibronectin	.006	.905	.377	.037	-.045
IL10	.146	.125	.880	-.102	.135
IL12a	-.183	-.031	.115	.793	-.093
IL12b	-.003	.827	-.111	-.018	.154
IL1a	.549	.439	.438	.410	.032
MMP9	.729	.232	-.016	-.229	.004
MR1	.082	.845	.368	.139	-.085
NOS2	.818	-.162	.223	.237	-.027
TGFb	.908	-.016	.092	-.123	-.052
TLR4	.884	.022	.146	.079	-.049
TNFa	.245	.394	.802	.093	.042

Extraction Method: Principal Component Analysis.

Table 4.4. Component matrix for the first round of PCA. Data was assessed via principal component analysis. Component 1 and component 2 explained 31.8% and 18.7% of the total variance in gene expression. An eigenvalue >1 was required for inclusion of the components that were generated.

	Component	
	1	2
CCL18	-.016	.753
Fibronectin	.057	.938
IL12b	-.039	.797
MMP9	.743	.209
MR1	.130	.870
NOS2	.829	-.114
TGFb	.924	-.013
TLR4	.887	.041

Extraction Method: Principal Component Analysis.

Table 4.5. Component matrix for the second round of PCA. Genes with a high weighting in either component 1 or component 2 were included in the second round of PCA. Data was assessed via principal component analysis. Component 1 and component 2 explained 38.8% and 33.6% of the total variance in gene expression. An eigenvalue >1 was required for inclusion of the components that were generated.

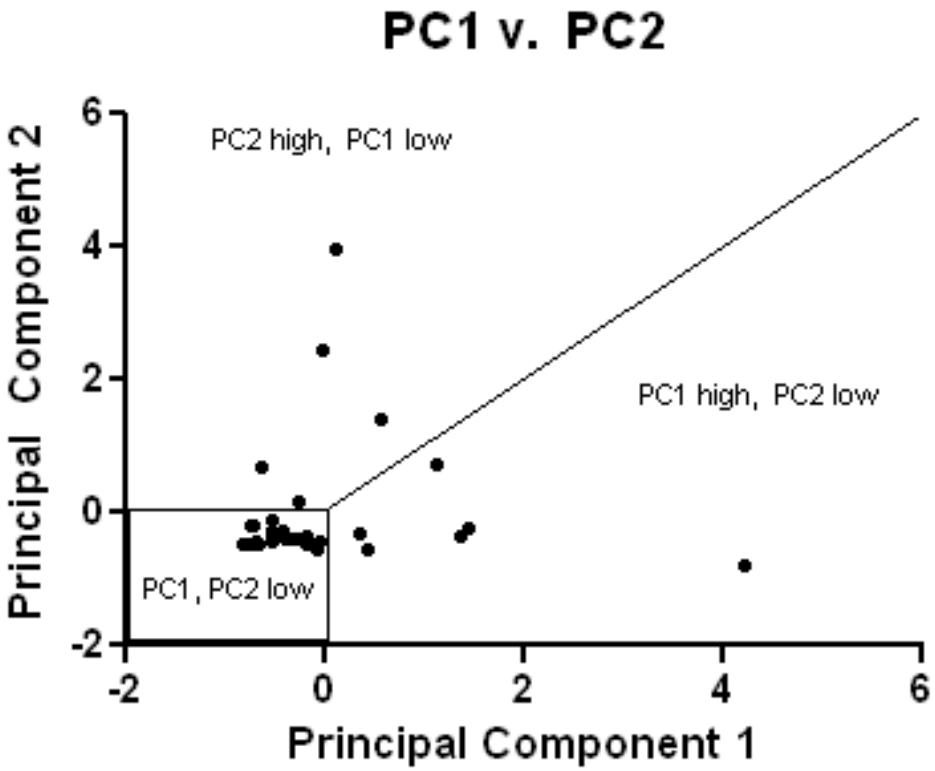

Figure 4.6. Plotting of principal components 1 and 2. Components 1 and 2 were graphed, and subjects were divided into one of three groups:one group with low values in both components 1 and 2, one group with greater values in component 1 than component 2, and one group with greater values in component 2 than component 1.

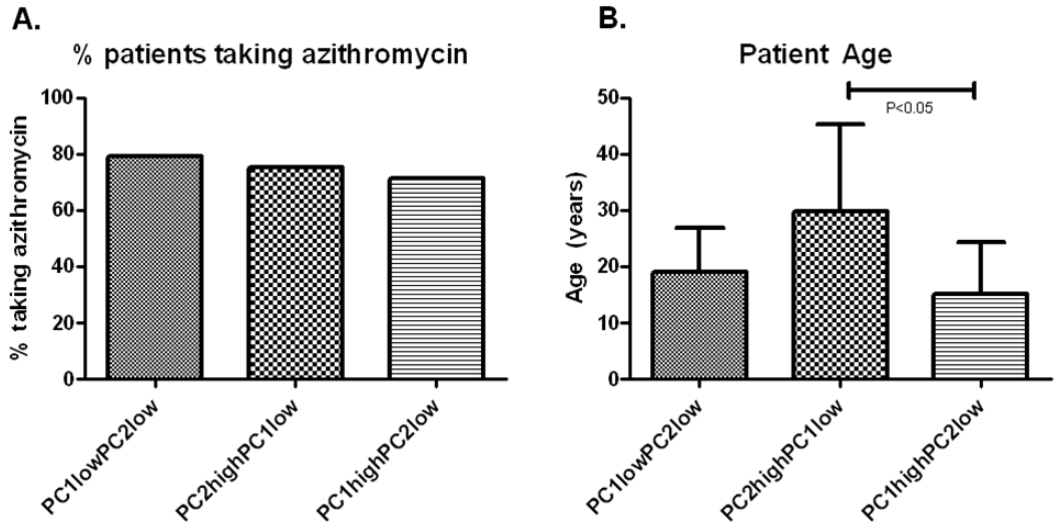

Figure 4.7. Subject demographics with PCA subgroups. Panel (A) describes the percentage of subjects who were receiving AZM; Panel (B) describes subject age. Statistical analysis of percentage of subjects receiving AZM was performed with Fisher's exact test for each possible comparison. Subject age was analyzed with a one way ANOVA with Tukey's multiple comparison test. Panel (B) represents mean ± SD for all samples.

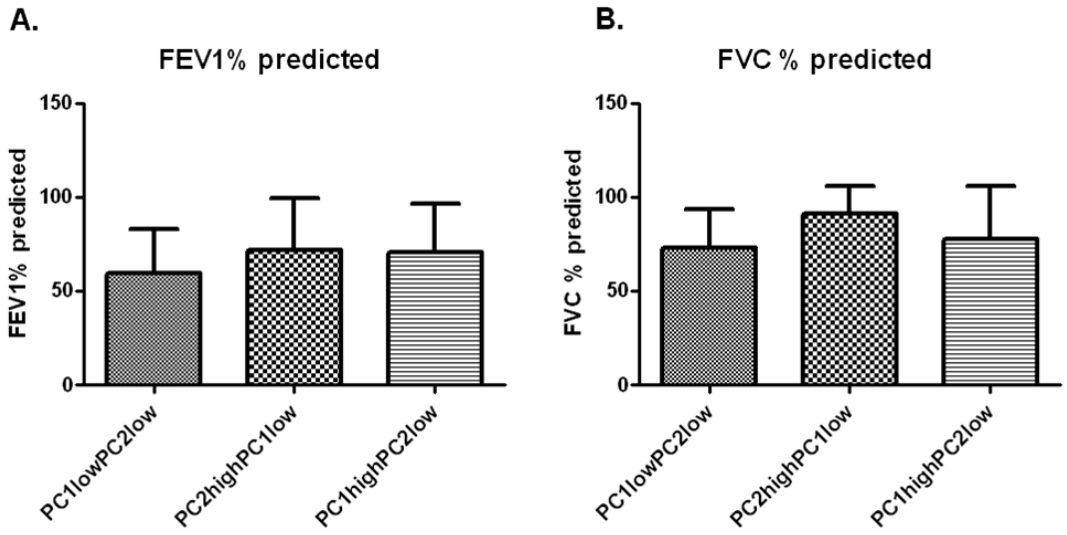

Figure 4.8. Parameters of lung function in PCA subgroups. Panel (A) describes FEV1% predicted in the three subgroups; (B) FVC% predicted in the three subgroups with PCA. Parameters of lung function were determined from chart review. Data represents mean ± SD of all samples. Samples were analyzed with a one way ANOVA with Tukey's multiple comparison test.

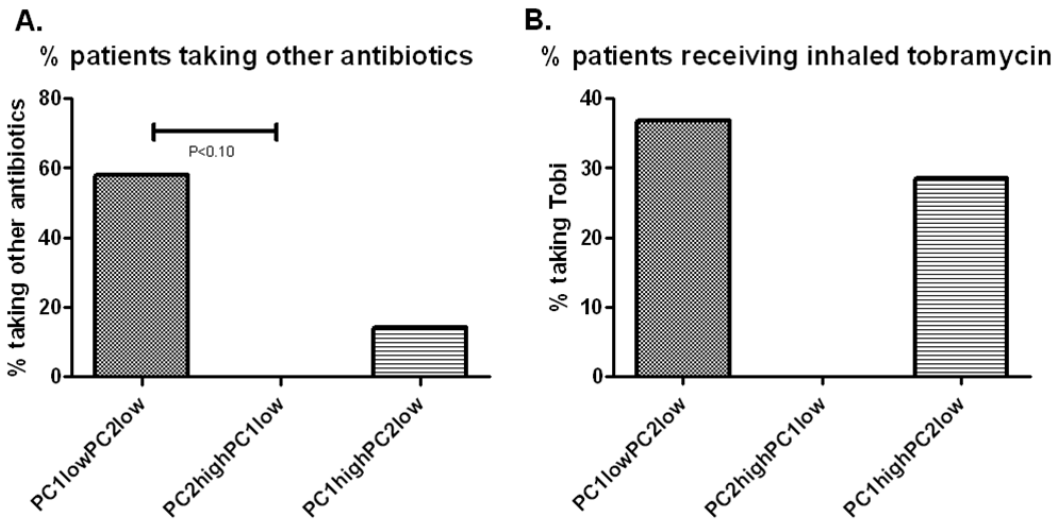

Figure 4.9. Other antibiotic usage in PCA subgroups. Panel (A) represents non-AZM oral and IV antibiotic usage in subjects receiving AZM. Antibiotic usage was determined from chart review. Statistical analysis of percentages were performed with Fisher's exact test for each possible comparison. Samples were deemed statistically significant with a $p < 0.1$.

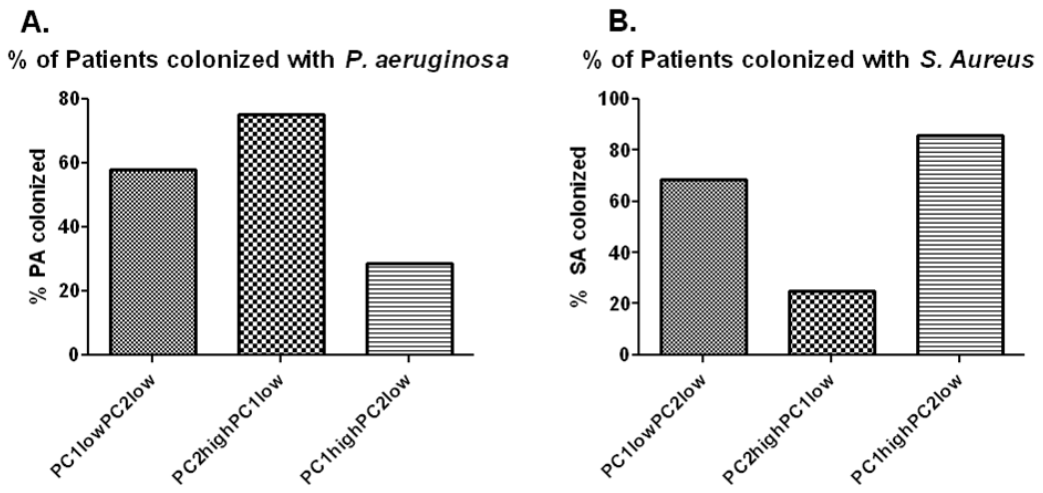

Figure 4.10. Bacterial colonization rates in PCA subgroups. Panel (A) represents the percentages of subjects colonized with *P. aeruginosa*; Panel (B) represents the percentages of subjects colonized with *S. Aureus*. Colonization rates were determined via chart review. Statistical analysis of percentages were performed with Fisher's exact test for each possible comparison. Samples were deemed statistically significant with a $p < 0.05$.

Chapter 5: Discussion

A. Results Overview

The goal of this work was to further identify the mechanism and importance of AZM dependent macrophage polarization. This was accomplished through a combination of cell culture, animal work, and clinical research. We utilized a series co-culture experiment to assess the importance of AZM dependent macrophage polarization on fibrogenesis in fibroblasts. We additionally examined the importance of AZM polarized macrophages in the context of *P. aeruginosa* pneumonia in the lungs of various mouse strains. We finally assessed gene expression in subjects with CF, and correlated gene expression to clinical parameters.

Further description of the phenotype of azithromycin polarized macrophages

We first assessed the ability of AZM to polarize macrophages to the M2 phenotype in the presence of both another cell type (fibroblasts), as well as in the presence of viable bacteria. This was done to confirm the results that we had previously seen *in vitro* [63]. While previous studies in our laboratory were descriptive in examining the effects of the drug on macrophages, here we extend the work to examine the function of macrophages treated with AZM, through both co-culture experiments to study the interaction with fibroblasts, and through our in vivo infection model. We confirmed through both the arginase assay and expression of the surface molecule MR that the macrophages in both our co-culture system and in infected mice are polarized by the drug to an M2-like phenotype.

We next examined expression and activation of the pro-fibrotic molecule TGFβ. Here we found that AZM increased both levels of active TGFβ, as well as the ratio of active to total TGFβ, and the amount of TGFβ1 mRNA. Work from others in our laboratory suggests that these increases in TGFβ activation are due at least in part to increases in molecules that cleave TGFβ from its inactive to

active form, including MMP9. Consistent with our findings for TGFβ, we found increases in fibronectin in the co-culture system, showing that AZM polarized macrophages act in a matter consistent with what we would expect from M2 macrophages. This suggests that function of AZM-induced macrophages is similar to that of cells polarized by IL4 and IL13.

Importance of M2 macrophages in response to *P. aeruginosa* pneumonia

We examined the role of M2 macrophages in *P. aeruginosa* pneumonia both in C57bl/6 mice as well as in IL4rαKO mice. In our C57bl/6 mice we found that AZM treatment resulted in greater numbers of cells expressing M2 markers, and fewer cells expressing M1 markers, as well as increased arginase activity. We further found that AZM shifts the influx of cells in the lungs of these animals away from a neutrophilic response, and towards a more monocytic cellular response. Importantly, C57bl/6 mice treated with AZM had significantly lower mortality from the infection, as compared to mice that did not receive AZM, while observing essentially no differences in the numbers of bacteria present in their lungs. We hypothesize that the shift away from the M1 phenotype and towards the M2 phenotype is responsible, at least in part, for these improvements. In essence, it is the overly zealous inflammatory response, rather than the bacteria, which results in the mortality associated with *P. aeruginosa* pneumonia in this model.

We observed similar, albeit less marked findings in our IL4rαKO mice, as well as IL4rαKO mice with cells adoptively transferred with Balb/c T cells and macrophages. While we did not observe differences in survival between these two groups, we did still see increases in monocytes in the lungs of animals that received macrophage from Balb/c mice, as well as decreases in neutrophils present in the lungs of these animals. When we treated IL4rαKO mice with AZM, we found that AZM was still able to polarize macrophages to the M2 phenotype in these mice. Most interestingly, we found increased localization of arginase 1 around small airways in the lungs of IL4rαKO mice treated with AZM, and decreased expression of iNOS. The clinical relevance of this shift in specific

location of arginase expression is potentially large. The peribronchiolar regions are impacted the most by the repeated inflammation and repair cycle in patients with CF, whereas the integrity of the alveoli are typically spared in this pathophysiology. This in itself could be largely responsible for the beneficial effects of AZM. Interestingly, other studies from our laboratory utilizing the Pseudomonas infection model have shown that the number of monocytes/macrophages infiltrating the airways is increased, corresponding with a decrease in neutrophil influx here [75]. The IHC data showing the location of heightened arginase expression supports these results. These findings show that AZM is able to polarize macrophages to the M2 phenotype independent of IL4 and IL13 function.

Mechanistic investigations into azithromycin-dependent M2 polarization

We further assessed the mechanism by which AZM polarizes macrophages to the M2 phenotype *in vitro*. We first found that AZM was able to increase arginase activity, a marker of M2 activation in IL4rαKO splenocytes stimulated *ex vivo*. We also found that AZM decreased activation of NF-κB while increasing levels of IKKβ present in the system. These findings suggest that one potential mechanism by which AZM polarizes macrophage to the M2 phenotype is IKKβ dependent, presumably via activation of IKKβ. This was further confirmed when we treated cells with the IKKβ inhibitor IKK-16. IKK-16 was able to decrease arginase activity with AZM treated cells, while exerting no effects on arginase activity in cells treated with IL4/13. While not confirming an exact mechanism for AZM dependent M2 polarization, it does further isolate molecular targets for future examinations. From this work, it does appear that signaling through intracellular cascades is altered, and therefore responsible for the changes in gene expression in macrophages exposed to AZM. To extend this, it was important for us to examine the role that IL4 and IL13 play. A possible explanation of the changes could be that autocrine IL4/IL13 secretion was being altered by the drug, thereby affecting the change in phenotype. This does not

appear to be the case however, because we show that AZM will polarize cells independently of IL4/IL13 signaling.

Phenotypic determinations in patients with CF

We collected 66 sputum samples from 30 subjects with CF and isolated mRNA. We performed qRT-PCR on these samples for a variety of genes for macrophage phenotype, inflammatory status, and fibrosis. We additionally performed chart review on these subjects allowing us to review their clinical status, as well as determine other parameters of their health. We first assessed correlations between various genes. Here we found that gene markers of M1 and M2 polarization correlated with inflammatory and fibrotic gene markers, respectively. We next compared various clinical parameters of the subjects. Here we found that the FEV1% predicted was significantly lower in subjects receiving AZM. We additionally found that older subjects had significantly lower FEV1% predicted than those who were younger. These two findings are consistent with the place of AZM in treatment of CF, and the decline that occurs in these subjects as they age.

Gene expression and AZM

We then correlated various gene markers of these subjects to their AZM treatment status. We found shifts in gene expression consistent with a shift to the M2 phenotype in the sputum samples of these subjects, as well as correlations between inflammatory cytokines and lung function. This confirmed the protein data that we have previously observed [115], showing that AZM increases markers of M2 polarization, and that in subjects with CF markers of the M1 phenotype are associated with better outcomes. This shows the potential importance of macrophage polarization in subjects with CF.

Principal component analysis

We finally utilized principal component analysis as a method of data reduction. We found two groupings, with one representing genes associated with

the M1 phenotype and one representing genes associated with the M2 phenotype. We then charted these two components, and found that our samples sorted into three different groups. Gene expression in one group showed markers of neither phenotype. Another group displayed increased expression of M1 activation, while a third displayed increased expression of M2 activation.

Clinical status in these subjects was then assessed. Our findings were consistent with those of others with the net Th2 shift that occurs in patients as they age [32]. The cytokines produced as part of this shift result in an alteration in macrophage polarization, as exemplified by the increased age observed in the group with high expression of M2 markers. We additionally observed differences in bacterial colonization between our groups, with subjects with high expression of M1 associated genes more likely to be colonized with *S. aureus*, and less likely to be colonized with *P. aeruginosa* than subjects with high expression of M2 markers. This again reflects the observations of others, with the shifts we observed in bacterial colonization status being similar to those observed by others in the past [119]. It is unknown whether these changes are related to the difference in macrophage polarization, or are related to the difference in subject age between the two groups.

B. Significance

IKKβ and macrophage polarization

We attempted to further isolate molecular targets by which AZM polarizes macrophages to the M2 phenotype. Based on the work by Fong et. al., we assessed IKKβ as a target for AZM. Their work utilized mice that were conditional knock-outs of IKKβ in either epithelial or myeloid cells. In mice with the IKKβ deficiency in epithelial cells, they found decreased inflammation as they expected. Surprisingly, however, in their mice with deficient IKKβ in myeloid cells, however, they found increased resistance to pulmonary infections with Group b Streptococci. They went on to find that macrophages with deficient

IKKβ signaling displayed increased markers of M1 activation, primarily measured by cytokine expression [68].

They then examined why eliminating IKKβ signaling in myeloid cells would lead to increased M1 signaling. They found that STAT1 phosphorylation was increased in cells with deficient IKKβ signaling, suggesting that IKKβ prevents the activation of STAT1. They hypothesize that this interaction is necessary in macrophages to allow for resolution of the immune response over time [68].

To attempt to determine if one of the ways that AZM polarizes macrophages to the M2 phenotype is via activation of IKKβ, we utilized a small molecule inhibitor of IKKβ to assess if IKKβ activation played a role. We found that inhibition of IKKβ activation with IKK-16 eliminated AZM dependent arginase activity, while exerting essentially no effect on IL4/13 dependent arginase activity. We did, however, find that extremely high concentrations of AZM were able to overcome this inhibition. This further confirms molecular targets by which AZM polarizes macrophages to the M2 phenotype. Due to technical limitations, we were unable to confirm that AZM in fact prevents phosphorylation of STAT1, confirming that this is the mechanism by which AZM polarizes macrophages to the M2 phenotype. In essence we were unable to detect p-STAT1 in our cells, including in positive controls (IFN +LPS stimulated cells). Future work in our laboratory will focus on alternative experiments to confirm that STAT1 activation is decreased with AZM treatment.

Breaking the cycle of inflammation and fibrosis

Disease progression in CF is characterized by repeated cycles of infection, inflammation, repair, and fibrosis [15]. We believe that the beneficial effects of AZM in these patients are due in part to decreasing the extent of the immune response to an acute flare of the disease. Figure 5.1 shows our proposed model for the beneficial effects of AZM. In the normal course of CF, there is a large inflammatory response consisting, among other cells, of M1

macrophages and neutrophils [44]. This overly zealous immune response, in the process of clearing the bacterial flare, results in the production of reactive oxygen species which leads to tissue damage in the lungs of these patients. After the initial inflammatory response, alternatively activated macrophages are up-regulated to help initiate the repair process. These cells are responsible for cleaning up the damage that occurred during the acute bacterial flare. They do this in part by internalizing the debris that was produced as part of the infection. M2 macrophages additionally up-regulate molecules leading to fibrosis, including fibronectin and collagen [38]. This process is necessary, allowing the lungs to repair. Excessive scarring, however, leads to a decline in airway function. This decline, then, increases the likelihood of a future flare occurring. This cycle of inflammation and fibrosis leads to a decline in lung function for the patient over time, and is responsible for much of the morbidity and mortality associated with CF.

Others have utilized similar models and observed similar findings with AZM. Tsai et. al. have utilized a *P. aeruginosa* infection model with a strain of mice with deficient CFTR function [100]. Unlike our findings, they observed that AZM treated mice displayed fewer bacteria in their lungs. They did, however observe a similar increase in survival and decrease in neutrophils influx as we observed with our mice. They also observed similar alterations in inflammatory cytokine production with their mice. While this group did not examine differences in macrophage activation status, in conjunction with our data it supports the hypothesis that the benefits of AZM are due in part to alterations in macrophage polarization.

With AZM, what we believe is occurring is that the initial inflammatory flare of the disease is being blunted. By shifting some of the macrophage polarization away from the M1 phenotype and towards the M2 phenotype during the initiation of inflammation, the immune response, while still strong enough to clear the infection, does not cause the same degree of damage as the dysregulated response would. There is then less repair and recovery necessary for the lungs

of these patients to recover from. This model helps to explain the seeming contradiction that exists with AZM treatment in CF. By decreasing the degree of an initial inflammatory flare, AZM improves lung function in patients with CF, even though it increases the amount of pro-fibrotic macrophages in the lungs.

Importance of alternatively activated macrophages in the response to extracellular bacteria

Characterizations into the importance of alternatively activated macrophages have primarily focused on intracellular bacteria and parasites. Kasmi et. al. assessed the importance of alternatively activated macrophages in host response to the intracellular pathogens *Mycobacterium tuberculosis* and *Toxoplasma Gondii* [124]. They found that these pathogens actually up-regulate the M2 marker arginase. This decreases intracellular arginine levels, and prevents the generation of a robust M1 dependent oxidative burst. They additionally utilized an Arg 1 knockout mouse, and found that these mice survived infection with intracellular bacteria more readily than wild type mice. They concluded that M1 macrophages play an important role in the destruction of intracellular bacteria, while M2 macrophages allow these bacteria to evade destruction.

Others have investigated the role of M2 produced arginase 1 with parasites including *S. mansoni*. Study of the inflammatory response to *S. mansoni* infection showed that mice with macrophages that lack arginase 1 succumb to Th2-driven pathology associated with the pathogen, related a lack of inhibition of the CD4+ T cell response. They concluded that arginase played an important role in the suppression of T cell dependent inflammation [85, 86].

Considerably less is known about the role of M2 macrophages with extracellular bacteria. This is primarily due to M2 macrophages not being present during the acute phase of these responses. We have shown that the inducement of the M2 phenotype during the acute phase of an infection improves survival in C57bl/6 mice with *P. aeruginosa* pneumonia. We have observed

similar trends with IL4rαKO mice adoptively transferred with functional macrophages. We hypothesize that this improvement is due in part to a blunting of the robust immune response that occurs in the context of an extracellular infection.

Future directions

While we were unable to determine an exact molecular mechanism by which AZM polarizes macrophages to the M2 phenotype, our investigations has greatly narrowed the number of targets that exist. The continuation of this research will further define these molecular targets. These investigations may allow the development of future therapeutic agents combining the beneficial immunomodulatory effects of AZM without the need for long term antibiotic usage.

Modulation of macrophage polarization may provide a new avenue for treatment of various infections. In many infections, it is the strong inflammatory response to infectious pathogens, rather than the pathogen itself, which is responsible for much of the damage and pathology that follows. AZM and other future AZM-like immunomodulatory drugs may be able to blunt the immune response, while still allowing for adequate clearance of the bacteria.

This work additionally provides the foundation for mechanistic investigations into specific molecular targets of M2 macrophages which lead to this immunomodulation. With AZM, we have an agent that is able to shift macrophage polarization to the M2 phenotype. AZM is able to modulate the immune system with few systemic complications, especially compared to other immunomodulators (e.g. corticosteroids, methotrexate, and cyclosporine), which profoundly suppress the immune system. This polarization is clinically relevant, however, as AZM functions as a relatively blunt instrument to affect these changes. It is conceivable that alterations in individual M2 effector proteins may be able to improve outcomes in a more selective manner. It is unknown which proteins expressed in M2 macrophages play important roles in the response to

extracellular pathogens. The determination of which specific proteins play an important role in the blunting of the inflammatory response to extracellular pathogens may allow for more specific modulation of the immune system. Novel therapeutics that allow for a shift in the balance of macrophage polarization may allow for improved outcomes in the context of infection.

C. Conclusions

This research provides additional insights into the role of M1 and M2 macrophages during acute infections and in CF. Our research has shown that shifting macrophage polarization away from the M1 phenotype and towards the M2 phenotype increases survival in mice during acute infections. This shift still allows for sufficient inflammation to clear the infection. We believe that it is the inflammatory response that causes much of the mortality, which is especially applicable in chronic inflammatory conditions like CF and COPD.

We conclude that shifts in macrophage phenotype towards an M2 polarization result in improved outcomes in *P. aeruginosa* pneumonia, and may be responsible for improvements associated with AZM treatment in patients with CF. We have previously shown that AZM shifts macrophage polarization away from the M2 phenotype in the presence of cytokines that would otherwise result in M1 polarization, and here we have expanded our knowledge of the functional role that AZM-exposed macrophages exhibit.

We additionally investigated potential molecular targets by which AZM polarizes macrophages to the M2 phenotype. We believe that AZM increases IKKβ activation, and, in a manner similar to what Fong et. al. described, preventing activation of STAT1 [68]. Further research is necessary to confirm the exact mechanism by which AZM effects these changes. Future research may lead to novel therapeutics that target specific aspects of alternative macrophage activation, as an immunomodulatory modality that is clinically effective in patients with chronic inflammatory lung diseases, while at the same

time are less toxic and immunosuppressive than therapies that are currently available.

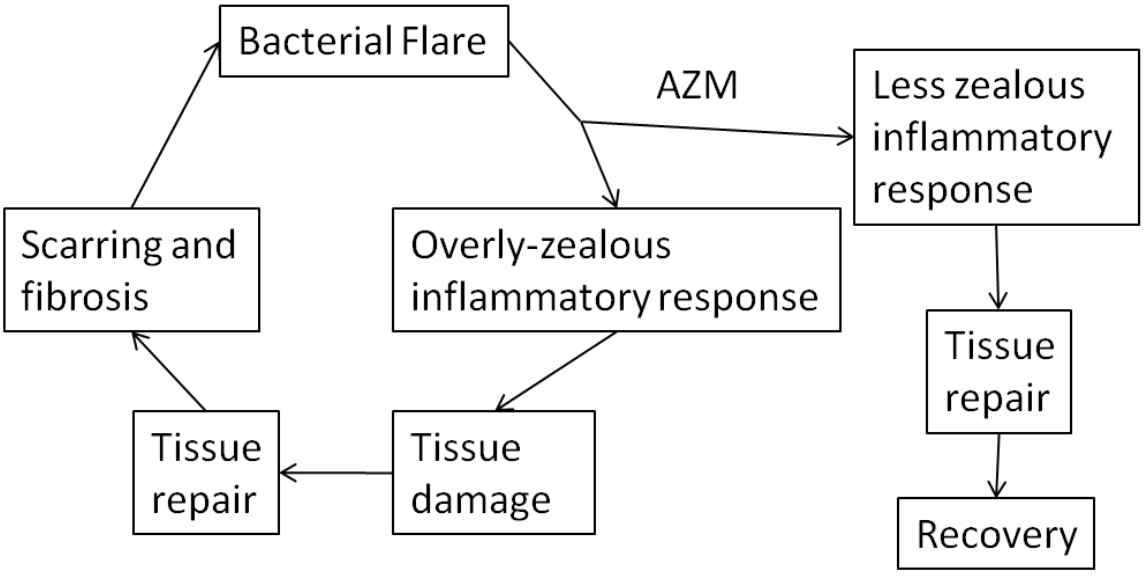

Figure 5.1. Proposed model for beneficial effects of AZM in patients with CF. Disease progression in CF is characterized by a cycle consisting of bacterial flares and a strong inflammatory response to the bacteria. This strong response leads to tissue damage, and eventually tissue repair. When excessive damage has occurred due to the immune response, scarring and fibrosis occurs, leading to future bacterial flares. We propose that AZM decreases the degree of the initial inflammatory response, resulting in less extensive damage.

REFERENCES

1. Gordon, S., *Alternative activation of macrophages.* Nat Rev Immunol, 2003. **3**(1): p. 23-35.
2. Gordon, S. and F.O. Martinez, *Alternative activation of macrophages: mechanism and functions.* Immunity. **32**(5): p. 593-604.
3. Mantovani, A., et al., *The chemokine system in diverse forms of macrophage activation and polarization.* Trends Immunol, 2004. **25**(12): p. 677-86.
4. Gough, D.J., et al., *IFNgamma signaling-does it mean JAK-STAT?* Cytokine Growth Factor Rev, 2008. **19**(5-6): p. 383-94.
5. Kovarik, P., et al., *Stat1 combines signals derived from IFN-gamma and LPS receptors during macrophage activation.* Embo J, 1998. **17**(13): p. 3660-8.
6. Bollrath, J. and F.R. Greten, *IKK/NF-kappaB and STAT3 pathways: central signalling hubs in inflammation-mediated tumour promotion and metastasis.* EMBO Rep, 2009. **10**(12): p. 1314-9.
7. Bonizzi, G. and M. Karin, *The two NF-kappaB activation pathways and their role in innate and adaptive immunity.* Trends Immunol, 2004. **25**(6): p. 280-8.
8. Timmer, A.M. and V. Nizet, *IKKbeta/NF-kappaB and the miscreant macrophage.* J Exp Med, 2008. **205**(6): p. 1255-9.
9. Munder, M., et al., *Th1/Th2-regulated expression of arginase isoforms in murine macrophages and dendritic cells.* J Immunol, 1999. **163**(7): p. 3771-7.
10. Morris, S.M., Jr., D. Kepka-Lenhart, and L.C. Chen, *Differential regulation of arginases and inducible nitric oxide synthase in murine macrophage cells.* Am J Physiol, 1998. **275**(5 Pt 1): p. E740-7.
11. Gibson, R.L., J.L. Burns, and B.W. Ramsey, *Pathophysiology and management of pulmonary infections in cystic fibrosis.* Am J Respir Crit Care Med, 2003. **168**(8): p. 918-51.
12. McKeon, D.J., et al., *Cystic fibrosis neutrophils have normal intrinsic reactive oxygen species generation.* Eur Respir J. **35**(6): p. 1264-72.
13. Davies, J.C., *Pseudomonas aeruginosa in cystic fibrosis: pathogenesis and persistence.* Paediatr Respir Rev, 2002. **3**(2): p. 128-34.
14. Flume, P.A., et al., *Cystic fibrosis pulmonary guidelines: chronic medications for maintenance of lung health.* Am J Respir Crit Care Med, 2007. **176**(10): p. 957-69.
15. Nichols, D.P., M.W. Konstan, and J.F. Chmiel, *Anti-inflammatory therapies for cystic fibrosis-related lung disease.* Clin Rev Allergy Immunol, 2008. **35**(3): p. 135-53.

16. Equi, A., et al., *Long term azithromycin in children with cystic fibrosis: a randomised, placebo-controlled crossover trial.* Lancet, 2002. **360**(9338): p. 978-84.
17. Saiman, L., et al., *Effect of azithromycin on pulmonary function in patients with cystic fibrosis uninfected with Pseudomonas aeruginosa: a randomized controlled trial.* Jama. **303**(17): p. 1707-15.
18. Saiman, L., et al., *Azithromycin in patients with cystic fibrosis chronically infected with Pseudomonas aeruginosa: a randomized controlled trial.* Jama, 2003. **290**(13): p. 1749-56.
19. Saiman, L., et al., *Heterogeneity of treatment response to azithromycin in patients with cystic fibrosis.* Am J Respir Crit Care Med, 2005. **172**(8): p. 1008-12.
20. Wolter, J., et al., *Effect of long term treatment with azithromycin on disease parameters in cystic fibrosis: a randomised trial.* Thorax, 2002. **57**(3): p. 212-6.
21. Ratjen, F.A., *Cystic fibrosis: pathogenesis and future treatment strategies.* Respir Care, 2009. **54**(5): p. 595-605.
22. Quinton, P.M., *Cystic fibrosis: a disease in electrolyte transport.* FASEB J, 1990. **4**(10): p. 2709-17.
23. Zielenski, J., *Genotype and phenotype in cystic fibrosis.* Respiration, 2000. **67**(2): p. 117-33.
24. Shute, J., et al., *Growth factors in cystic fibrosis - when more is not enough.* Paediatr Respir Rev, 2003. **4**(2): p. 120-7.
25. Di, A., et al., *CFTR regulates phagosome acidification in macrophages and alters bactericidal activity.* Nat Cell Biol, 2006. **8**(9): p. 933-44.
26. Parkins, M.D. and J.S. Elborn, *Newer antibacterial agents and their potential role in cystic fibrosis pulmonary exacerbation management.* J Antimicrob Chemother. **65**(9): p. 1853-61.
27. Aaron, S.D., et al., *Infection with transmissible strains of Pseudomonas aeruginosa and clinical outcomes in adults with cystic fibrosis.* Jama. **304**(19): p. 2145-53.
28. Douglas, T.A., et al., *Acquisition and eradication of P. aeruginosa in young children with cystic fibrosis.* Eur Respir J, 2009. **33**(2): p. 305-11.
29. Bjarnsholt, T., et al., *Pseudomonas aeruginosa biofilms in the respiratory tract of cystic fibrosis patients.* Pediatr Pulmonol, 2009. **44**(6): p. 547-58.
30. Govan, J.R. and V. Deretic, *Microbial pathogenesis in cystic fibrosis: mucoid Pseudomonas aeruginosa and Burkholderia cepacia.* Microbiol Rev, 1996. **60**(3): p. 539-74.
31. Oliver, A., et al., *High frequency of hypermutable Pseudomonas aeruginosa in cystic fibrosis lung infection.* Science, 2000. **288**(5469): p. 1251-4.
32. Hartl, D., et al., *Pulmonary T(H)2 response in Pseudomonas aeruginosa-infected patients with cystic fibrosis.* J Allergy Clin Immunol, 2006. **117**(1): p. 204-11.

33. Borowitz, D., R.D. Baker, and V. Stallings, *Consensus report on nutrition for pediatric patients with cystic fibrosis.* J Pediatr Gastroenterol Nutr, 2002. **35**(3): p. 246-59.
34. Mosser, D.M., *The many faces of macrophage activation.* J Leukoc Biol, 2003. **73**(2): p. 209-12.
35. Mosser, D.M. and J.P. Edwards, *Exploring the full spectrum of macrophage activation.* Nat Rev Immunol, 2008. **8**(12): p. 958-69.
36. Parnham, M.J., et al., *Modulation of neutrophil and inflammation markers in chronic obstructive pulmonary disease by short-term azithromycin treatment.* Eur J Pharmacol, 2005. **517**(1-2): p. 132-43.
37. Legssyer, R., et al., *Azithromycin reduces spontaneous and induced inflammation in DeltaF508 cystic fibrosis mice.* Respir Res, 2006. **7**: p. 134.
38. Fairweather, D. and D. Cihakova, *Alternatively activated macrophages in infection and autoimmunity.* J Autoimmun, 2009. **33**(3-4): p. 222-30.
39. Pechkovsky, D.V., et al., *Alternatively activated alveolar macrophages in pulmonary fibrosis-mediator production and intracellular signal transduction.* Clin Immunol. **137**(1): p. 89-101.
40. Mori, M. and T. Gotoh, *Regulation of nitric oxide production by arginine metabolic enzymes.* Biochem Biophys Res Commun, 2000. **275**(3): p. 715-9.
41. Mori, M., *Regulation of nitric oxide synthesis and apoptosis by arginase and arginine recycling.* J Nutr, 2007. **137**(6 Suppl 2): p. 1616S-1620S.
42. Mori, M. and T. Gotoh, *Arginine metabolic enzymes, nitric oxide and infection.* J Nutr, 2004. **134**(10 Suppl): p. 2820S-2825S; discussion 2853S.
43. Wojnarowski, C., et al., *Cytokine expression in bronchial biopsies of cystic fibrosis patients with and without acute exacerbation.* Eur Respir J, 1999. **14**(5): p. 1136-44.
44. McGrath, L.T., et al., *Oxidative stress during acute respiratory exacerbations in cystic fibrosis.* Thorax, 1999. **54**(6): p. 518-23.
45. Bruscia, E.M., et al., *Macrophages directly contribute to the exaggerated inflammatory response in cystic fibrosis transmembrane conductance regulator-/- mice.* Am J Respir Cell Mol Biol, 2009. **40**(3): p. 295-304.
46. Mills, C.D., et al., *M-1/M-2 macrophages and the Th1/Th2 paradigm.* J Immunol, 2000. **164**(12): p. 6166-73.
47. Moser, C., et al., *Improved outcome of chronic Pseudomonas aeruginosa lung infection is associated with induction of a Th1-dominated cytokine response.* Clin Exp Immunol, 2002. **127**(2): p. 206-13.
48. Meneghin, A. and C.M. Hogaboam, *Infectious disease, the innate immune response, and fibrosis.* J Clin Invest, 2007. **117**(3): p. 530-8.
49. Jakubzick, C., et al., *Therapeutic targeting of IL-4- and IL-13-responsive cells in pulmonary fibrosis.* Immunol Res, 2004. **30**(3): p. 339-49.
50. Taylor, M.D., et al., *F4/80+ alternatively activated macrophages control CD4+ T cell hyporesponsiveness at sites peripheral to filarial infection.* J Immunol, 2006. **176**(11): p. 6918-27.

51. Weber, M.S., et al., *Type II monocytes modulate T cell-mediated central nervous system autoimmune disease.* Nat Med, 2007. **13**(8): p. 935-43.
52. Elizur, A., C.L. Cannon, and T.W. Ferkol, *Airway inflammation in cystic fibrosis.* Chest, 2008. **133**(2): p. 489-95.
53. Rao, S. and J. Grigg, *New insights into pulmonary inflammation in cystic fibrosis.* Arch Dis Child, 2006. **91**(9): p. 786-8.
54. Song, E., et al., *Influence of alternatively and classically activated macrophages on fibrogenic activities of human fibroblasts.* Cell Immunol, 2000. **204**(1): p. 19-28.
55. Prasse, A., et al., *A vicious circle of alveolar macrophages and fibroblasts perpetuates pulmonary fibrosis via CCL18.* Am J Respir Crit Care Med, 2006. **173**(7): p. 781-92.
56. Friedman, P.J., I.R. Harwood, and P.H. Ellenbogen, *Pulmonary cystic fibrosis in the adult: early and late radiologic findings with pathologic correlations.* AJR Am J Roentgenol, 1981. **136**(6): p. 1131-44.
57. Retsema, J., et al., *Spectrum and mode of action of azithromycin (CP-62,993), a new 15-membered-ring macrolide with improved potency against gram-negative organisms.* Antimicrob Agents Chemother, 1987. **31**(12): p. 1939-47.
58. Zhanel, G.G., et al., *Review of macrolides and ketolides: focus on respiratory tract infections.* Drugs, 2001. **61**(4): p. 443-98.
59. Scaglione, F. and G. Rossoni, *Comparative anti-inflammatory effects of roxithromycin, azithromycin and clarithromycin.* J Antimicrob Chemother, 1998. **41 Suppl B**: p. 47-50.
60. Schultz, M.J., *Macrolide activities beyond their antimicrobial effects: macrolides in diffuse panbronchiolitis and cystic fibrosis.* J Antimicrob Chemother, 2004. **54**(1): p. 21-8.
61. Tateda, K., et al., *Azithromycin inhibits quorum sensing in Pseudomonas aeruginosa.* Antimicrob Agents Chemother, 2001. **45**(6): p. 1930-3.
62. Kanoh, S. and B.K. Rubin, *Mechanisms of action and clinical application of macrolides as immunomodulatory medications.* Clin Microbiol Rev. **23**(3): p. 590-615.
63. Murphy, B.S., et al., *Azithromycin alters macrophage phenotype.* J Antimicrob Chemother, 2008. **61**(3): p. 554-60.
64. Cai, Y., et al., *Effectiveness and safety of macrolides in cystic fibrosis patients: a meta-analysis and systematic review.* J Antimicrob Chemother. **66**(5): p. 968-78.
65. Beigelman, A., et al., *Azithromycin attenuates airway inflammation in a noninfectious mouse model of allergic asthma.* Chest, 2009. **136**(2): p. 498-506.
66. Blasi, F., et al., *Long-term azithromycin use in patients with chronic obstructive pulmonary disease and tracheostomy.* Pulm Pharmacol Ther. **23**(3): p. 200-7.
67. Shultz, D.B., et al., *Activation of a subset of genes by IFN-gamma requires IKKbeta but not interferon-dependent activation of NF-kappaB.* J Interferon Cytokine Res, 2007. **27**(10): p. 875-84.

68. Fong, C.H., et al., *An antiinflammatory role for IKK{beta} through the inhibition of "classical" macrophage activation.* J Exp Med, 2008.
69. Daley, J.M., et al., *The phenotype of murine wound macrophages.* J Leukoc Biol, 2009.
70. Mishra, B.B., U.M. Gundra, and J.M. Teale, *STAT6(-/-) mice exhibit decreased cells with alternatively activated macrophage phenotypes and enhanced disease severity in murine neurocysticercosis.* J Neuroimmunol.
71. Nelms, K., et al., *The IL-4 receptor: signaling mechanisms and biologic functions.* Annu Rev Immunol, 1999. **17**: p. 701-38.
72. Rutschman, R., et al., *Cutting edge: Stat6-dependent substrate depletion regulates nitric oxide production.* J Immunol, 2001. **166**(4): p. 2173-7.
73. Weng, M., et al., *Alternatively activated macrophages in intestinal helminth infection: effects on concurrent bacterial colitis.* J Immunol, 2007. **179**(7): p. 4721-31.
74. Cheung, P.S., E.C. Si, and K. Hosseini, *Anti-inflammatory activity of azithromycin as measured by its NF-kappaB, inhibitory activity.* Ocul Immunol Inflamm. **18**(1): p. 32-7.
75. Feola, D.J., et al., *Azithromycin alters macrophage phenotype and pulmonary compartmentalization during lung infection with Pseudomonas.* Antimicrob Agents Chemother. **54**(6): p. 2437-47.
76. Martinez, F.O., et al., *Transcriptional profiling of the human monocyte-to-macrophage differentiation and polarization: new molecules and patterns of gene expression.* J Immunol, 2006. **177**(10): p. 7303-11.
77. Duluc, D., et al., *Interferon-gamma reverses the immunosuppressive and protumoral properties and prevents the generation of human tumor-associated macrophages.* Int J Cancer, 2009. **125**(2): p. 367-73.
78. Laskin, D.L., et al., *Macrophages and tissue injury: agents of defense or destruction?* Annu Rev Pharmacol Toxicol, 2011. **51**: p. 267-88.
79. Byers, D.E. and M.J. Holtzman, *Alternatively activated macrophages as cause or effect in airway disease.* Am J Respir Cell Mol Biol. **43**(1): p. 1-4.
80. Kitowska, K., et al., *Functional role and species-specific contribution of arginases in pulmonary fibrosis.* Am J Physiol Lung Cell Mol Physiol, 2008. **294**(1): p. L34-45.
81. Bartram, U. and C.P. Speer, *The role of transforming growth factor beta in lung development and disease.* Chest, 2004. **125**(2): p. 754-65.
82. Koli, K., et al., *Latency, activation, and binding proteins of TGF-beta.* Microsc Res Tech, 2001. **52**(4): p. 354-62.
83. Lawrence, D.A., *Latent-TGF-beta: an overview.* Mol Cell Biochem, 2001. **219**(1-2): p. 163-70.
84. Koli, K., et al., *Transforming growth factor-beta activation in the lung: focus on fibrosis and reactive oxygen species.* Antioxid Redox Signal, 2008. **10**(2): p. 333-42.
85. Herbert, D.R., et al., *Alternative macrophage activation is essential for survival during schistosomiasis and downmodulates T helper 1 responses and immunopathology.* Immunity, 2004. **20**(5): p. 623-35.

86. Pesce, J.T., et al., *Arginase-1-expressing macrophages suppress Th2 cytokine-driven inflammation and fibrosis.* PLoS Pathog, 2009. **5**(4): p. e1000371.
87. Arkwright, P.D., et al., *TGF-beta(1) genotype and accelerated decline in lung function of patients with cystic fibrosis.* Thorax, 2000. **55**(6): p. 459-62.
88. Hesse, M., et al., *Differential regulation of nitric oxide synthase-2 and arginase-1 by type 1/type 2 cytokines in vivo: granulomatous pathology is shaped by the pattern of L-arginine metabolism.* J Immunol, 2001. **167**(11): p. 6533-44.
89. Gratchev, A., et al., *Alternatively activated macrophages differentially express fibronectin and its splice variants and the extracellular matrix protein betaIG-H3.* Scand J Immunol, 2001. **53**(4): p. 386-92.
90. Jainchill, J.L., S.A. Aaronson, and G.J. Todaro, *Murine sarcoma and leukemia viruses: assay using clonal lines of contact-inhibited mouse cells.* J Virol, 1969. **4**(5): p. 549-53.
91. Ralph, P. and I. Nakoinz, *Phagocytosis and cytolysis by a macrophage tumour and its cloned cell line.* Nature, 1975. **257**(5525): p. 393-4.
92. Corraliza, I.M., et al., *Determination of arginase activity in macrophages: a micromethod.* J Immunol Methods, 1994. **174**(1-2): p. 231-5.
93. Nacucchio, M.C., et al., *Short communication. Role of agar beads in the pathogenicity of Pseudomonas aeruginosa in the rat respiratory tract.* Pediatr Res, 1984. **18**(3): p. 295-6.
94. van Heeckeren, A.M. and M.D. Schluchter, *Murine models of chronic Pseudomonas aeruginosa lung infection.* Lab Anim, 2002. **36**(3): p. 291-312.
95. Corbel, M., et al., *Involvement of gelatinases (MMP-2 and MMP-9) in the development of airway inflammation and pulmonary fibrosis.* Cell Biol Toxicol, 2002. **18**(1): p. 51-61.
96. Wynn, T.A., et al., *Quantitative assessment of macrophage functions in repair and fibrosis.* Curr Protoc Immunol. **Chapter 14**: p. Unit14 22.
97. Cigana, C., B.M. Assael, and P. Melotti, *Azithromycin selectively reduces tumor necrosis factor alpha levels in cystic fibrosis airway epithelial cells.* Antimicrob Agents Chemother, 2007. **51**(3): p. 975-81.
98. Lawrence, T., *The nuclear factor NF-kappaB pathway in inflammation.* Cold Spring Harb Perspect Biol, 2009. **1**(6): p. a001651.
99. Sugiyama, K., et al., *Differing effects of clarithromycin and azithromycin on cytokine production by murine dendritic cells.* Clin Exp Immunol, 2007. **147**(3): p. 540-6.
100. Tsai, W.C., et al., *Azithromycin increases survival and reduces lung inflammation in cystic fibrosis mice.* Inflamm Res, 2009. **58**(8): p. 491-501.
101. Noben-Trauth, N., et al., *An interleukin 4 (IL-4)-independent pathway for CD4+ T cell IL-4 production is revealed in IL-4 receptor-deficient mice.* Proc Natl Acad Sci U S A, 1997. **94**(20): p. 10838-43.

102. Spencer, L., L. Shultz, and T.V. Rajan, *Interleukin-4 receptor-Stat6 signaling in murine infections with a tissue-dwelling nematode parasite.* Infect Immun, 2001. **69**(12): p. 7743-52.
103. Ostrand-Rosenberg, S., et al., *Resistance to metastatic disease in STAT6-deficient mice requires hemopoietic and nonhemopoietic cells and is IFN-gamma dependent.* J Immunol, 2002. **169**(10): p. 5796-804.
104. Waelchli, R., et al., *Design and preparation of 2-benzamido-pyrimidines as inhibitors of IKK.* Bioorg Med Chem Lett, 2006. **16**(1): p. 108-12.
105. Weissman, B.A. and S.S. Gross, *Measurement of NO and NO synthase.* Curr Protoc Neurosci, 2001. **Chapter 7**: p. Unit7 13.
106. Boxenbaum, H. and C. DiLea, *First-time-in-human dose selection: allometric thoughts and perspectives.* J Clin Pharmacol, 1995. **35**(10): p. 957-66.
107. Mahmood, I., *Interspecies scaling: predicting clearance of anticancer drugs in humans. A comparative study of three different approaches using body weight or body surface area.* Eur J Drug Metab Pharmacokinet, 1996. **21**(3): p. 275-8.
108. Foulds, G., R.M. Shepard, and R.B. Johnson, *The pharmacokinetics of azithromycin in human serum and tissues.* J Antimicrob Chemother, 1990. **25 Suppl A**: p. 73-82.
109. Morissette, C., E. Skamene, and F. Gervais, *Endobronchial inflammation following Pseudomonas aeruginosa infection in resistant and susceptible strains of mice.* Infect Immun, 1995. **63**(5): p. 1718-24.
110. Stotland, P.K., D. Radzioch, and M.M. Stevenson, *Mouse models of chronic lung infection with Pseudomonas aeruginosa: models for the study of cystic fibrosis.* Pediatr Pulmonol, 2000. **30**(5): p. 413-24.
111. Tam, M., G.J. Snipes, and M.M. Stevenson, *Characterization of chronic bronchopulmonary Pseudomonas aeruginosa infection in resistant and susceptible inbred mouse strains.* Am J Respir Cell Mol Biol, 1999. **20**(4): p. 710-9.
112. Hoffmann, N., et al., *Novel mouse model of chronic Pseudomonas aeruginosa lung infection mimicking cystic fibrosis.* Infect Immun, 2005. **73**(4): p. 2504-14.
113. Doring, G. and E. Gulbins, *Cystic fibrosis and innate immunity: how chloride channel mutations provoke lung disease.* Cell Microbiol, 2009. **11**(2): p. 208-16.
114. Hankinson, J.L., J.R. Odencrantz, and K.B. Fedan, *Spirometric reference values from a sample of the general U.S. population.* Am J Respir Crit Care Med, 1999. **159**(1): p. 179-87.
115. Murphy, B.S., et al., *Characterization of macrophage activation states in patients with cystic fibrosis.* J Cyst Fibros. **9**(5): p. 314-22.
116. Razvi, S., et al., *Respiratory microbiology of patients with cystic fibrosis in the United States, 1995 to 2005.* Chest, 2009. **136**(6): p. 1554-60.
117. Prasse, A., et al., *CCL18 as an indicator of pulmonary fibrotic activity in idiopathic interstitial pneumonias and systemic sclerosis.* Arthritis Rheum, 2007. **56**(5): p. 1685-93.

118. Raes, G., et al., *Arginase-1 and Ym1 are markers for murine, but not human, alternatively activated myeloid cells.* J Immunol, 2005. **174**(11): p. 6561; author reply 6561-2.
119. Emerson, J., et al., *Changes in cystic fibrosis sputum microbiology in the United States between 1995 and 2008.* Pediatr Pulmonol. **45**(4): p. 363-70.
120. Fahy, J.V., et al., *Safety and reproducibility of sputum induction in asthmatic subjects in a multicenter study.* Am J Respir Crit Care Med, 2001. **163**(6): p. 1470-5.
121. Gershman, N.H., et al., *Fractional analysis of sequential induced sputum samples during sputum induction: evidence that different lung compartments are sampled at different time points.* J Allergy Clin Immunol, 1999. **104**(2 Pt 1): p. 322-8.
122. Kim, C.K., et al., *Bronchoalveolar lavage cellular composition in acute asthma and acute bronchiolitis.* J Pediatr, 2000. **137**(4): p. 517-22.
123. Strumpf, I.J., et al., *Safety of fiberoptic bronchoalveolar lavage in evaluation of interstitial lung disease.* Chest, 1981. **80**(3): p. 268-71.
124. El Kasmi, K.C., et al., *Toll-like receptor-induced arginase 1 in macrophages thwarts effective immunity against intracellular pathogens.* Nat Immunol, 2008. **9**(12): p. 1399-406.

VITA

Theodore James Cory, Doctoral Candidate

Birth

February 3, 1982
St. Louis Park, MN

Education

Drake University
Pharm.D. with honors: May 2006
Cumulative GPA 3.5
The University of Kentucky
Entered graduate program Fall 2006
Ph.D. candidate, Clinical and Experimental Therapeutics Track, Pharmaceutical Sciences Graduate Program
Anticipated Graduation: August 2011
Cumulative GPA 3.6

Research Experiences

2006-present: Graduate Student in the lab of Dr. David Feola. Research into the effect of azithromycin on classically and alternatively activated macrophage phenotype

Work Experience

TA duties at the University of Kentucky have included Therapeutics, Pharmacokinetics, and patient care laboratories
2006-2011: Float pharmacist, Wal-Mart

Honors/Awards

Spring 2011: First Place, University of Kentucky Rho Chi Research Day, graduate student division
Spring 2011: Recipient, Helton Travel award (College of Pharmacy)
Fall 2010-Spring 2011: Recipient, Graduate School Academic Year Fellowship.
Spring 2010: Member, Rho Chi honor society
Fall 2009: Recipient, Glavinos Travel Award (College of Pharmacy)
Dean's List (GPA>3.5): Spring 2001, Fall 2001, Spring 2002, Spring 2003, and Fall 2003
Spring 2001: Recipient CRC Press award for chemistry
President's List (GPA=4.0): Fall 2000
Eagle Scout, 1997

Publications

Sabeva NS, McPhaul CM, Li X, Cory TJ, Feola DJ, Graf GA. Phytosterols Differentially Influence ABC Transporter Expression, Cholesterol Efflux and Inflammatory Cytokine Secretion in Macrophage Foam Cells. *Journal of Nutritional Biochemistry* November 24, 2010. Epub ahead of print

Murphy BS, Bush HM, Sundareshan V, Davis C, Hagadone J, Cory TJ, Hoy H, Hayes Jr D, Anstead MI, Feola DJ. Characterization of Macrophage Activation States in Patients with Cystic Fibrosis. *Journal of Cystic Fibrosis* 2010:9(5):314-322.

Feola DJ, Garvy BA, Cory TJ, Birket SE, Hoy H, Hayes Jr D, and Murphy BS. Azithromycin alters macrophage phenotype and pulmonary compartmentalization during *Pseudomonas* pneumonia. *Antimicrobial Agents and Chemotherapy*. 2010:54:2437-47.

Murphy BS, Sundareshan V, Cory TJ, Hayes D Jr, Anistead MI, Feola DJ. Azithromycin Alters Macrophage Phenotype. *Journal of Antimicrobial Chemotherapy.* 2008:61:554-60.

Fogarty B, Heppert K, Cory T, Hulbutta K, Martin R, and Lunte S. Rapid Fabrication of Poly(Dimethylsiloxane)-based Microchip Capillary Electrophoresis Devices using CO_2 Laser Ablation. *The Analyst*. 2005;130(6):924-930.

Presentations

Macrophage Polarization in Inflammatory Lung Disease. University of Kentucky Pharmacy Practice and Science Seminar Series. April 8, 2011

Decreased Inflammatory Cytokine Gene Expression in Cystic Fibrosis Patients. T. Cory, S. Birket, B. Murphy, H. Bush, and D. Feola. Keystone Symposia: Immunity in the Respiratory Tract: Challenges of the Lung Environment, February 26-March 3, 2011. Vancouver, BC, Canada.

Gene Expression Analysis of Macrophage and Inflammatory Proteins in Sputum Samples of Cystic Fibrosis Patients. T. Cory, S. Birket, B. Murphy and D. Feola. Autumn Immunology Conference, November 19-22, 2010, Chicago, IL

Azithromycin Polarizes Macrophages to an Alternatively Activated Phenotype Independent of IL4/13 Receptor Function. Departmental Seminar, presented Spring 2010

Effect of Azithromycin on Collagen Production in a Co-Culture System. T. Cory, S. Birket, B. Murphy and D. Feola. Autumn Immunology Conference, November 21-24, 2009. Chicago, IL.